ABSTRACT

Title of Dissertation:	STRATEGIES FOR SMALL RNA LOADING INTO EXTRACELLULAR VESICLES
	Alex Pottash
Doctor of Philosophy, 2022
Dissertation directed by:	Associate Professor, Dr. Steven M. Jay, Fischell Department of Bioengineering

Small RNAs are an exciting class of therapeutics with significant untapped therapeutic potential, due to their ability to affect cell behavior at the RNA level. However, delivery of RNA is a challenge due to its size and labile nature. Extracellular vesicles (EVs) are promising as delivery vehicles due to their natural role as physiological intercellular microRNA transporters, and research has shown that EVs have significant advantages compared to competing technologies such as lipid nanoparticles. Specifically, EVs more readily transport through biological barriers, deliver RNA more efficiently, and are less immunogenic. However, intrinsic microRNA content in EVs is low and thus active small RNA loading strategies are needed to enable therapeutic use. Consequently, a variety of small RNA loading methods for EVs have been developed. These include endogenous and exogenous approaches. Exogenous approaches, in which EVs are loaded directly, have been shown to enable loading of hundreds to thousands of small RNAs per EV, but they are not readily amenable to scalable production processes. Endogenous approaches, in which EVs are loaded by upstream manipulation of the producer cell, are compatible with large

scale EV production, but loading by these approaches is inconsistent and has scarcely been quantitatively analyzed. The work in this dissertation is focused on enabling small RNA therapeutics via EV delivery. The lack of an ideal small RNA loading approach for EVs is addressed by tackling important issues of both endogenous and exogenous loading. First, the loading capacity of several common endogenous loading methods was optimized and quantitatively analyzed. Additionally, new approaches to endogenous small RNA loading involving genetic manipulation of the RNA structure and the microRNA cellular processing pathway were developed and evaluated. Finally, exogenous loading via sonication was applied to enable delivery of a novel microRNA combination that was identified via a rational selection process. This combination of miR-146a, miR-155, and miR-223 was found to have potentially synergistic anti-inflammatory activity, and EV-mediated delivery of the combination opens the possibility for therapeutic application in inflammatory diseases and conditions such as sepsis. Overall, this work both improves understanding of current techniques for small RNA loading into EVs and opens new opportunities for advanced strategies, bringing EV-based small RNA therapeutics closer to clinical application.

STRATEGIES FOR SMALL RNA LOADING INTO EXTRACELLULAR VESICLES

by

Alex Pottash

Dissertation submitted to the Faculty of the Graduate School of the
University of Maryland, College Park, in partial fulfillment
of the requirements for the degree of
Doctor of Philosophy
2022

Advisory Committee:
Associate Professor Dr. Steven Jay, Chair
Professor Dr. William E. Bentley
Associate Professor Dr. Edward Eisenstein
Professor Dr. Christopher Jewell
Associate Professor Dr. Amy J. Karlsson, Dean's Representative

Dedication

To my parents and my bubbe and my brothers and Ayelet and my nieces who support me.

To Michael, for letting me crash on your couch for a year in 2018.

To all my friends and extended family.

To Luc and Monique Chamberland, your support meant so much.

To Sarah, j'taime. I'm sorry for staying in lab too late. Thank you for everything.

Acknowledgements

I would like to thank my advisor Steven Jay for all his enthusiasm and valuable guidance over the last 5+ years. He was such a role model to me as a scientist and leader, and gave me the independence to develop my ideas while pushing me to do my very best. I will feel honored to be able to tell people I trained in his lab, and I hope to be as wonderful a mentor as he is. Thank you for your patient and consistent support and for all the opportunities you gave me. I'd also like to thank frequent collaborator Dr. Wei Chao.

I am grateful to my committee, Dr. Chris Jewell, Dr. Amy Karlsson, Dr. Ed Eisenstein, and Dr. Bill Bentley, for giving me feedback and guidance in various forms throughout my PhD. I would especially like to thank Dr. Bentley for giving me my start in his lab seven years ago.

This work was financially supported in part by the NIH T32 Graduate Training Program in Host-Pathogen Interactions. I would like to thank Dr. Kevin McIver, Dr. Vincent Lee, Dr. David Mosser, and Teresa Thompson for their support and the opportunity to be a part of their program.

I am grateful to Dr. John Fisher, Teresa Moore, Bill Churma, Tracy Chung, Tanisha Lee, Alexa Marcos, Ron Noble, Mari Andrews, Catherine Carroll, and everyone else in the Fischell Department who helped me over the years and did so much in the background for this dissertation.

Man then goes out to his work,
to his labor until the evening.

How many are the things You have made, O LORD;
You have made them all with wisdom;
the earth is full of Your creations.

[…] vast and wide,
with its creatures beyond number,
living things, small and great.

(Psalms 104: 23-25)

A different exposition for "small and great":
these are the scholars, the small and the great,
who sharpen their teeth on one another's arguments.

(The Midrash on Psalms)

Table of Contents

List of figures

List of abbreviations

Ago2: Argonaute 2

EV: extracellular vesicle

GFP: green fluorescent protein

HDV: hepatitis delta virus

HEK293T: human embryonic kidney cell line

MSC: mesenchymal stem cell

MVB: multivesicular body

NoDice: Dicer-knockout HEK293T cells

nt: nucleotide

NTA: nanoparticle tracking analysis

PBS: phosphate-buffered saline

Pol II: RNA polymerase II

RT-PCR: reverse transcription – polymerase chain reaction

scr: scramble

SD: standard deviation

SEM: standard error of the mean

Nucleic acids

RNA: ribonucleic acid

RNAi: RNA interference

miRNA: microRNA

pri-miRNA: primary-miRNA

pre-miRNA: precursor-miRNA

mRNA: messenger RNA

siRNA: short interfering RNA

shRNA: short hairpin RNA

ssRNA: single-stranded RNA

dsRNA: double-stranded RNA

DNA: deoxyribonucleic acid

cDNA: complementary DNA

Chapter 1: Introduction

Extracellular vesicles (EVs) are increasingly studied as diagnostic and therapeutic agents in medicine. EVs are cell-derived membrane-delimited nanoparticles that have been shown to play a large role in physiological and pathological paracrine and endocrine signaling via intercellular transfer of proteins, lipids, and RNA. In particular, microRNA (miRNA), which are 19-23 nucleotide (nt) RNA molecules that play an important regulatory role in cell biology, are enriched within EVs and are implicated as key drivers of their bioactivity [1]. Thus, EVs have been extensively studied as a platform for delivery of therapeutic miRNA as well as the functionally and structurally homologous short interfering RNA (siRNA) (miRNA and siRNA are collectively termed "small RNA"). A significant breakthrough occurred in 2011, when scientists loaded EVs with non-endogenous small RNA for delivery to the brain in a preclinical model [2]. Since then, numerous methods for the enrichment of specific small RNA in EVs have been developed, including "endogenous" methods wherein the parental cell is manipulated for overexpression of desired RNA into EVs and "exogenous" methods wherein the extracellular vesicles are first isolated and then directly enriched with RNA. Yet, despite years of research, there is still no consensus approach to small RNA loading of EVs, and a relative lack of quantitative understanding of the capabilities of the different methods in use constitutes a barrier to translation of EV-based therapies. The native miRNA content of EVs is subject to much debate and controversy in the field. Some labs have found miRNA content to be extremely enriched in EVs isolated from cell culture, with specific abundant miRNAs reaching above one or even ten copies per EV [3], [4]. Other labs have found much less miRNA content within EVs, both isolated from cell culture and bodily fluids, with some estimates of total miRNA

concentration at around one copy per EV or much less [5]–[8]. These discrepancies are likely attributable to a combination of factors, such as EV isolation methods and quantification scheme. The lower estimates have caused some to question the underlying premises that extracellular miRNAs play a significant physiological role, given the stoichiometric requirements for recipient cell target knockdown.

The work in this dissertation addresses the need for increased knowledge of miRNA loading approaches to EVs in multiple ways. **Chapter 2** provides an overview of current approaches as well as background on the physiological roles of EVs and miRNA and potential clinical applications for and alternatives to EV-mediated miRNA delivery. The subsequent three chapters cover techniques spanning both the endogenous and exogenous loading method space. **Chapter 3** examines the endogenous loading methods of electroporation and cationic transfection. Each method was optimized to maximize miRNA delivery into the parental cell and the produced EVs were quantitatively analyzed for miRNA loading. **Chapter 4** explores the possibilities and complexities of DNA overexpression of miRNA as an endogenous loading strategy. The effects of plasmid design, RNA secondary structure, and cellular engineering on miRNA production and secretion were investigated. **Chapter 5** builds on prior work from the advisor's group that examined the exogenous method of sonication of EVs for loading of a single small RNA species. Here, the possible therapeutic advantage of loading multiple different RNA species into a single EV population using this method was investigated. Employing a rationally designed *in vitro* screen, we identified a specific combination of miRNAs that exhibited maximal anti-inflammatory bioactivity. We then examined the secreted proteome of macrophage cells for targets of the combination-miRNA-loaded EVs and finally assessed the efficacy of these EVs in

a murine endotoxemia model. Finally, **Chapter 6** summarizes the work presented in the previous chapters, places it within the greater context of the field, and points out the future directions necessary to continue to develop EVs as miRNA delivery vehicles. The **Appendix** includes various ongoing work that could benefit the RNA delivery field.

Chapter 2: Background

RNA interference (RNAi) is a well-studied biological phenomenon that is still emerging as a therapeutic technology. Discovered by Fire and Mello in 1998, RNAi describes the silencing of specific protein translation based on messenger RNA (mRNA) sequence complementarity of small (~19-23 nt) RNAs such as endogenous microRNA (miRNA), exogenous small interfering RNA (siRNA), or small hairpin RNA (shRNA) [9]. RNAi has potentially far-reaching therapeutic potential due to the central role of RNA in many diseases. Thus far, however, only three small RNA pharmaceuticals have been approved for clinical use, all of which deliver to the liver. The major obstacle to further small RNA translational successes is delivery to the cytoplasm of specific cells of therapeutic interest.

The human body has evolved to prevent the unregulated transport of genetic material as a matter of survival. As a result, numerous biological barriers to RNAi delivery exist (Figure 1), including: a) extracellular RNA nucleases, b) cellular membranes that repulse charged macromolecules, c) circulating phagocytic cells, d) clearance by the liver and kidneys, and e) intracellular degradation in the lysosome. These barriers have necessitated design of RNAi delivery strategies, including, prevalently, vehicles such as lipid nanoparticles and polymer-based systems. Such approaches have been shown to be effective for delivery to the liver but can exhibit immunogenicity and be cleared by the reticuloendothelial system (RES).
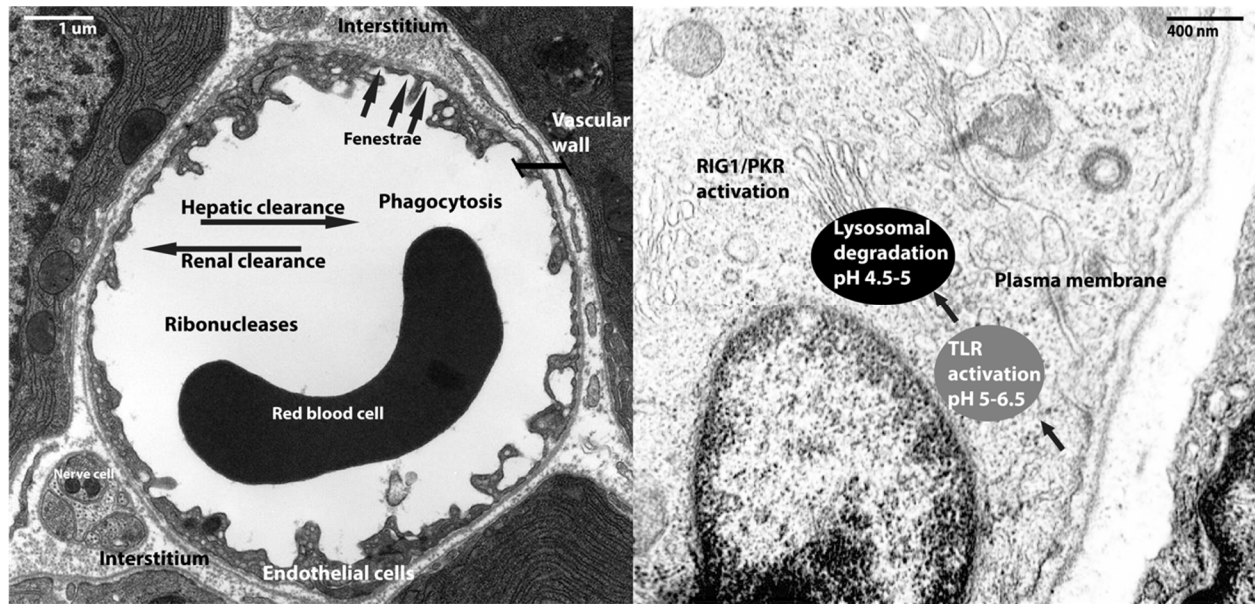
Figure 1. Barriers to RNA delivery. Left: RNA in circulation is vulnerable to RNase degradation and phagocytosis, and access to targeted tissue is blocked by physical barriers (e.g., endothelial and epithelial layers) and renal and hepatic clearance. Right: Cytoplasmic delivery is impaired by the plasma membrane, degradation within lysosomes, and nonspecific dsRNA immune activation. The latter can occur within the endosome by activating a Toll-like receptor (TLR) or in the cytoplasm by activating RIG1 or protein kinase R (PKR). Images courtesy of Louisa Howard at Dartmouth University. Reprinted with permission from [409].

Almost immediately after the discovery of RNAi, attempts to produce small RNA therapies began. Since then, findings on the intricacies of small RNA biology and their development as therapeutics have mostly gone hand-in-hand since their discovery. In the following sections, we will discuss the history and promises of small RNA, as well as relevant details about their biogenesis and natural function.

Biology and clinical potential of small RNA

History of RNAi

In the 1990s, various groups had found that introducing single-stranded RNA (ssRNA) that was complementary to a specific mRNA would cause "quelling" of that mRNA. Fire and Mello, in a 1998 paper that garnered them the 2006 Nobel Prize, showed that double-stranded RNA (dsRNA), not ssRNA, was the trigger for RNA interference in *C. elegans* [10]. This work indicated that complementary RNA does not inhibit mRNA activity by direct hybridization, but rather a completely novel mechanism. In following years, various details about the RNAi process were discovered: inhibitory dsRNA were being processed into small 21-23 nt RNAs (2000) [11], [12], that synthetic small RNAs were capable of silencing (2001) [13], that this worked in mammalian cells (2001) [14], that Dicer protein produced small RNAs (2001) [15], that Argonaute 2 (Ago2) protein was the effector protein (2006) [16], [17], and so on. Other minor and major details of RNAi biology continue to be elucidated to this date.

miRNA biogenesis and function

The miRNA biogenesis pathway varies for specific miRNAs, but canonically proceeds as follows [18]–[20] (Figure 2). First, primary miRNA (pri-miRNA) is transcribed by RNA Polymerase II (Pol II) from intragenic regions of the genome, occasionally within a family of related miRNAs. Next, these RNAs are cleaved at the base of a hairpin structure by a Drosha/DGCR8 complex to become a hairpin-shaped precursor miRNA (pre-miRNA) that typically ranges from 50-70 nucleotides long. This pre-miRNA is shuttled from the nucleus to

6

the cytoplasm by a Exportin-5/RanGTP complex. In the cytoplasm, the enzyme Dicer cleaves off the pre-miRNA hairpin to produce a miRNA duplex similar to siRNA. Based partly on strand thermodynamics, one strand of the miRNA duplex is degraded while the other is loaded into the RNA-induced silencing complex (RISC), which is composed of Ago2, Dicer, TRBP and other proteins. From here, the mature miRNA is capable of guiding Ago2-mediated binding to fully- or partly-complementary target RNA sequences via Watson-Crick base pairing, whereupon Ago2 performs cleavage of the target, which is subsequently destroyed. Other Argonaute proteins (Ago1, Ago3 and Ago4) can also be loaded with small RNA and repress other RNAs; however, they are expressed at lower levels and do not cleave their targets [21]. These cytoplasmic processes generally occur at localized foci known as P-bodies (processing-bodies) and GW-bodies (so-called for their enrichment with the GW182 protein) [22], [23], though these structures are not required for function [24].

Some non-canonical exceptions to the miRNA biogenesis pathways have been elucidated (Figure 3) [20], [25]. Briefly, mirtrons (such as miR-877) are miRNAs derived from gene introns that are spliced into pre-miRNAs and therefore do not require Drosha processing. Due to its short length, miR-451 is Dicer-independent and its 5' strand is selectively loaded directly in Ago2, whereupon it undergoes 3' progressive trimming by the PARN enzyme into a mature sequence [26]–[30]. Some miRNAs (such as miR-320) bypass Drosha and Exportin-5, as they are modified with a 5' 7-methylguanosine (m7G) cap during transcription and exported via Exportin-1 to the cytoplasm, where the 3' strand is selectively loaded [31]. Other RNAs use enzymes to tweak their processing via minor modifications, for example let-7 is mono-uridylated by TUT7 and TUT2 enzymes during biogenesis [32]. Finally, unexpected RNA precursors like small nucleolar RNA

7

(snoRNA) and transfer RNA (tRNA) can be processed into small RNA that are loaded into Ago2 [25]. Additionally, miRNA can have effects besides those of target knockdown, including activation of toll-like receptors [33]. Other interesting exceptions to the canonical pathway exist [25].
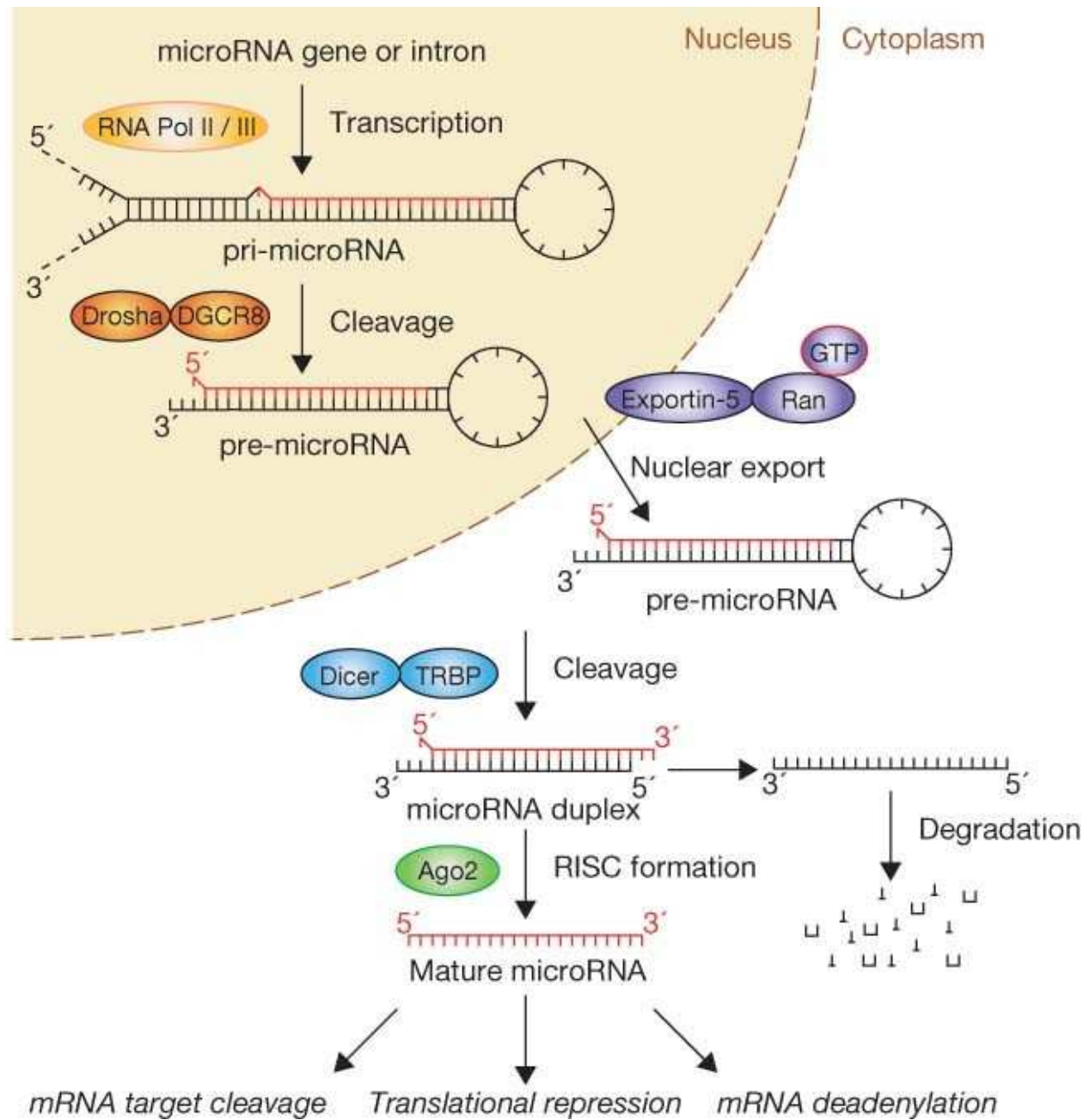
Figure 2. miRNA biogenesis pathway. Reprinted with permission from [34].
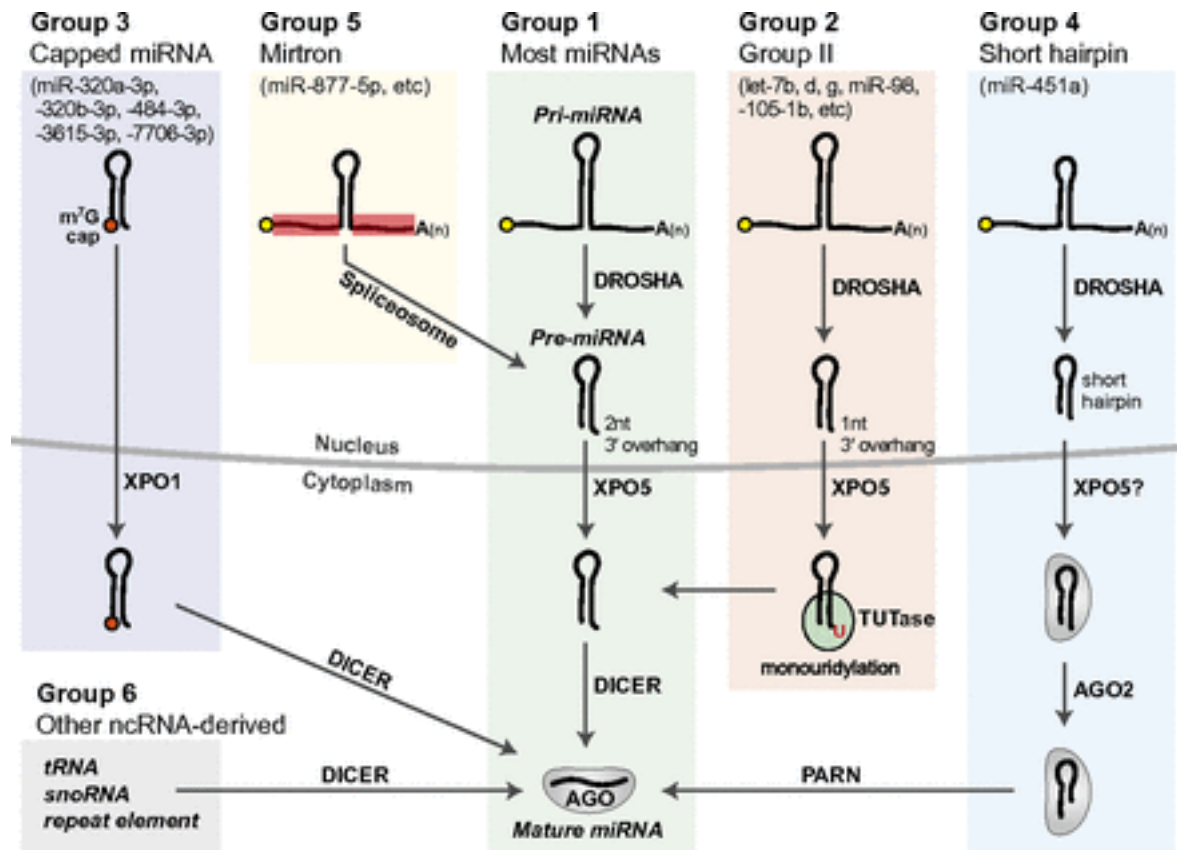
Figure 3. Non-canonical miRNA biogenesis, reprinted with permission from [20].

Once miRNAs are loaded into Ago2, they have the capacity to downregulate mRNA through partial complementary sequences primarily in their 3' untranslated region (UTR). It is estimated that 30-50% of genes are regulated by miRNAs [35], [36]. Single miRNAs can also target hundreds of different mRNA species; likewise particular mRNAs can be targeted by multiple miRNAs [37]. Furthermore, the "competing endogenous RNA (ceRNA)" theory posits that miRNA levels are regulated by their targets as much as the opposite [38]. Thus, miRNA can be sponged by "miRNA response elements (MREs)", such as long non-coding RNAs (lncRNAs) like circular RNA (circRNA), pseudogenes, and simple mRNAs. This leads to an idea of cellular

RNA as an equilibrium consisting of a complex network of MREs that is constantly shifting and may behave in opaque and unpredictable ways.

Small RNA therapeutic development and clinical promise

The therapeutic potential of RNAi was immediately noticed after discovery. siRNA drug development companies were quickly founded, with the first in-human clinical trial for an siRNA-based drug begun in 2004. Despite the hype, clinical trial failures coupled with negative press led to a waning of interest in RNAi drugs. However, recent successes have led to resurgence in interest. In 2018, the first siRNA-based drug, patisiran became FDA-approved, followed by givosiran and lumasiran. These three drugs were developed by Alnylam, and all target the liver.

Certain technical challenges had to be overcome in order develop these drugs. Patisiran utilizes a lipid nanoparticle-encapsulated siRNA, while the other two drugs utilize N-acetylgalactosamine (GalNAc)-conjugated siRNA. Lipid nanoparticles are highly developed vehicles that mostly evade the immune system, and accumulate in the liver [39]. GalNAc is a carbohydrate moiety that binds strongly to a hapatocyte receptor [40]. Additionally, these siRNA molecules have extensive chemical modifications that allow them to evade degradation during extracellular transport and to bias strand selection in the cell, among other functions [41]. These developments were critical towards the development of liver-targeting siRNA therapies; however, further technical challenges remain for targeting other tissues.

EV biology and use as therapeutic vehicle

The discovery in 2007 by Valadi *et al.* that EVs (including exosomes, microvesicles, and apoptotic bodies) transfer RNA species opened a new frontier of knowledge on intercellular communication [42]. Previously, EVs, which are secreted by most—if not all—cell types and are prevalent in all body fluids, were considered a form of cellular waste disposal. Since Valadi *et al.*, an entire field of studying the natural pathways of EV biogenesis, composition, and function has emerged. This research has borne out that EV-mediated RNA transfer plays an important role in healthy physiology as well as pathologic progression.

EV physiology

"Extracellular vesicle" is a broad term that is defined as a cell product that has a lipid bilayer and cannot replicate. This is used to describe any number of vesicles secreted by cells, including exosomes, microvesicles, and apoptotic bodies. Each of these are extremely heterogenous, made up of diverse lipids, proteins, and RNA species. Exosomes originate in multivesicular bodies in the cell and are 30-150 nm in diameter. Microvesicles originate from the cell surface and range from 100-1000 nm. Apoptotic bodies originate from the outward blebbing of apoptotic cells and are 500-2000 nm wide. These bodies contain the nuclear fractions and organelles of the apoptotic cell and are undesirable for therapeutic use. There are currently no established methods for isolating these populations from one another, thus most refer to them as a group, "extracellular vesicles," or EVs.

EVs are increasingly the focus of studies for their role in intercellular communication. All cell types release EVs, and many different roles have been proposed and verified for EVs in healthy

11

physiological and pathophysiological function, as both paracrine and endocrine signalers. These roles range from response to exercise [43], neonatal development [44], interkingdom gut-microbiota communication [45], and brain cell crosstalk [46], to SARS-CoV-2 infection [47], heart disease [48], and immune suppression by tumor cells [49].

As indicated above, EVs subpopulations are defined based on their biogenesis pathways [50]. Exosomes are formed within multivesicular bodies (MVBs), which are part of the endosomal system. Within MVBs, intralumenal vesicles (ILVs) are formed through invagination of the endosome by the cytoplasm; this process is initiated by the concentration of tetraspanins and recruitment of the ESCRT (endosomal sorting complexes required for transport) complex. Other ESCRT-independent pathways, perhaps dependent on sphingolipid ceramide, may also lead to MVB budding. ILVs accumulate within the MVB until the MVB fuses with the plasma membrane, at which point the ILVs are released into the extracellular environment and become exosomes. Microvesicle biogenesis is less defined, and in general is likely caused by the outward budding of the plasma membrane due to phospholipid concentration and actin-myosin contraction.

The contents of EVs are dependent on the species, individual, cell type, cell phenotype, and biogenesis pathway [51]. The contents of EVs reflect the contents of the parental cell. In terms of protein content, exosomes are generally enriched with proteins that are involved in biogenesis, like tetraspanins such as CD63 and CD9, and ESCRT proteins such as ALIX or TSG101. For lipid content, there are certain lipids which are enriched in EVs, such as sphingomyelin, cholesterol, phosphatidylserine, and others. Microvesicle lipid content largely resembles plasma

membrane content. The nucleic acid content of EVs is extremely diverse and enriched in shorter sequences (<200 nucleotides), including rRNA and tRNA fragments, YRNA, piRNA, mRNA, and miRNA (with the latter receiving the bulk of the attention).

EV fate is determined by both specific factors such as extravesicular protein- and lipid-mediated interactions and generic uptake mechanisms [52]. For example, EVs produced by oligodendrocytes are taken up preferentially by microglia, rather than neurons, and EVs collected from primary neurons are only internalized by other neurons, as compared to EVs from a neuroblastoma cell line, which are also internalized by astrocytes [53], [54]. Additionally, EVs that display CD47 or do not display phosphatidylserine have been shown to have extended half-lives in blood circulation, most likely due to evasion of the RES [55], [56]. Upon interaction of surface proteins/lipids with the cell membrane, EVs deliver their cargo by either fusing directly with the cell membrane or through endocytosis. After endocytosis, EVs can fuse with the endocytic membrane, releasing their contents into the cytoplasm, or be degraded in the lysosome.

EV miRNA content

In 2009, it was shown that GW182-enriched P-bodies (referred to as GW-bodies) localize with MVBs and that miRNA biogenesis and activity was intimately entangled with EV biogenesis, with GW182 serving as a possible link between the two pathways [57], [58]. Other connections have been found, including identifying Ago2 and Alix as binding partners [59]. One study found evidence that miRNA secretion was suppressed by interacting with complementary mRNA, since this sequestered the miRNA in P-bodies, away from the MVB [60]. However, this finding has recently been challenged by another group [61]. These connections are still murky but indicate a

profound link between miRNA biology and EV biology, and illuminating this link could help elucidate other questions surrounding miRNA secretion.

To a first approximation, the miRNA content of EVs reflect the contents of the parental cells, however to a second approximation, there can be significant enrichments or exclusions in EV content compared to the parental cell, including specific miRNA sequences. Some studies have seen a high correlation (r > 0.9) between cell and EV miRNA profiles [62], [63], while others have seen a weaker correlation (r = 0.5-0.7) [64], [65]. Other studies have shown that certain miRNA species are an enriched fraction of EV-associated miRNA when compared to their fraction of cellular miRNA [60], [66]–[72]. This led to the discovery of various RNA-binding proteins (RBPs), such as HuR, SYNCRIP, hnRNPA2B1, and others, that bind in sequence-specific manner to miRNA and increase secretion [68], [69], [71]–[75]. Specific motifs like GGAG and CGGGAG, when added to the 3' end of miRNA sequences, led to increases in secretion due to RBP binding [68], [72]. Additionally, nontemplated uridylation is enriched in EV-associated miRNA, indicating that chemical modifications could mark RNA for secretion [76]. All of these results indicate that miRNA secretion is an "active, selective" process, whereby favored sequences are exported for intracellular communication or degradation.

Despite these results, however, there has been pushback on this idea, favoring a "passive, nonselective" process whereby miRNA sequence plays a minor or nonexistent role in determining secretion. Detractors point to other factors, such as RNA size, stability, local concentration, availability, and random stochasticity that may be much more important for secretion [51], [77]–[80]. In this view, RBPs and specific sequences (perhaps high in GC-

14

content) may not actively promote secretion, but rather sequester miRNA from cellular RNAi machinery or degradation. Interestingly, a study by Chen *et al.* showed that mesenchymal stem cell (MSC)-derived EVs are more highly enriched in pre-miRNA than mature miRNA, perhaps due to this sequestration [81]. Additionally, while 29% of the HEK293T-derived EV proteome was found to be RNA-binding proteins, only 0.9% were found to be "miRNA related" [82]. Furthermore, stable tRNA halves were preferentially secreted into EVs, indicating that stability is important towards secretion [83].

An additional explanation for the phenomenon could be the "law of small numbers," whereby since some miRNAs are expressed at a low amount and if EV-associated miRNAs are a tiny sampling of total cellular miRNA, random noise could generate outliers that are not necessarily the result of an active process. For example, if one copy of miR-000b is expressed in a cell, and by chance that copy is randomly secreted, data analysis would return that miR-000b is 100% selectively secreted. This would be a fallacy.

There is also controversy surrounding the absolute abundance of EV-associated miRNA. Some estimates measure the total concentration of all miRNAs in EVs to be approximately one copy per EV and much less for individual sequences [5], [7], [84]. Others find specific miRNAs to be enriched to the ones or tens of copies per EV [3], [4]. Absolute quantification is difficult and depends on factors like EV isolation method and quantification scheme.

Low estimates of EV-associated miRNAs have led some to question the role that they might play in physiology [5], [7], [84]. It has been demonstrated that ~300-2000 copies of siRNA are

required for 50% knockdown of a given mRNA in cells [85]–[87]. Stoichiometric evaluation of the system therefore necessitates the delivery of thousands of EVs to a single cell in order to achieve knockdown, which detractors find unlikely in most situations *in vivo*. However, there are other considerations which may alter the calculation. First, quantification of both miRNAs and EVs is difficult and subject to error and may be wrong. Secondly, miRNA cargo may not be evenly distributed among EVs. Chevillet *et al.* proposed a "low occupancy" model, whereby most EVs contain no miRNA, while some contain many copies of miRNA (Figure 4) [6]. In this model, one or ten highly loaded delivered EVs may be sufficient to modify a single cells expression. Finally, experiments looking at small RNA requirements used traditional unmodified siRNA, which may or may not represent trafficked EV-associated miRNA [81].
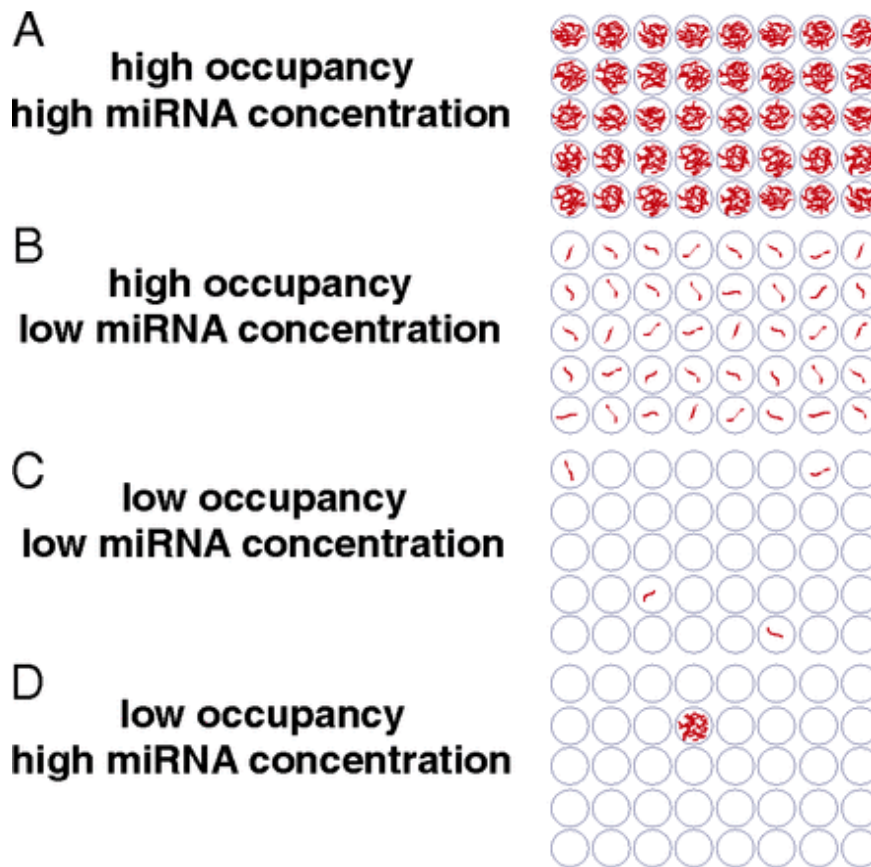
Figure 4. Different proposed models for miRNA occupancy within EVs. Reprinted with permission from [6].

EVs as therapeutic cargo vehicles

EVs have intrinsic bioactivity that makes them attractive for therapeutic development, and "character" that is reflective of their producer cell. Thus, EVs can often recapitulate a cell-based therapy without some of the risks of cell therapies, such as tumorigenesis. Two main areas to which researchers have sought to apply EVs therapies are cardiovascular and immune therapy. EVs from cardiac progenitor cells, CD34+ stem cells, and MSCs have all been shown to improve heart health [88]–[90]. Dendritic cells pulsed with tumor antigen will release EVs presenting that antigen alongside co-stimulatory molecules. These EVs can be used as cancer vaccines, and are currently in clinical trials [91].

With regard to use as a vehicle for therapeutic cargo, EVs may demonstrate superiority to synthetic nanoparticles, as shown in Figure 5. For example, EVs have a great safety profile including low immunogenicity and toxicity when compared to synthetic alternatives [92], [93].

	Safety profile	Extra-hepatic delivery	Endosomal escape	Manufacturing proficiency
Lipid nanoparticles (LNPs)	yellow	red	red	green
N-Acetylgalactosamine (GalNAc)	green	red	red	green
Adeno-associated virus (AAV) vectors	red	green	green	yellow
EVs	green	?	green	yellow

Figure 5. Comparison of various delivery vehicles according to current knowledge. Safety profile describes the immunogenicity and toxicity of the vehicle. Extra-hepatic delivery describes the ability of the vehicle to deliver to internal targets outside the liver. Endosomal escape describes the ability of the vehicle to enter the cytoplasm after endocytosis. Manufacturing proficiency describes knowledge and viability of different techniques to be used at an industrial scale. Red, yellow, and green describe how well each technique fulfills each parameter. Question marks refer to gaps in knowledge.

They achieve rates of endosomal escape of 20-30%, compared to 1-2% for synthetic

nanoparticles [5], [94]. Additionally, those nanoparticles are often limited in delivery to the liver

and lung, whereas EVs may enable targeting and delivery to other organs. Finally, EV

production and manufacturing is still being developed in order to put it on par with other

vehicles. These characteristics have led researchers to use EVs as delivery vehicles for

exogenous cargo loading, including therapeutic small RNA. For loading desired RNA, there

have been many approaches, shown in Figure 6. They can be grouped into two broad categories:

direct EV manipulation, or *exogenous loading*, and producer cell manipulation, or *endogenous*

loading. A comparison of multiple exogenous and endogenous techniques is shown in Figure 7,

including current gaps in knowledge.
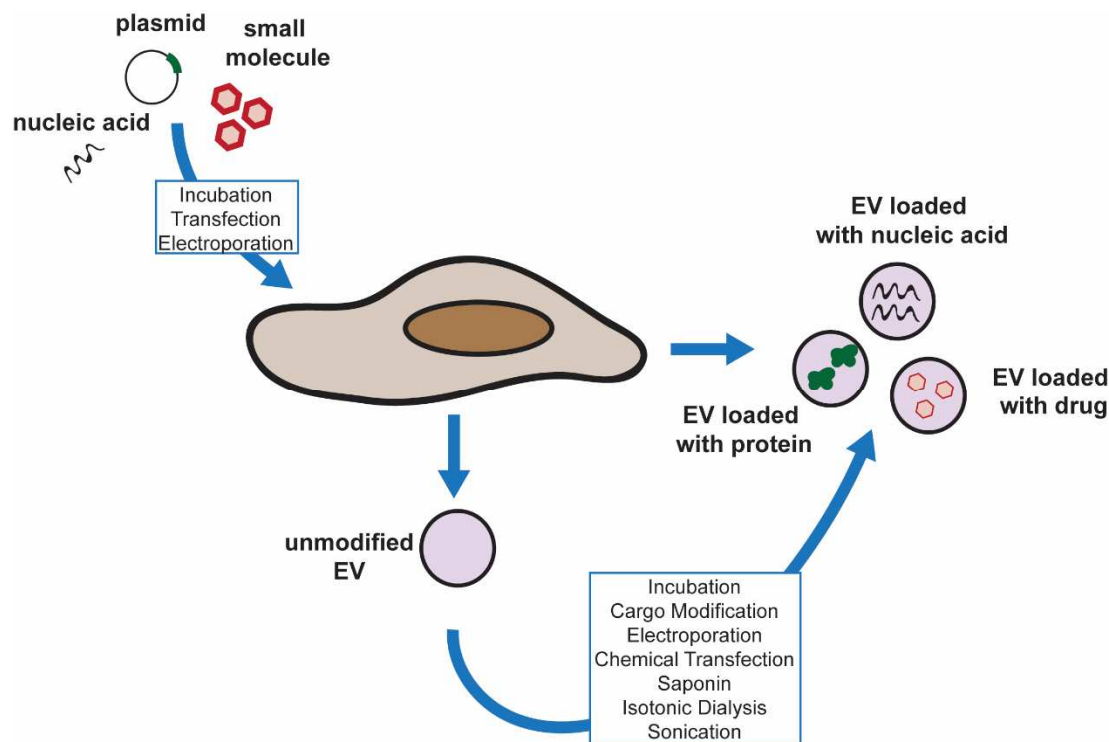
Figure 6. Different methods for loading cargo in EVs.
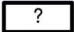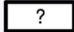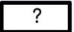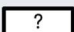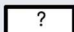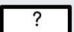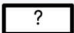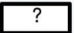
		EV loading efficiency	EV integrity	Scalability	Optimization still needed
Exogenous	Electroporation	red	red	red	green
Exogenous	Sonication	green	yellow	red	green
Endogenous	Electroporation	?	?	green	?
Endogenous	Cationic transfection	?	?	yellow	?
Endogenous	DNA overexpression	?	green	green	?

Figure 7. Comparison of various exogenous and endogenous loading techniques according to current knowledge. EV loading efficiency describes the copies RNA/EV. EV integrity describes structural and functional soundness of final product. Scalability describes ability to scale up to a high-throughput industrial process. Optimization still needed describes further research required to optimize this technique. Red, yellow, and green describe how well each technique fulfills each parameter. Question marks refer to gaps in knowledge.

EV exogenous loading methods

Exogenous loading means that the desired cargo to be loaded is added to the vesicles after secretion from the cell. Thus, the cargo does not interact with the producer cells at all, rather with the purified EV product. This strategy requires either a means of membrane disruption to allow RNA to enter, or decoration of the outside of EVs via chemical conjugation or chemical mediator. There are obvious negative consequences of these techniques: membrane disruption can lead to irreparable damage or aggregation and addition of chemicals can lead to a reduction of RNA or EV bioactivity due to diminished uptake or processivity. Another negative trait of exogenous loading techniques is it is likely a less efficient manufacturing process, due to the requirement to isolate EVs before loading. Endogenous loading techniques theoretically require no downstream process after isolation. Finally, exogenous techniques can lead to loading that is non-intravesicular, whereby RNA can become associated with the EV surface but not within the EV lumen. miRNA that is extravesicular may be detected in RNA quantification assays, but may not be protected from RNA degradation and is likely not delivered in an efficient manner.

19

For some hydrophobic cargo, such as curcumin, passive incubation is enough to achieve EV loading; however, for hydrophilic molecules such as RNA, despite reports to the contrary [95], this strategy is widely dismissed. Efforts to make siRNA hydrophobic by conjugating to lipids such as cholesterol succeed in loading the EVs, but only on the outside of the membrane, leaving the RNA vulnerable to degradation and possibly leading to inefficient delivery [96]. Additionally, lipids, especially cholesterol, can be promiscuous in spontaneously moving from membrane to membrane, which could cause a shedding of cholesterol-conjugated RNA to other vesicles, lipoproteins, or cells without requiring traditional EV uptake [97]–[100]. This effect would also likely be exacerbated by addition of a large hydrophilic RNA molecule [101]. This could very conceivably be a benefit towards delivery, especially in situations of cellular convergence towards an injury site [102]. Further development of lipid-conjugation along with chemical modifications to evade nuclease activity has made this technology a viable option, though the downstream effects of extensive loading on attributes such as EV surface charge and membrane character need to be determined [103]–[106] Like the first ever study to load miRNA into EVs [2], a majority of studies that exogenously load cargo employ electroporation, by which an electric field applied to the EVs rips holes in the bilayer and allows cargo to enter. This loading technique may load a limited amount of nucleic acid, however it induces significant aggregation of RNA cargo and causes EV aggregation and fusion [107]–[110]. EV electroporation should likely be retired as a loading strategy. Saponin is a detergent-like molecule that causes pore to open in EVs, allowing for cargo to enter. Unfortunately, however, it is difficult to remove saponin from the preparations, making it unfeasible as a loading method [111]. This is similar to the commercial product Exo-Fect, which has an unknown chemical

formulation, but high loading efficiency [112]. Further characterization needs to be performed on Exo-Fect to determine if it is a viable solution. In another technique, EVs are placed in hypotonic solution, causing the membrane to swell and form pores, so cargo can enter. However, after the solution is restored to isotonic, the EVs have modified size and charge, which ultimately inhibits cellular uptake [111]. Heat shock in the presence of calcium chloride has been employed, with limited loading efficiency [112], [113]. Our lab has previously developed a pH gradient-based loading technique, inspired by a similar technique originally used to load lysosomes [114]. This technique showed high loading efficiency and is promising for further development. Sonication has also been used at a loading method. Our lab has optimized a protocol for sonication loading that has shown much less RNA aggregation with sonication when compared to electroporation and a high loading efficiency [107]. We have also seen sonication cause an increase in nominal EV size and a slight decrease in uptake. However, sonication is a simple technique that allows for relatively high loading and easy application.

EV endogenous loading methods

EVs can also be loaded through the manipulation of the producer cell. This option poses much less risk of damaging the vesicles, guarantees intravesicular loading, and is likely more scalable since cells can be manipulated in high-throughput fashion before EV production [115]. However, there are potential downsides to endogenous loading techniques. Firstly, transfection may stress the cell and introduce foreign materials with an unknown effect. Secondly, unintended effects of cellular manipulation may lead to undesired or unknown changes to the EV product. More challengingly, introduction of any RNA transcript will have unique and unpredictable structure- and sequence-specific cellular effects that may change cellular phenotype and secretome.

Therefore, a thorough analysis of producer cell phenotype and EV composition would be required for every sequence that is tested. This effect also makes recipient cell changes difficult to attribute to specific RNA delivery and activity, when invariably the producer cell is more influenced by the RNA than the recipient cell. This producer cell priming effect may, in the end, be a benefit of this technique. Lastly, there are likely hard limits to cellular loading. As discussed above, some estimates claim that miRNAs are normally secreted at an average rate of one copy within one EV. While it is unknown if this rate is fixed or can be increased, some exogenous techniques reliably load thousands of copies of EVs.

As with exogenous loading, small molecules can be loaded via simple incubation. For example, MSCs incubated with Paclitaxel produce EVs loaded with the drug [74]. For small RNA, introduction via producer cells has traditionally been accomplished by transfection of the desired RNA or introduction of a DNA sequence for overexpression of a precursor (Figure 6). This DNA sequence could be transiently expressed or integrated into the genome. Transfecting the desired RNA sequence is more straightforward in that the only cellular process required is export, whereas DNA overexpression requires navigation of the miRNA biogenesis pathway.

Two methods for transfection of cells are electroporation and cationic transfection. Electroporation is a physical process in which an electric field applied to cells causes a temporary rupture in the cellular membrane through which molecules can enter the cytoplasm and is well-established for the introduction of plasmid DNA and small RNA. Protocols are generally optimized for specific cells in parameters such as wave form, field strength, pulse length, gap size, pulse number, and others. Electroporation of siRNA into cells has long been

used for inducing target knockdown, especially into cell lines refractory to other forms of transfection [116]. In studies of DNA electroporation, aggregation is important for the uptake and delivery of long DNA; approximately 75% of delivered DNA is taken up through endocytosis [117], [118]. siRNA, due to their smaller size, enter the cell passively through pores in the membrane during the electroporation step and have direct access to the cytoplasm [119]. Studies have also examined the diffusion of DNAs in the cytoplasm after electroporation and seen that diffusion of small DNA is mostly unhindered by actin or other cell components [120]–[122]. We could find only two papers that employed endogenous loading using electroporation [123], [124]. Wang *et al.* saw a 315-fold relative increase in miR-101 content in EVs and quantified the absolute concentration to be about 10 pg miR-101 per 1 μg MSC EVs [123]. Potential downsides of electroporation include possible siRNA aggregation and stress induced by electroporation. siRNA aggregation has not specifically been studied in the context of cellular electroporation, and could have a negative effect on cell health, quantification, and contamination.

Cationic lipids or polymers bind with anionic nucleic acids, mediate entry into the cell, and may assist with endosomal escape into the cytoplasm. This also a well-established method for small RNA transfection, with many commercially available reagents that may differ in formulation and effective concentrations. This strategy for loading miRNA into EVs has been used in a number of publications, with predictably variable loading efficiencies. Potential downsides of cationic transfection are the introduction of foreign lipids or chemicals that may end up in the final EV product, and stress caused by high doses of reagent.

DNA overexpression is potentially the most scalable strategy, since cells with stable genome integration can merely be grown and their EVs collected with nucleic acid synthesis or specialized equipment and can also avoid the problem of contamination. This technique is well established and optimized for expression of shRNA in cellular model, but has also been applied for loading into EVs [4], [125]–[131]. This technique generally only leads to modest fold-increases in miRNA, partly due to bottlenecks in the miRNA biogenesis pathway (shown in Figure 2). Recent work by Reshke *et al.* innovated a way to evade part of the miRNA biogenesis pathway, by packaging a desired mature RNA sequence within the pre-miR-451 scaffold [4]. miR-451 does not interact with the Dicer enzyme due to its short length, and is possibly the most naturally enriched miRNA within EVs. Additionally, only the 5' strand of miR-451 is loaded into Ago2. Packaging a desired sequence in the pre-miR-451 scaffold reconstituted this secretion behavior, and was found to enrich the EV-associated miRNA to one copy/EV. Reshke *et al.* saw knockdown of their target in the small intestine and liver at a much reduced dose compared to synthetic nanoparticles [4].

Application of EV-based miRNA therapy – Sepsis[1]

As mentioned above, small RNA has much promise as a novel therapeutic modality. Previously "undruggable" targets are newly available for drugging by leveraging the inherent system of RNA regulation found in the cell. Due to the centrality of RNA in most cellular functions, for many diseases there is reason to pursue an RNA-focused strategy. Therefore, there are many different diseases one could seek to treat with small RNA. Given the composition of our EV-based miRNA treatments, we decided to pursue a disease that lies at the intersection of EVs and

---

1 This section is partly adapted with permission from [408].

miRNA. Our previous work in the lab has found that EV-associated miRNA is significantly altered in septic patients, and that extracellular single-stranded miR-146a-5p is a large contributor to inflammation and disease progression [33], [132], [133]. While it is still unclear to what extent pathological EV-associated miRNA is necessary in sepsis progression, these agents are clearly implicated in pro-inflammatory signaling. Theoretically, then, replacement or displacement by anti-inflammatory EV-associated miRNA would lead to less inflammation and better outcomes.

Sepsis is a dysregulated host immune response to infection that is distinguished by a heterogeneous and complex pathophysiology [134]. At point of onset, sepsis is characterized by an unstable cascade involving the excessive activation of inflammatory mediators that can prompt widespread microvascular dysfunction and systemic inflammation [135]. The resulting overcompensation by the immune system can develop into an immunosuppressant state, during which inflammation is reduced but persistent, and the patient becomes susceptible to recurrent and nosocomial secondary infections [136]. Immune dysregulation can ultimately lead to multiple-organ failure, the major cause of death in sepsis patients [135], [137]. At this time, there are no drugs specifically approved for the treatment of sepsis, and while widespread adoption of sepsis management protocols including administration of antibiotics, fluid resuscitation, and hemodynamic support has significantly improved outcomes, patient recovery remains inconsistent [138]. As a result, sepsis is the leading cause of death of hospitalized patients, and with an estimated 48.9 million cases of sepsis worldwide and 11 million sepsis-related deaths reported in 2017, it persists as a major global health problem [139]. These discouraging statistics

have driven numerous efforts to develop therapeutic strategies, but the failures of several clinical trials in the past decades have led for some to call for new directions in sepsis treatment [140].

General pathology

Sepsis is an exceedingly complex clinical condition with a range of symptoms that occurs when an infection leads to a dysregulated systemic immune response. These symptoms can include: fever, leukocytosis or leukopenia, hypotension, organ failure, and death [141]. Within the context of local pathogen presence, the immune response is necessary for survival. Sepsis arises from an inability to contain that pro-inflammatory response to the local environment. This is how an adaptive immune response becomes maladaptive. Once systemic inflammation begins, it is difficult for the body to return to homeostasis. Sepsis is often characterized by significant systemic inflammation and coagulation activation, the two key components that lead to widespread microvascular thrombi deposition, tissue perfusion impairment, and gross clotting dysfunction, a condition termed sepsis-induced coagulopathy (SIC). Once sepsis causes low blood pressure, it is referred to as "septic shock."

As the interface between blood and organs, the endothelial cell lining plays immensely important roles in normal physiological function, including regulation of hemostasis, vasomotor control, and immunological function. Additionally, the endothelium is responsible for maintaining solute transport and osmotic balance. Dysfunctional endothelium in sepsis therefore leads to severe downstream effects that can result in death. There are many processes that contribute to and are affected by endothelial dysfunction. In small local infection scenarios, microvascular changes are beneficial to stopping the spread of pathogens. In sepsis, a positive feedback cascade is initiated

and subsequently mediated by innate immune cells such as neutrophils, monocytes, macrophages, and endothelial cells. Initially, activation of these cells via bacterial components such as lipopolysaccharide (LPS) leads to the release of pro-inflammatory cytokines and reactive oxygen species (ROS). Over-exposure of host cells to these factors can lead to undesirable processes such as glycocalyx shedding. The glycocalyx is the multicomponent gel-like barrier comprised of proteoglycans and glycoproteins. The glycocalyx is involved in processes such as the vascular barrier function, hemostasis, leukocyte and platelet adhesion, the transmission of shear stress to the endothelium, and anti-inflammatory and antioxidant defenses. Without the glycocalyx, edema can occur, and endothelial adhesion molecules are exposed, allowing for leukocyte adhesion and transmigration. Vasodilation is promoted via altered nitric oxide production. Additionally, hemostasis can be disrupted, by overexpression of tissue factor (TF), for example, allowing for the activation of the complement cascade and coagulation factors. These molecules activate the endothelium further, degrade endothelial junctions, and lead to further permeability. Pro-thrombic factors are produced, leading to microthrombosis. Eventually, microthrombi formation, capillary obstruction, tissue edema by capillary leak, and neutrophil recruitment, leads to organ dysfunction, failure, and eventually death. In this way, local microvascular changes that defend against infection in healthy function are adaptive, in sepsis become systemic and maladaptive.

Native EV role in sepsis

Sepsis is capable of inducing systemic dysfunction that can simultaneously affect the cardiovascular, respiratory, neurological, hematologic, hepatic, and/or renal system(s) [142]. As endogenous EVs are ubiquitous throughout human tissue, bodily fluids, and within the

27

circulation [143], there is reason to assume that EVs naturally play a role in the pathogenesis of sepsis. In fact, during the development of sepsis, endogenous EVs undergo fluctuations in both relative quantities and functional effects, making them integral in the progression of pathophysiological conditions [144]–[147]. Specifically, in sepsis and subsequent organ damage, endogenous EVs have been implicated as critical immunomodulatory factors that can regulate inflammation [148]–[157], coagulation [158]–[166], apoptosis [167], and vascular dysfunction [153], [168]–[172]. The ability of EVs to trigger, amplify, and sometimes suppress immune responses during disease can be attributed to the presence of distinct membranous proteins or lipids (e.g. phosphatidylserine, integrins, major histocompatibility complexes) and to differential luminal cargo (e.g., miRNAs, proteins) [173], [174]. There is much research dissecting these attributes and the mechanisms through which they work, as it can prove not only beneficial in the development of an EV therapeutic but also in clarifying the complex pathophysiology of sepsis. For example, Xu et al. showed that circulating plasma EVs in a cecal ligation and puncture (CLP) murine model of sepsis were not only more abundant when compared with healthy mice but also contained different miRNA and had pro-inflammatory effects on bone marrow-derived macrophages (BMDMs) [33]. This immunomodulation was shown to be partially mediated by EV-associated miRNAs (i.e., miR-34a, miR-122, miR-146a) that signal via a TLR7-myeloid differentiation primary response 88 (TLR7-MyD88)-dependent mechanism [33]. This research led to further investigation of the TLR7 signaling mechanism using a loss-of-function approach by Jian and colleagues that showed TLR7 signaling contributes to inflammation, organ injury, and mortality in murine sepsis [175]. These studies reveal important EV mechanisms as well as expose the cellular mechanisms contributing to sepsis and end-organ injury. The importance of endogenous EVs in sepsis was further highlighted in a study by Essandoh and colleagues in

which GW4869, a neutral sphingomyelinase inhibitor that partially blocks the release of EVs, was used to successfully reduce the number of EVs and proinflammatory cytokines emitted from lipopolysaccharide -stimulated macrophages [176]. This EV reduction was correlated with decreased systemic inflammation as well as diminished cardiac dysfunction and mortality in a CLP mouse model [176]. Overall, these outcomes confirm the importance of endogenous EVs in sepsis and highlight the potential of inhibiting or exploiting this dynamic as a promising intervention.

The research discussed thus far has focused on how EVs within the body can serve to initiate and perpetuate sepsis. However, it is important to note that endogenous EVs can also lend protection during sepsis. Dalli et al. showed that neutrophil-derived EVs (nEVs) containing alpha-2-macroglobulin (A2MG), an antiprotease shown to be upregulated in nEVs in septic patients [177], were able to mitigate bacterial titers, reduce systemic inflammation, and enhance survival in murine sepsis [178]. Additionally, a study by Gao and colleagues found that administration of murine septic EVs into a CLP mouse model suppressed inflammatory cytokine production (i.e., tumor necrosis factor-alpha; TNF-α), alleviated liver and lung tissue injury, and significantly prolonged survival [179]. When applied to engineered vascular constructs comprising human arterial smooth muscle cells, EVs from septic human patients were able to increase the expression of IL-10 and consequently reverse LPS-induced hyporeactivity and reduce oxidative stress [170]. Endogenous EVs can also serve as sepsis biomarkers to inform treatment strategy and timing, especially in critically ill patients [180]. As an example, in human septic patients, Dakhlallah and colleagues showed that circulating EVs had significantly higher loads of DNA methyltransferase (DNMT) mRNA, which regulates gene expression [181]. Specifically, more

severely ill patients showed increases in the ratio of de novo methylating factors DNMT3A and DNMT3B to the maintenance methylating factor DNMT1 encapsulated within these circulating EVs [181]. Research has also shown sepsis-induced differential expression of other EV-associated molecules, including miRNAs [153], [181]–[184]. Overall, the clear importance of endogenous EVs in sepsis demonstrates the efficacy of targeting or exploiting EVs as a potent sepsis treatment. Consequently, research on endogenous EVs and their roles in sepsis continues to grow and reveal numerous in vivo functions and diagnostic capabilities in preclinical sepsis models [151], [153], [154], [156], [162], [171], [172], [182], [185]–[193], as well as in human patients [145], [148], [155], [161], [167], [183], [184], [189], [194]–[212].

Role of extracellular miRNA in sepsis

Extracellular miRNAs play a large role in the progression and outcome of sepsis, depending on the source and identity of the miRNA. In work from our lab, extracellular RNA from septic mice were shown to induce a robust immune response in healthy animals and were inhibited by specific anti-miRNA antagonists [33]. Additionally, we have shown that EV-associated single-stranded miR-146a-5p, but not double-stranded, is a pro-inflammatory ligand for TLR7, and associated with sepsis predictors in human patients [132], [133]

In mice, sepsis severity and thrombosis both have a positive correlation with amount of extracellular RNA [213], [214]. Likewise, in humans, studies on specific extracellular RNA show they are modulated in sepsis patients, and are correlated with survival [215]. It appears that miR-150, miR-146a, and miR-223 are downregulated in patients with poorer outcomes, while miR-15/16 and miR-122 are overexpressed in those patients. It remains unclear if these

correlations are driving poor outcomes or merely markers for them. However, there is some evidence for the mechanisms of these miRNAs. For example, miR-223 has been shown to downregulate ICAM-1 (a surface molecule responsible for leukocyte adhesion and infiltration) and other targets in endothelial cells [216]. Similarly, miR-146a has been shown to known to target IRAK-1 (a signaling molecule for multiple TLRs) and regulate innate immune function [217], while other studies show a pro-inflammatory character. While the full mechanisms of extracellular RNA in the context of sepsis are still unknown, it is clear that the lack of homeostasis in sepsis extends to extracellular miRNA.

Alternative miRNA delivery approaches[2]

While RNA is trafficked within viruses and EVs, most naturally occurring RNA transport is protein-associated or protein-mediated. Key players include apolipoprotein A-1 (ApoA1) – which constitutes the primary protein component of high-density lipoprotein (HDL) – as well as Ago2, retroviral capsids such as activity-regulated cytoskeleton-associated protein (Arc), and possibly others (Figure 8). Leveraging biological phenomena involving proteins has already proven to be a successful formula for therapeutic development as evidenced by the clinical success of monoclonal antibodies and insulin analogs, among many others. Thus, protein-based RNAi delivery offers a biomimetic strategy with the potential to overcome some of the obstacles that hinder synthetic systems for RNAi therapy.

---

2 This section is partly adapted with permission from [409].
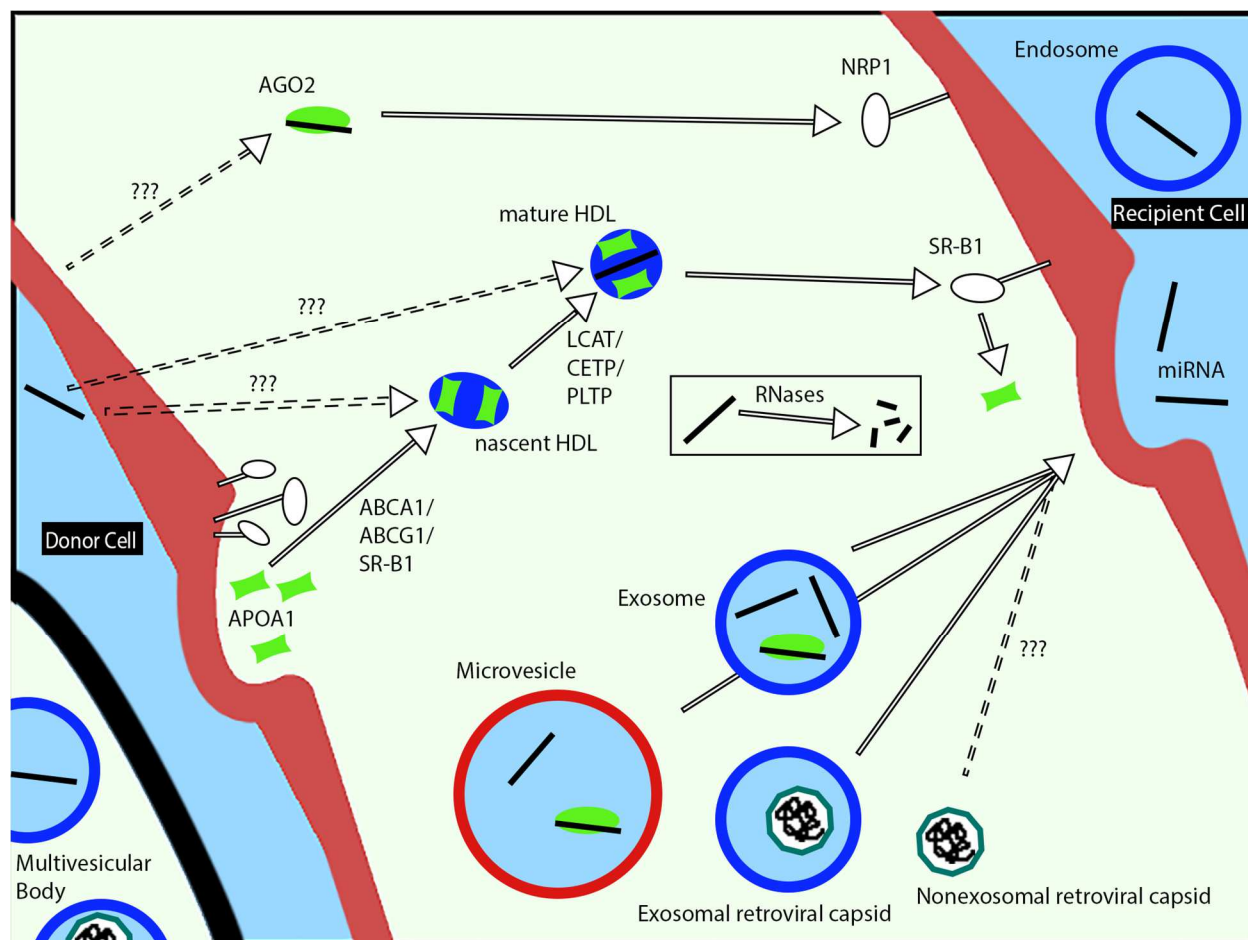
Figure 8. Physiological RNA vehicles, reprinted with permission from [409].

A feature of protein-based therapeutic systems is manipulability, or "engineerability." Many molecular attributes that contribute to optimal pharmacologic efficacy – such as low immunogenicity, avoidance of renal and other forms of clearance, and prevention of opsonization-mediated phagocytosis and degradation – can be incorporated into proteins via straightforward genetic engineering techniques. Protein size, charge, post-translational modification, and binding affinity to both cargo (e.g., RNA) and target moieties can all be manipulated using rational design or directed evolution approaches. For example, conjugation of a therapeutic protein to the Fc domain or albumin-binding domain can markedly extend its half-

life [218]. These same domains, along with a variety of others, could also be appended to increase protein size, an important determinant of molecular pharmacokinetics. Molecules greater than 60 kDa avoid renal clearance, while molecular weight is inversely related to endothelial permeability and tissue penetrance (and smaller molecules are more highly influenced by target binding affinity) [219].

With regard to optimizing RNAi delivery, protein-based vehicles (and all vehicles in general) must accomplish protection of the RNA strand, evasion of clearance, cell/tissue targeting, cell penetration, and RNAi lysosomal escape. Theoretically, this could result in a Rube Goldberg-esque chimera containing a) an RNA-binding domain, b) a tissue-targeting domain, c) an endocytic domain, d) an endosomolytic domain (this is often added as a second agent), e) a half-life enhancing domain, and f) multiple flexible linkers. Unfortunately, any such vehicle would likely have low translational potential due to its complexity. Thus, attempts at engineering protein vehicles for small RNA delivery to date have in most cases focused on more practical approaches, including leveraging biomimicry. Here, we present a summary of the progress in the field, organized by vehicle RNA-binding domain. Beyond what is presented here, the **Appendix** contains further descriptions of protein-based RNA delivery vehicles.

Lipoproteins

High density lipoprotein (HDL) is a heterogeneous, complex circulating particle consisting of mainly phospholipids, cholesterol and proteins, with the primary protein component (>70%) being apolipoprotein A-1 (ApoA1). Much has been described about the role of HDL in cholesterol efflux and its effects on cardiovascular function, but appreciation of the importance

of HDL in extracellular RNA transport is more recent. In 2011, Vickers *et al.* reported that miRNA is found in complex with HDL and showed that the HDL-associated miRNA in healthy and atherosclerotic patients differed. HDL was further found to accept miRNA from macrophage cell line J774 *in vitro*, with subsequent capability to deliver miRNA to hepatoma cell line Huh7 via scavenger receptor class B type 1 (SR-B1) [220]. Wagner *et al.* reported that HDL facilitated transport of low levels (5-10 copies/cell) of miRNAs to endothelial cells *in vitro* [221]. *Tabet et al.* showed that native HDL delivered high levels of miR-223, a downregulator of intercellular adhesion molecule-1 (ICAM-1) mRNA , resulting in ICAM-1 knockdown in endothelial cells *in vitr*o [216]. Additionally, many studies have examined low density lipoprotein (LDL) association with miRNA, with the consensus being that levels of miRNA associated with LDL are much lower than HDL [222]. Meanwhile, a recent study has observed that a significant amount of lipoprotein-RNA is non-host derived [223]. HDL delivers cargo via at least one known receptor, SR-B1, which is widely expressed in macrophages as well as in tissues such as fat, endothelium, intestines, and brain (HDL can cross the blood-brain barrier) [224]. The highest expression occurs in the liver and steroidogenic tissues that utilize cholesterol for bile and hormone synthesis, respectively [225]. Expression is also high in many tumors [226]. SR-B1 binds to HDL and forms a non-aqueous channel between the lipoprotein and the plasma membrane, through which lipophilic molecules can travel bidirectionally (down a concentration gradient) [225]. Therefore, HDL achieves a direct cytoplasmic delivery. Controversially, there have been reports that SR-B1 also mediates HDL endocytosis and resecretion, potentially playing a role in non-lipid delivery. In hepatocytes, HDL is resecreted deplete of cholesterol, while in macrophages, HDL is resecreted replete with cholesterol, indicating that cell type and cholesterol level play a role in HDL function [227]. There are still open questions as to how miRNA is taken

34

up, binds to, and is delivered by HDL, what the true axis of communication is, and the role of non-host organism-derived RNA.

Due to its size, long half-life (5.8 days for ApoA1), anti-inflammatory nature, and low toxicity, HDL has recently received attention as drug delivery vehicle, mainly targeting the liver or tumors [228]–[230]. Additionally, the amphipathic nature of HDL allows for loading of hydrophobic, hydrophilic, or amphipathic molecules. HDL can be isolated from native blood samples (nHDL) or reconstituted *in vitro* with recombinant ApoA1 (rHDL), most commonly with a cholate method [231]. Reconstitution has multiple advantages, such as availability and low risk of contamination, and depending on the lipids used, rHDL can mimic nHDL at any stage of maturity.

Long before the discovery of miRNA-HDL complexes in blood, molecular engineers had experimented with cholesterol-conjugated siRNA and antisense oligonucleotides [232]–[234]. Especially of note is the knockdown of apolipoprotein B (ApoB) in non-human primates via chol-siRNA injection in 2006 by Zimmermann *et al* [235]. In 2007, researchers associated with Alnylam Pharmaceuticals published a wide-ranging study of various lipophilic siRNA conjugates and their relative efficacy in murine hepatic delivery [236]. They showed that the lipophile-siRNAs that preferentially associated with HDL rather than albumin (or remained unbound) were most effective in knocking down the target (ApoB) mRNA in the liver. Strikingly, pre-incubating cholesterol-siRNA (chol-siRNA) with native HDL before injection led to ~2- to 4-fold less plasma ApoB (produced in the liver) when compared to chol-siRNA injected alone. The authors examined the biodistribution of chol-siRNA, with greatest uptake in liver,

kidney, adrenal, and ovary tissues. They also demonstrated that HDL-mediated delivery depends on SR-B1 and, interestingly, lipophilic-siRNA delivery depends on SidT1, a mammalian homologue to the Sid1 transmembrane protein that regulates systemic RNA transport in *C. elegans.* In 2012, another group associated with Alnylam, Nakayama *et al.,* compared the liver delivery of chol-siRNA reconstituted with either recombinant ApoA1 or apolipoprotein E (ApoE) [237]. ApoE primarily binds to the LDL Receptor (LDLR), which may have led to greater liver delivery, and therefore siRNA efficacy, of ApoE-rHDL over ApoA1-rHDL. The authors also saw that adding 4 chol-siRNA molecules for every 1 rHDL (of either type) led to siRNA buildup on the plasma membrane *in vitro,* as opposed to cytoplasmic buildup seen with 1:1 loading. This indicates that there may be a limit to how much siRNA can be loaded using this cholesterol-conjugated method before it interferes with receptor binding. A possible solution to this problem was introduced by Shahzad *et al.*, who applied a different strategy for delivery of non-cholesterol-conjugated siRNA; they loaded anionic siRNA into the core of rHDL by neutralizing with cationic oligolysine peptides [226]. This approach may increase the siRNA loading capacity of rHDL. The group used siRNA against STAT3 and FAK in mouse models of ovarian and colorectal cancer, alone or in combination with chemotherapeutics. Results showed that in three different models, including a resistance model, STAT3-rHDL monotherapy or in combination with docetaxel or oxaliplatin averaged ~72% and ~93% decrease in tumor weight, respectively. Liver function was not impacted and empty rHDL did not affect tumor weight. Additionally, the authors reported that siRNA was distributed evenly to 80% of a given tumor after injection. An analysis by Ding *et al.,* which utilized ApoA1-incorporated liposomes at a diameter of ~90 nm, nevertheless showed that SR-B1-mediated chol-siRNA uptake is similar to cholesteryl ester selective uptake [238]. Alternatively, some groups have utilized ApoA1

mimetic peptides [239]–[241], gold-templated nanoparticles [242], [243] and ApoA1-incorporated liposomes [238], [244]–[247] to deliver siRNA. This review will not cover those strategies in detail.

There have been relevant attempts to further engineer the HDL molecule for enhanced drug delivery. Some groups have sought to enhance targeting capabilities by incorporating targeting moieties to HDL to help direct delivery to the liver [248] or tumor [249]. Some groups have encapsulated various packages within the core, such as super paramagnetic nanoparticles for guided targeting [250], or hydrophobic chemotherapeutics [251]–[253] and Vitamin E [254] for cancer therapy. Any incorporation or encapsulation method may increase the size of the rHDL molecule, which could impact delivery. Additionally, naturally occurring variants of ApoA1, including the Milano and Paris mutants, have been discovered. These variants, R173C and R151C mutants, respectively, perform greater cholesterol efflux due to more transient cholesterol binding [255], [256]. Their behavior in a system of siRNA delivery is currently unknown.

Argonaute 2

Argonaute 2 (Ago2) is the catalytic center of the RNA-induced silencing complex (RISC) that accepts miRNA and siRNA, protects it from degradation, and cleaves complementary mRNA in the cytoplasm. Ago2 has been well-studied within the cell, but in 2011, Arroyo *et al.* and Turchinovich *et al.* reported that a majority of miRNA in circulation was not associated with vesicles, but rather protein – specifically ~100 kDa Ago2 [62], [257]. The distribution of miRNA among the two fractions was uneven, indicating a sorting mechanism. Arroyo *et al.* estimated that potentially 90% of extracellular miRNA were Ago2-bound. A 2016 paper from Prud'homme

et al. identified neuropilin-1 (Nrp1) as a receptor for extracellular Ago2, and demonstrated functionalized delivery in multiple cell lines [258]. Nrp1 is also a receptor for vascular endothelial growth factor (VEGF) and Semaphorin 3, among others, and is expressed widely in endothelial, immune, and many cancer cells, as well as others, including in the developing brain and heart [259], [260]. The results above suggest a major intercellular communication system based on protein-mediated miRNA delivery. This communication system would be privileged; endogenous miRNA must compete for Ago2 loading, but exogenous miRNA would be pre-loaded and ready for mRNA cleavage. However, there are currently more questions surrounding extracellular Ago2 than answers. Ago2 secretion mechanisms are currently unknown, though may be related to one of many binding partners, such as Hsp90 or Hsc70 [261]. It is also unknown if Ago2 has any mechanism for targeting specific tissues.

A 2018 paper from Li *et al.* developed a strategy for delivering Ago2 pre-assembled with a desired siRNA sequence. Briefly, they screened various polyamine polymers to find one that was able to deliver the Ago2-siRNA combination *in vitro*, finding that the polyamine with the most highly dense side chain performed the best. Applying this complex *in vivo*, the authors saw a downregulation of the target and extended survival in a mouse melanoma model. This strategy of encapsulating Ago2 and siRNA within a polyamine polymer is a novel strategy but does not fully exploit the natural delivery capacity of Ago2.

Retroviral capsids

Activity-Regulated Cytoskeleton-Associated protein (Arc) is a major regulator involved in synaptic plasticity and maturation, learning, and memory [262]. Arc is an early immediate

neuronal gene that regulates synaptic plasticity through AMPA receptors, which are involved in rapid synaptic transmission. Arc mRNA moves to the dendritic spines where it is locally translated and begins engaging with the endocytic machinery to regulate the AMPA receptors [263]. Regulation of Arc expression is essential for normal cognition and long-term memory storage. Abnormal Arc expression has been implicated in various neurological and neurodevelopmental disorders such as Alzheimer's disease, Angelman syndrome, Fragile X syndrome, and schizophrenia [262]. Previous studies have noted the similarity between viral proteins and Arc, as it is composed of structural elements also found in Group-specific antigen (Gag) polyproteins encoded in retroviruses and retrotransposons, including human immunodeficiency virus type 1 (HIV-1) [264].

In 2018, Pastuzyn *et al.* and Ashley *et al.* reported a novel mechanism by which genetic information (mRNA) is transferred between neurons via Arc [264], [265]. Arc encapsulates mRNA into viral-like capsids for delivery to neighboring neurons within EVs. When purified in bacterial systems, Arc spontaneously self assembles into oligomeric structures with biochemical properties similar to Gag proteins. Arc capsids are double-shelled structures measuring 32 nm in diameter and are capable of binding RNA nonspecifically, which was found to be a requisite for normal capsid formation. It is hypothesized that Arc is co-expressed with, and encapsulates and delivers, Arc mRNA, which may constitute a positive feedback system of Arc expression. Arc proteins are secreted within EVs, the uptake of which is thought to be dictated by targeting moieties on the lipid surface while the capsid itself protects and transfers the mRNA. It was also shown that Arc capsids delivered functional mRNA even without EV encapsulation [264].

Segel *et al.* in 2021 demonstrated the power of harnessing retroviral intercellular communication for therapeutic delivery [266]. Their team discovered that among potential retroviral *gag* genes, the PEG10 protein forms capsids that are secreted within extracellular vesicles and preferentially export PEG10 mRNA. This preferential loading is mediated primarily by the PEG10 UTR sequences, which, when added to a desired mRNA sequence, leads specific secretion of that mRNA. Segel *et al.* used this knowledge to package spCas9 mRNA into EVs for delivery of CRISPR machinery for gene editing in recipient cells. Further developments of this technology are likely to yield new avenues for biomimetic long RNA delivery.

Outlook for EV-based small RNA therapeutics

There are currently around 35 active clinical trials for siRNA, including three miRNA mimics, and three FDA-approved siRNA drugs [267]. There is also currently around 20 active clinical trials for EVs [92]. Among all of these trials, there are two that are small RNAs loaded into EVs: miR-124 mimic electroporated into MSC-derived EVs for ischemic stroke treatment (at Isfahan University), and anti-KRAS siRNA electroporated into MSC-derived EVs for metastatic pancreatic cancer (at the MD Anderson Cancer Center in Houston). Additionally, there are numerous trials using extracellular vesicles for treatment of Covid-19, indicating a high level of confidence in EV therapies [268]. For EV-based small RNA therapies to truly fulfill their potential in the clinic, many technical challenges need to be overcome, including standardization, manufacturing, cargo loading, delivery, and others. In the following chapters, we will focus on cargo loading and manufacturing.

Chapter 3: Quantification of endogenous miRNA loading into EVs[3]

Introduction

Techniques for loading cargo into EVs broadly fall into two categories: exogenous loading, loading the EVs after isolation from the parental cell, or endogenous loading, transfecting the parental cell and allowing cell machinery to load the EVs. Exogenous loading techniques, such as simple co-incubation [95], sonication [107], pH-loading [114], electroporation [2], and use of chemically-modified RNA [104], [105] or chemical-mediated EV transfection [112], among others, are common. Using these techniques, researchers can achieve high loading concentrations, sometimes reaching to thousands of copies per EV [105], [107], [112]. However, manipulating the EVs directly can damage their superstructure, degrade proteins, cause aggregation, require RNA chemical modifications, and inhibit function, and throughput is generally low, meaning that manufacturing at scale can be slow, laborious, and costly.

Endogenous loading, on the other hand, does not require any EV manipulation after secretion or RNA chemical modifications, allows for high-throughput cellular transfection, and guarantees intravesicular loading. These characteristics are desirable yet ultimately meaningless unless endogenous techniques can provide high loading efficiency. In this aim, we examine the absolute EV loading efficiency of two common miRNA transfection techniques: cellular cationic transfection and cellular electroporation.

---

3 **A. E. Pottash**, L. Kuo, D. Levy, S. M. Jay, "Comparison of endogenous loading methods for small RNA loading into extracellular vesicles," In preparation.

Electroporation is a physical process in which an electric field applied to cells causes a temporary rupture in the cellular membrane through which molecules can enter the cytoplasm. This technique is well-established for the introduction of plasmid DNA and small RNA and has also been previously applied towards miRNA loading into EVs. Electroporation of nucleic acids directly into EVs, although still commonly employed, has been largely discredited by our lab and others as a loading technique due to RNA aggregate formation, in addition to low loading efficiency [107], [109], [110]. To our knowledge, there are two papers that employed endogenous loading using electroporation [123], [124]. Wang *et al.* saw a 315-fold relative increase in miR-101 content in EVs and quantified the absolute concentration to be about 10pg miR-101 per 1μg MSC EVs [123].

Cationic lipids or polymers bind with anionic nucleic acids, mediate entry into the cell, and may assist with endosomal escape into the cytoplasm. This also a well-established method for small RNA transfection, with many commercially available reagents that may differ in formulation and effective concentrations. This strategy for loading miRNA into EVs has been used in a number of publications [269]–[274].

In this chapter we will examine these two endogenous loading techniques, first by optimizing their transfection in order to distinguish relevant design parameters, then by determining the maximum possible loading conditions. Finally, we determine the loaded concentration at this maximum loading condition and compare between the two techniques.

Methods

<u>Cell culture</u>

Human embryonic kidney HEK293T cells were cultured in Dulbecco's modified Eagle's medium (DMEM) (Corning 10-013-CV; Corning, NY, USA) supplemented with 10% fetal bovine serum (FBS) and 1% penicillin/streptomycin in T175 tissue culture polystyrene flasks. For EV collection, normal FBS was replaced by EV-depleted FBS. FBS was EV-depleted via 100,000 x g centrifugation at 4°C for 16 h where the supernatant was retained.

<u>Extracellular vesicle isolation</u>

Conditioned media was collected and subjected to differential centrifugation. Briefly, the supernatant was centrifuged at 1,000 x g for 10 min, 2,000 x g for 20 min, 10,000 x g for 30 min, for each of which the supernatant was retained, and finally, 100,000 x g for 2 h, after which the pellet was resuspended in phosphate-buffered saline (PBS) and collected. This resuspension was washed 2x using Nanosep 300-kDa MWCO spin columns (OD300C35; Pall, Port Washington, NY, USA). The washed EVs were resuspended in PBS and filtered using an 0.2-μm syringe filter. EV size distribution and concentration were determined by nanoparticle tracking analysis (NTA) via a NanoSight LM10. Each sample was analyzed in triplicate using consistent acquisition settings. Total EV protein was determined via bicinchoninic acid assay (BCA) following manufacturer's protocol. Relative levels of relevant protein components were determined via western blotting. Alix (ab186429; Abcam, Cambridge, MA, USA), TSG101 (ab125011; Abcam), GAPDH (2118L; Cell Signaling Technology) and CD63 (25682-1-AP; Thermo Fisher). Primary antibodies were added at a 1:1000 dilution, except for GAPDH

(1:2000). Secondary antibody IRDye 800CW anti-Mouse and anti-Rabbit (926-32210 and 926-32211; LI-COR Biosciences, Lincoln, NE, USA) were added at 1:10000 dilution, and membranes were imaged on a LI-COR Odyssey CLX Imager.

Cellular cationic transfection

HEK293T were seeded at 1.75 million cells in a T75 tissue culture polystyrene flask. The next day, cells were treated with miR-146a mimic (Dharmacon) transfection reagent prepared according to manufacturer's instruction immediately before addition to cells. 18 h later, the cell media was removed, and cells were washed 10x with PBS supplemented with calcium chloride and magnesium chloride. Two days later, cell media was collected for EV isolation and cell lysate for RNA isolation and analysis. The reagents utilized were HiPerfect (Qiagen), RNAiMAX (Thermo Fisher), X-tremeGENE (Sigma-Aldrich), and branched polyethylenimine (PEI) (Sigma-Aldrich; 408727). For PEI transfection, the protocol of Wirth *et al.* was followed [275]. For comparison of transfection reagents, 200 pmol of RNA was used for a final concentration of 13.3 nM RNA.

Cellular electroporation

HEK293T were trypsinized and passed through a cell strainer to achieve single-cell suspension. Cells were resuspended in electroporation buffer at 5 million cells/mL (final concentration) and mixed with desired amount of miRNA mimic. These mixtures were electroporated in 100 μL aliquots, before being diluted in 900 μL of growth media and spun down. After a second wash and spin, 1.5 million cells were seeded in a T75 tissue culture polystyrene flask. The next day,

cells were washed 1x with PBS. Two days later, cell media was collected for EV isolation and cell lysate for RNA isolation and analysis. For comparison of electroporation protocols, 250 nM of RNA was used. Electroporation was tested using three different protocols and two different buffers. Program "1" refers to the Q-001 protocol on Nucleofector 2b Device (Lonza) using Ingenio Cuvettes (Mirus Bio). Program "2" refers to the A-023 protocol on the same device. Program "3" refers to the HEK293T pre-set protocol on the Gene Pulser Xcell Electroporation System (Bio-rad) using Gene Pulser Cuvettes (Bio-rad). Program "A" refers to Opti-mem buffer (Thermo Fisher) and Program "B" refers to Ingenio Electroporation Solution (Mirus Bio).

Cell viability assay

Cell viability was determined via the XTT Cell Viability Kit (Cell Signaling #9095) according to manufacturer's instruction.

RT-PCR

EVs were resuspended in 700 µL Qiazol spiked with 2 fmol cel-miR-39 (Norgen Biotek) per sample. RNA was isolated using miRNeasy Kit (Qiagen) and complementary RNA (cDNA) was produced using miScript RT II Kit (Qiagen) using the same amount of starting RNA according to manufacturer's protocol. 2 µL cDNA product along with primers and water was added to Ssoadvanced Universal SYBR Green Supermix (Biorad) according to manufacturer's protocol. A QuantStudio 7 Flex qPCR System was used to detect the signal from each well. The reaction cycle consisted of 98C (1 min), and 40 cycles of 98°C (10 s) and 60°C (20 s)**.** The primers used were miR-146a fwd: (5'-GAGAACTGAATTACATGGGT-3'), miR-146a rev: (5'-CAGGTCCAGTTTTTTTTTTTTTTT-3'), cel-miR-39 fwd: (5'-

GTCACCGGGTGTAAATCAG-3'), cel-miR-39 rev: (5'-

GGTCCAGTTTTTTTTTTTTTTTTCAAG-3'), actin fwd: (5'-

ACTTAGTTGCGTTACACCCTT-3'), actin rev: (5'- GTCACCTTCACCGTTCCA-3'). As an

RNA standard for absolute quantification, 40 pmol miR-146a-5p miRNA mimic was reverse

transcribed including spike-in, and serially diluted 10-fold six times.

Aggregation

RNA aggregation was assessed by electroporating miRNA mimic spinning the sample in a

Nanosep 300-kDa MWCO spin column and washing 2x with PBS. The retentate was then

resuspended in PBS and quantified for RNA content using Quant-it microRNA Assay Kit

(Thermo Fisher; Q32882) and the included standard.

Statistical analysis

Data are presented as mean ± SD, except for SEM (standard error of the mean) where noted.

One-way ANOVAs with Dunnett's multiple comparison test were used to determine statistical

significance ($p < 0.05$) in RT-PCR experiments and plasmid/reporter fluorescence experiments.

All statistical analysis was performed with Prism 8 (GraphPad Software, La Jolla, CA). Notation

for significance in figures were as follows: ns = $p > 0.05$, * = $p \leq 0.05$; ** = $p \leq 0.01$; *** = $p \leq$

0.001; **** = $p \leq 0.0001$.

Results

Optimization of cellular electroporation for EV loading

Cellular electroporation protocols typically vary in parameters such as wave form, field strength, pulse length, etc. Three protocols previously optimized for the HEK293T cell line were tested, using two buffers commonly used for electroporation. To differentiate between these programs, cells were electroporated in the presence of 250 nM miR-146a mimic and after three days examined the cellular RNA content via RT-PCR (Fig. 9a). Some programs resulted in large increases in cellular RNA, but not others. Additionally, EVs collected from these cells had undetectable levels of RNA. Previous work has shown that when electroporated in cuvettes with metal electrodes, RNA can aggregate into large insoluble particles [109], [276]. Therefore, we tested for aggregation by electroporating the RNA without any cells present (Fig. 9b). Interestingly, the same groups that had high levels of cellular miR-146a also had some degree of aggregation, implicating that the increase in cellular RNA was due to RNA aggregation. The undetectable levels of EV-associated RNA indicated that aggregates were likely not co-isolating during the EV isolation process; this was previously noted by Kooijmans *et al.* [109]. It is difficult to assess the variable effect of the electroporation program on cellular RNA, since the Nucleofector 2b Device parameters and Ingenio Electroporation Solution composition are proprietary information.

To prevent RNA aggregation, the chelator EDTA was employed to sequester metal ions during electroporation. RNA aggregation was measured as a function of EDTA concentration for two protocols, (Program B2 and Program B3) (Fig. 9c). Aggregation was inhibited in dose-dependent fashion for Program B2, with complete inhibition at 5 mM EDTA. Thus, we tested

A Cellular miR-146a after electroporation

B Aggregation after electroporation

C EDTA effect on miRNA aggregation

D EDTA effect on cell viability
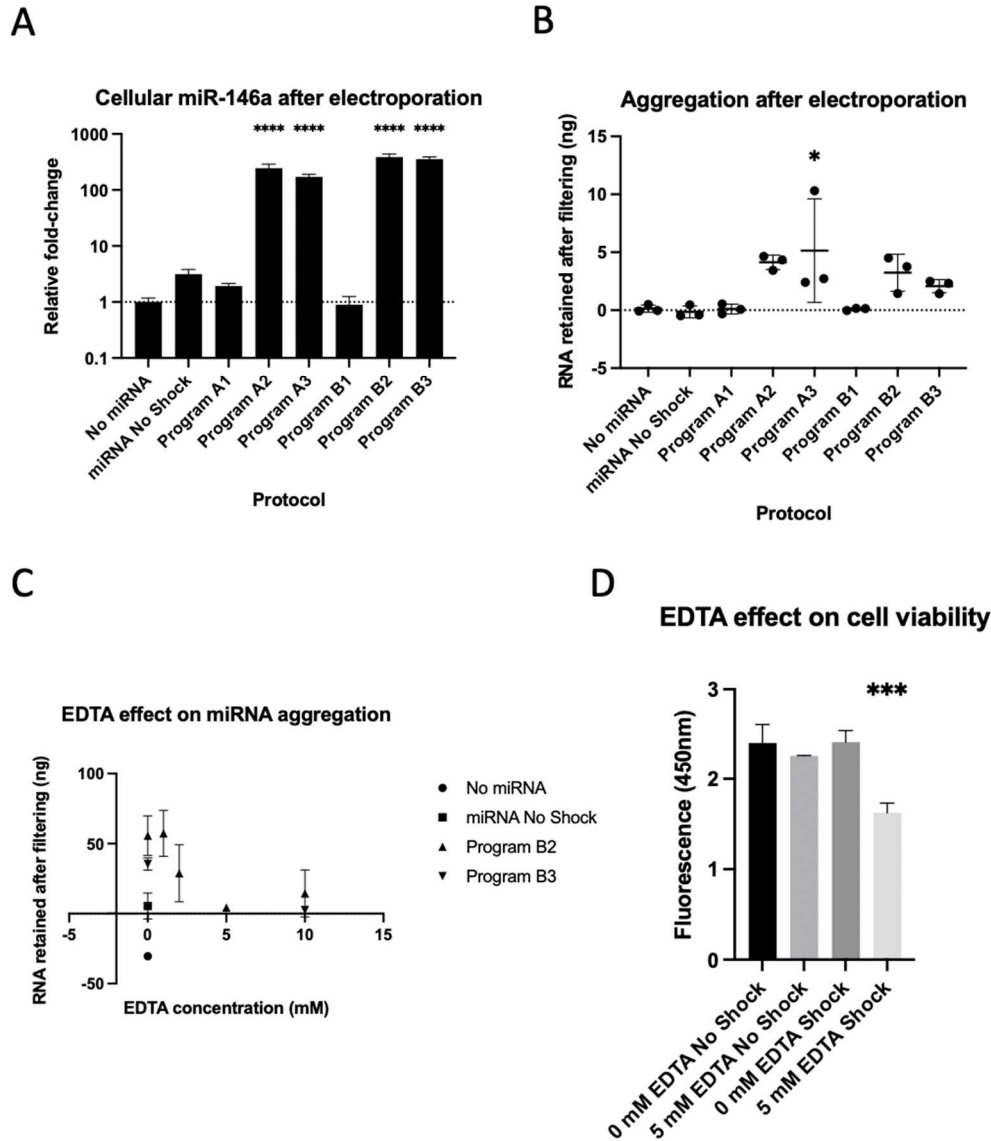
Figure 9. Aggregation of RNA during electroporation. (A) Relative fold-change of miR-146a in cells electroporated with the indicated protocol as measured by RT-PCR. (B) RNA aggregation as measured by RNA retention during filtration after electroporation with the indicated protocol. (C) RNA aggregation after electroporation over a range of EDTA concentrations. (D) Cell viability after electroporation measured via XTT assay. (ns = $p > 0.05$, * = $p \le 0.05$; ** = $p \le 0.01$; *** = $p \le 0.001$; **** = $p \le 0.0001$).

electroporation in cells using Program B2 supplemented with 5 mM EDTA. Unfortunately,

however, EDTA caused a decrease in cell viability (Fig. 9d). Given these results, we decided to

continue without EDTA with the risk of RNA aggregates in cells.

Quantification of EV-associated RNA from electroporation

To determine the maximum loading capability of electroporation, we executed a dose curve for electroporation up to and including the max tolerable dose, which was previously determined to be 10 mM (data not shown). NTA data showed a similar size distribution between the different electroporating doses (Fig. 10a). The cellular RNA rose with electroporation dose, but reach a plateau after 4 mM, with only a slight increase between 4 mM and 10 mM (Fig. 10b). At the 4 mM electroporation dose, miR-146a was loaded into EVs at 1.302 (SEM = 0.520) copies/EV (Fig. 10c).
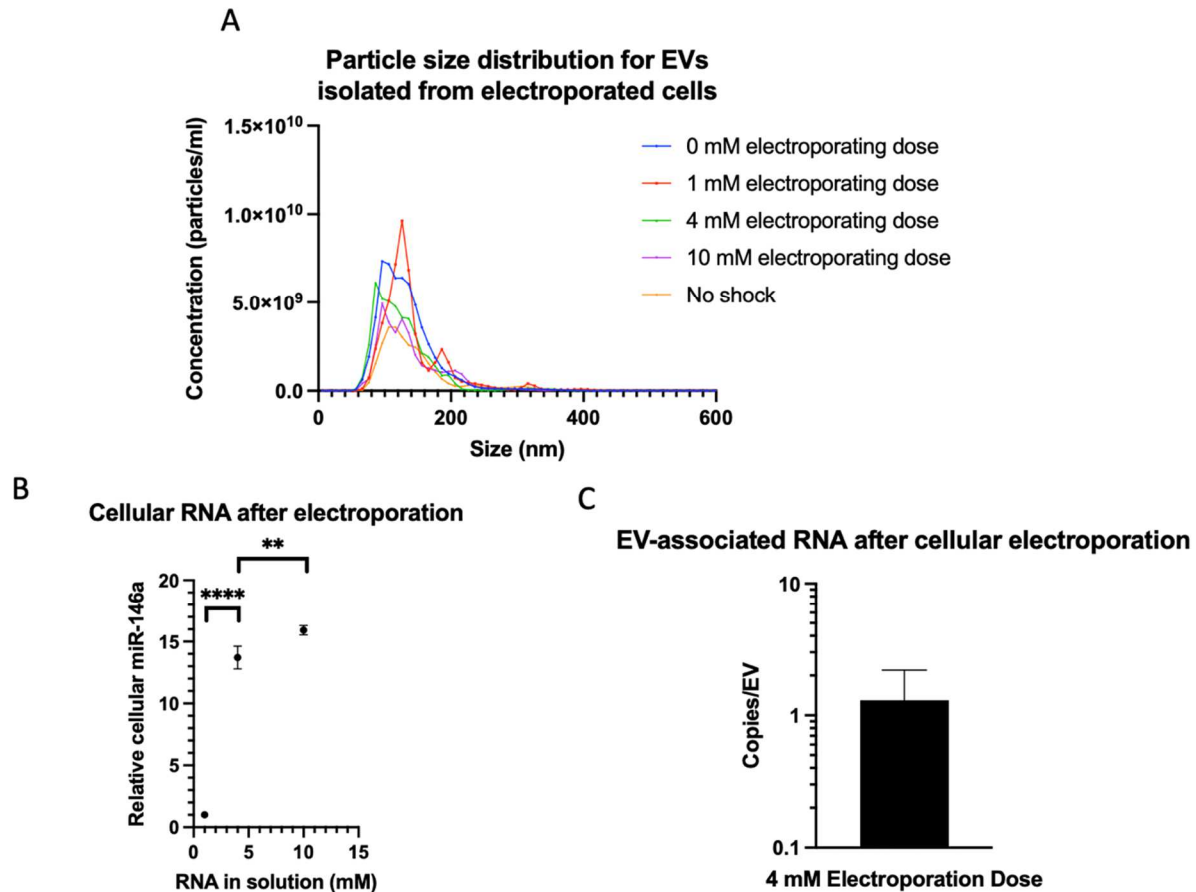
Figure 10. miR-146a loading into EVs using electroporation. (A) EV particle count and size distribution after cellular electroporation as measured by NTA. (B) Relative cellular miR-146a content after electroporation at a range of doses as measured by RT-PCR. (C) miR-146a copies per EV as measured by RT-PCR and NTA. (ns = p > 0.05, * = p ≤ 0.05; ** = p ≤ 0.01; *** = p ≤ 0.001; **** = p ≤ 0.0001).

Comparison of cationic transfection reagent for EV loading

To develop a working protocol for the enrichment of miR-146a in cells for subsequent re-packaging into EVs, four different cationic transfection reagents were compared. Reagent formulation differences may impact both RNA transfection efficiency and the fate of transfected molecules. To differentiate between the four reagents, the maximum dose of miR-146a mimic (Dharmacon) that HEK293T cells could tolerate before experiencing toxicity was determined for each reagent via XTT assay (Fig. 11a). The results indicated that some reagents were more toxic than others and allowed for much higher RNA doses during transfection. Next, cells were transfected at the max tolerable dose with Cy3-tagged miR-93 (Dharmacon) to determine the appropriate length of time to transfect our cells before EV collection (Fig. 11b). For all reagents, the fluorescent signal peaked at 18 hours, before declining slightly at 24 hours. This decline is possibly attributable to cellular digestion of the fluorescent tag. In terms of total fluorescence, X-tremeGENE had the highest signal, but when the fluorescent signal is normalized by dose added, RNAiMAX exceeds the others. Finally, cells were transfected with miR-146a with each reagent for 18 h, and two days later EVs were collected. Nanoparticle tracking analysis (NTA) was performed on the isolated EV sample to determine particle count. RT-PCR performed on collected EVs showed a highest amount of EV-associated RNA in the RNAiMAX and HiPerfect groups, respectively (Fig. 11c). The X-tremeGENE and PEI groups, along with the negative control groups, were not determined, due to the low sensitivity of the assay. Moving forward, we continued with HiPerfect since the max tolerable dose was greater in that group.
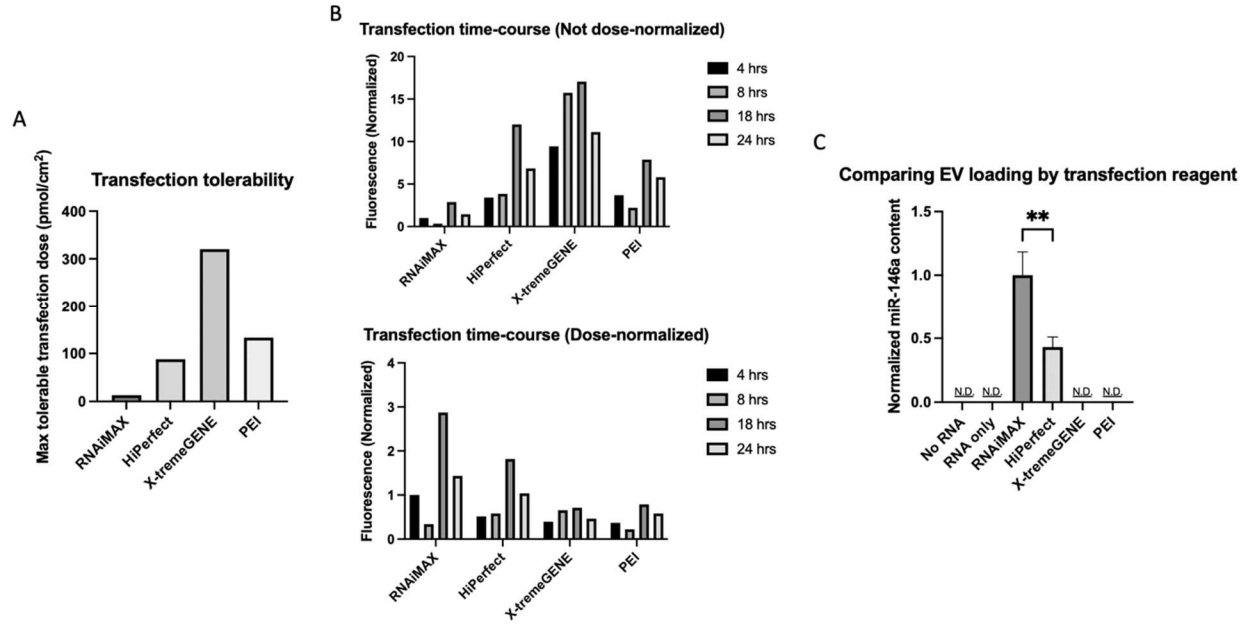
Figure 11. Optimization of cationic transfection protocol. (A) Maximum transfection dose before cell growth was inhibited for variable transfection reagents as measured by XTT assay. (B) Time course of transfection for variable transfection reagents using fluorescently tagged RNA. (C) EV-associated miR-146a after transfection with variable transfection reagents as measured by RT-PCR (N.D. = Not Detected). (ns = p > 0.05, * = p ≤ 0.05; ** = p ≤ 0.01; *** = p ≤ 0.001; **** = p ≤ 0.0001).

Quantification of EV-associated RNA from cationic transfection

To determine the maximum loading capability of cationic transfection, a dose curve for

RNA/HiPerfect up to and including the max tolerable dose was performed. NTA data from these

EVs showed a significant increase in mean particle size the highest transfecting dose (mean size

= 218.0 ±9.3 nm) compared to other doses, including nontransfection EVs (mean size = 163.5

±8.3 nm), due to a large EV population at ~300 nm (Fig. 12a). Cellular miR-146a increased

linearly (R^2=0.952) with the transfecting dose, indicating a non-saturation even at the highest

dose (Fig. 12b). On the contrary, EV-associated RNA followed an exponential growth curve in

relation to transfecting dose (R^2=0.999) (Fig. 12c). At the max tolerable dose, miR-146a was

loaded into EVs at 1.043 (SEM = 0.277) copies/EV. Additionally, to control for the possibility

that reagent-associated miR-146a was being retained in the cell media and co-isolating during

51

the EV isolation process, the protocol was performed without any cells at the highest dose,

finding a low but detectable number of particles and nonnegligible amount of miR-146a, at 0.078

(SEM = 0.023) copies/EV. After adjusting for particle count, reagent-associated miR-146a

accounted for 4.3% of the final EV-associated miR-146a concentration.
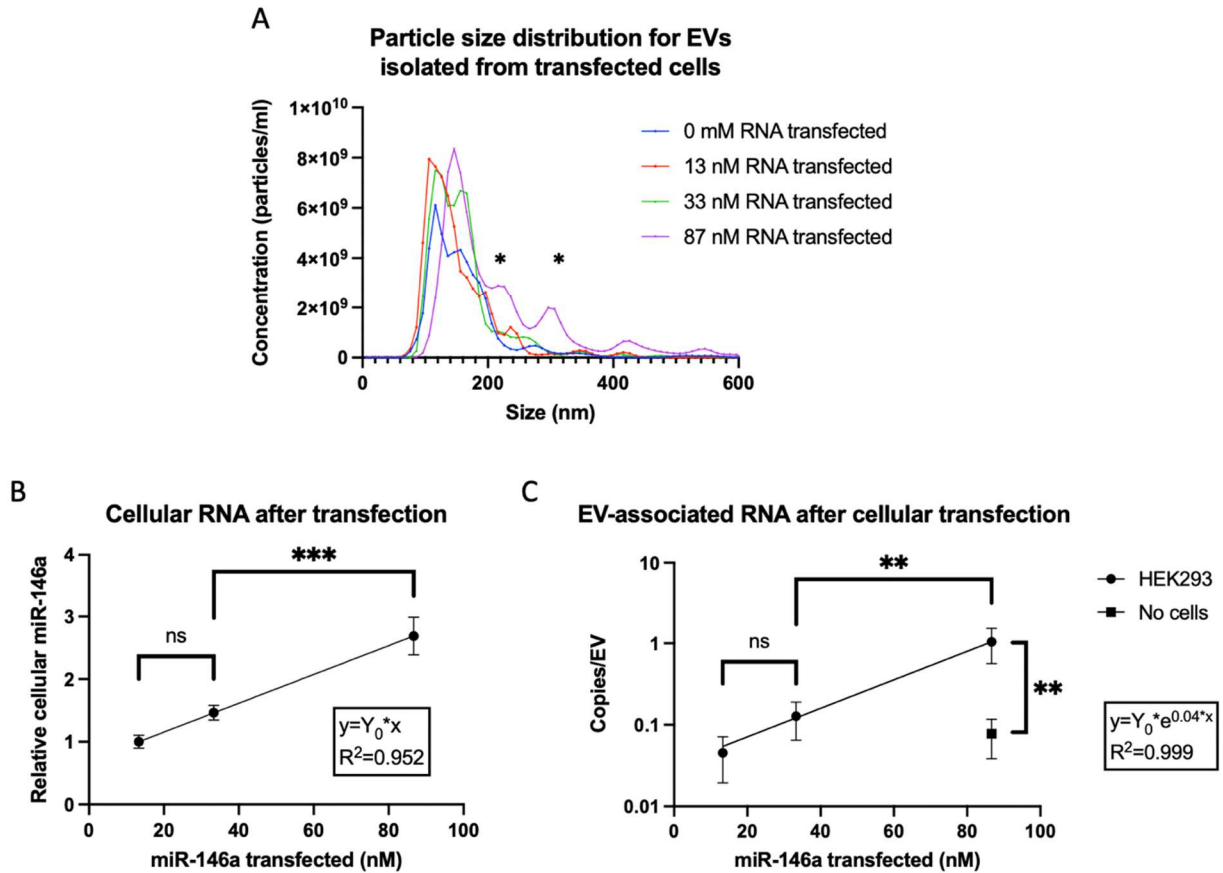
Figure 12. miR-146a loading into EVs using cationic transfection. (A) EV particle count and size distribution after cationic transfection as measured by NTA. (B) Relative cellular miR-146a content after cationic transfection at a range of doses as measured by RT-PCR. (C) miR-146a copies per EV as measured by RT-PCR and NTA. (ns = p > 0.05, * = p ≤ 0.05; ** = p ≤ 0.01; *** = p ≤ 0.001; **** = p ≤ 0.0001).

Discussion

Our lab has previously studied exogenous strategies for unlabeled miRNA loading into EVs, including sonication-mediated, electroporation-mediated, and pH-mediated methods. Here, we examine basic endogenous strategies for RNA loading, using both cationic-mediated transfection and electroporation. Both strategies were successful in enriching miR-146a within EVs to a considerable degree, while each also presented technical difficulties that may compromise the quality of the final product and require further problem solving. Unfortunately, in this study, due to their proprietary nature, we were unable to assess the impact of specific electroporation parameters or chemical compositions on cellular or EV enrichment.

In our electroporation studies, we screened a limited set of electroporation programs and saw enrichment in the cell. However, we also detected siRNA aggregation. Despite our attempts to prevent aggregation, we could not do so without causing cellular toxicity. Given that siRNA aggregates have not been found to co-isolate with EVs [109], we proceeded to apply our optimized protocol to cellular loading. We saw a large increase in cellular miR-146a at 4 mM transfecting dose, but none further at 10 mM, indicating saturation. Using 4 mM transfecting dose, the maximum loading efficiency for this strategy that we achieved was 1.302 (SEM = 0.520) copies/EV. This is a high enrichment of the desired sequence into EVs; however, concerns linger about siRNA aggregation and their impact on cellular function and final EV quality.

Electroporation of siRNA into cells has long been used for inducing target knockdown, especially into cell lines refractory to other forms of transfection [116]. In studies of DNA electroporation, aggregation is important for the uptake and delivery of long DNA; approximately 75% of delivered DNA is taken up through endocytosis [117], [118]. siRNA, due to their smaller size, enter the cell passively through pores in the membrane during the electroporation step and have direct access to the cytoplasm [119]. Studies have also examined the diffusion of DNAs in the cytoplasm after electroporation and seen that diffusion of small DNA is mostly unhindered by actin or other cell components [120]–[122]. However, siRNA aggregation has not specifically been studied in the context of cellular electroporation. Three outcomes are possible: (1) siRNA aggregation is negligible in this context; (2) siRNA aggregation enhances endocytosis by the cell and a portion of the RNA is incorporated into extracellular vesicles; (3) siRNA aggregates interfere with cellular function. While siRNA aggregates are thought to successfully inhibit their target mRNA in recipient cells, it is necessary to follow up to see the fate of aggregated RNA. Other technical solutions may be required to prevent aggregation fully.

In our optimization of cationic transfection for EV loading, we saw a mixed outcome for transfection reagents loading EVs. At the same RNA dose, RNAiMAX and HiPerfect led to enrichment in the EV fraction, while X-tremeGENE and PEI did not. Due to the proprietary nature of the reagent composition, it is impossible to speculate why there was a divergence in EV enrichment. The reagents were not tested for knockdown ability, so we cannot speculate about endocytic pathway or secretion vs. RNAi pathway preferences. We continued with HiPerfect since the max tolerable dose was ~6.5x greater than RNAiMAX.

At the highest cationic transfecting dose, we achieved 1.043 (SEM = 0.277) copies/EV. However, we also recovered miR-146a in negative control group conducted without any cells present. After adjusting for particle count, reagent-associated miR-146a accounted for 4.3% of final miR-146a content in the group with cells present. This result, obtained after washing ten times, indicates a contamination of final EV product with transfection material in the form of transfection reagent that is carried over in the extracellular media. For this reason, a further examination of potential transfection reagents for reagents that do not co-isolate with EVs is essential. Additionally, forms of contamination that are not as easily detected, such as incorporation of reagent chemicals like lipids into the final EV product need to be analyzed for presence and effect on downstream function. The appearance of a large particle population at ~300 nm in the highest transfecting dose, indicates that some contamination from the reagent may be leading to larger EVs.

Within the range of transfecting doses we applied, cellular miR-146a increased linearly (R^2=0.952) with the transfecting dose and did not saturate even at the max tolerable dose. On the other hand, EV-associated miR-146a increased exponentially (R^2=0.999) with transfecting dose. This result echoes that of Squadrito *et al.*, who observed a similar relationship between miRNA expression levels and secretion [60]. This relationship indicates that optimization of cell transfection is incredibly important, as transfection efficiency grants accelerating returns. The source of transfection toxicity is unknown, but relevant if trying to maximize cellular RNA levels. If the reagent is the source of toxicity, then a less toxic transfection reagent may allow for greater loading. If the RNA itself is the source of toxicity, other solutions need to be pursued,

including engineering the cell or making changes to the RNA secondary structure to discourage toxicity or interaction with cellular RNA machinery.

Both endogenous strategies yielded results in the range of one copy per EV, spurring us to speculate whether this is near the limit for endogenous loading strategies. Some estimates say that the total concentration of all miRNAs in EVs is approximately one copy per EV (depending on the EV source; less in HEK293T-derived EVs), and much less for individual sequences [5], [84], [110]. These estimates are controversial, as mentioned in Chapter 2, and comparing our results to those depends on factors like EV isolation method and quantification scheme.

Additionally, transfection delivers supraphysiological levels of RNA. Jin *et al.* found that their cationic transfection (using the DharmaFECT 1 reagent) with 100 nM miRNA mimic led to 1-2 million copies per HeLa cell, dwarfing the estimated 100,000 copies of mature miRNA per cell by a factor of ten [277]. Given that the cytoplasmic concentration of a given miRNA generally dictates its EV concentration, it is thus likely that our transfected RNA comprises the vast majority of extracellular RNA. It is also to be expected that at these drastic levels the transfected RNA is saturating miRNA-related cellular processes. Therefore, given the inherent limitations of cellular production, we hypothesize that one copy per EV may be approaching the limit of endogenous loading.

This value is lower than reported for exogenous loading techniques, which can reach into the thousands of miRNA per EV [105], [107], [112]. While raw copy number of EV-associated miRNAs may not correlate completely with intravesicular quantity or functional delivery, this

gap is considerable. Interestingly, Reshke *et al.* find that by overexpressing a desired siRNA

sequence within a pre-miR-451 secondary structure, they enrich the sequence to one copy per

EV [4]. Other works have shown that including a sequence motif within the RNA strand or

overexpressing an RNA-binding protein may lead to preferential loading into EVs [278]. These

approaches and others could be combined with transfection-based strategies to further enhance

efficiency of RNA secretion within EVs and inhibit off-target effects.

Conclusion

For endogenous loading, manipulating parental cells can lead to unintended changes in the cell

that may impact the final EV product. This can occur through introduction of incidental

byproducts of transfection, like reagent or aggregated RNA, or through off-target effects via the

RNAi machinery of the cell (though the latter may in fact enhance the therapeutic product or be

the primary component of it). In this aim, we examined the loading efficiency of endogenous

loading techniques and saw a similar result of approximately one copy per EV.

Chapter 4: Development of a DNA overexpression system for endogenous miRNA loading[4]

Introduction

RNA secretion within extracellular vesicles is a topic with great relevance to RNA biology and therapeutic development. microRNAs make up a significant fraction of RNA in EVs, and much research has been devoted to understanding the mechanism of secretion, which has become controversial [79]. Many publications have demonstrated that EV-associated miRNAs are not merely representative of cellular miRNA, leading some to argue that a sorting process is selectively loading certain miRNA species over others, involving sequence-dependent RNA-binding proteins [60], [66]–[72]. Thus, some previous attempts to improve secretion of desired small RNA have added short motifs to the mature RNA sequence, achieving modest increases in secretion [68], [72], [73]. Others are skeptical of this view, arguing that other factors, including differential RNA stability, subcellular localization, random stochasticity, and the "law of small numbers" cause a nonselective loading regime [51], [77]–[80]. Regardless, it has been shown that alteration of the cellular miRNA profile leads to changes in the EV profile, and overexpression of a specific miRNA in the cell will lead to increased abundance in the EV fraction [60].

In the canonical miRNA biogenesis pathway, primary miRNAs (pri-miRNAs) are transcribed by RNA Polymerase II (Pol II) and cleaved at the base of a hairpin structure by Drosha to become hairpin-shaped precursor miRNAs (pre-miRNAs) that typically range from 50-70 nucleotides

---

4 **A. E. Pottash**, E. Powsner, L. Kuo, D. Levy, S. M. Jay, "Manipulation of microRNA genesis pathway leads to enhanced extracellular vesicle loading," In preparation.

long. This pre-miRNA is shuttled from the nucleus to the cytoplasm by Exportin-5. In the cytoplasm, Dicer cleaves off the pre-miRNA hairpin to produce a miRNA duplex similar to siRNA. One strand of the miRNA duplex is preferentially loaded into Argonaute-2 (Ago2). From here, the mature miRNA is capable of guiding Ago2-mediated cleavage and degradation of complementary RNA targets. Natural variations on the biogenesis pathway include intronic miRNAs that bypass Drosha, such as miR-15b and miR-126, and short complementary miRNAs that bypass Dicer, of which miR-451 is the only currently known example.

Due to its short length, pre-miR-451 evades Dicer, but rather is loaded directly into Ago2 where it undergoes 3' trimming to become a mature miR-451 [26]–[30]. Recent work by Reshke *et al.* has demonstrated that miR-451 is preferentially secreted by cells into EVs. Replacing the mature miR-451 sequence with a desired sequence against SOD1 or green fluorescent protein (GFP) led to massive enrichment in EVs (to 1 copy/EV in some cases), implying that enhanced secretion it is independent of the mature miR-451 sequence, but rather dependent on the unique structure of the pre-miR-451, which determines how it interacts with members of the miRNA biogenesis pathway [4]. Additionally, there have been reports that pre-miRNA is enriched over mature miRNA in MSC-derived EVs [81].

In this chapter, we will examine various strategies that may enhance the expression, bioactivity, and secretion of miR-146-5p, by tweaking interactions with miRNA biogenesis proteins. Throughout this process, however, we will not alter the mature sequence of miR-146-5p. Optimization of this process may allow for supremely scalable production of specific miR-loaded EVs, at comparable levels to previous endogenous loading techniques.

Methods

<u>Cell culture</u>

The Dicer-knockout cell line NoDice was a generous gift from the Bryan Cullen lab at Duke University [279]. Human embryonic kidney HEK293T and NoDice cells were cultured in Dulbecco's modified Eagle's medium (DMEM) (Corning 10-013-CV; Corning, NY, USA) supplemented with 10% fetal bovine serum (FBS) and 1% penicillin/streptomycin in T175 tissue culture polystyrene flasks. For EV collection, normal FBS was replaced by EV-depleted FBS. FBS was EV-depleted via 100,000 x g centrifugation at 4°C for 16 h where the supernatant was retained.

<u>Plasmid cloning</u>

pCMV-GFP was a gift from Connie Cepko (Addgene plasmid # 11153; http://n2t.net/addgene:11153 ; RRID:Addgene_11153). U6-scr, U6-pri, U6-pre, U6-pri451, and U6-pre451 oligo sequences were designed based on miRBase sequences and ordered from Twist Biosciences. The scramble sequence (5'-gacgagauauaagcagucuugu-3') was designed using the Invivogen Scramble siRNA tool and was placed into a hsa-miR-15a-derived scaffold. The plasmid was linearized via EcoRI, and the NEBuilder HiFi DNA Assembly Kit (New England Biolabs) was used to insert the oligos upstream of the CMV promoter. In order to remove the CMV enhancer, the plasmids were linearized via SpeI/SnaBI digestion and the NEBuilder HiFi DNA Assembly Kit was used to bridge the ends. In order to insert the HDV sequence, the plasmids were linearized via SpeI/SnaBI digestion and the NEBuilder HiFi DNA Assembly Kit

was used to insert the HDV oligo (Integrated DNA Technologies) downstream of the terminal TT of the miR-146a scaffold. pKmyc-Exp5 was a gift from Ian Macara (Addgene plasmid # 12552 ; http://n2t.net/addgene:12552 ; RRID:Addgene_12552). pKMyc was a gift from Ian Macara (Addgene plasmid # 19400 ; http://n2t.net/addgene:19400 ; RRID:Addgene_19400). LSB-hsa-miR-146a-5p was a gift from Ron Weiss (Addgene plasmid # 103248). LSB-hsa-miR-126-3p was a gift from Ron Weiss (Addgene plasmid # 103192 ; http://n2t.net/addgene:103192 ; RRID:Addgene_103192).

DNA transfection and EV production

For plasmid transfection, cells were seeded in a T75 or T175 at 6666 cells/cm^2. The next day, cells were treated with 83.3ng of plasmid per mL of cell culture media using Lipofectamine 3000 (Thermo Fisher) via manufacturer's instructions. Briefly, for a T75 flask, plasmid (1250 ng) was added to Opti-Mem (91.25 µL) (Thermo Fisher) in a 1.5 mL tube. After vortexing to ensure homogenous composition of plasmid in Opti-Mem, P3000 reagent (2.4 µL) was added, and the solution was vortexed a second time. In another 1.5 mL tube, lipofectamine reagent (5.1 µL) was added to Opti-Mem (91.25 µL). The lipofectamine solution was added to the plasmid/P3000 solution and vigorously pipetted up and down at least 15 times and then left at room temperature for at least 10 min. The lipofectamine solution with the DNA plasmid of interest was then added directly to the 15 mL of media in the flask and the flask was swirled to disperse the reagent. The flask was left to incubate undisturbed for 1 h at 37°C. After 1 h, the media was aspirated from the cells. Fresh media was added, and the next day, media was replaced with EV-depleted media. Media was collected when the cells reached confluency, usually 2 days after transfection. For Exportin-5 co-expression, each plasmid was co-transfected at half the normal dose.

Extracellular vesicle isolation

Conditioned media was collected and subjected to differential centrifugation. Briefly, the supernatant was centrifuged at 1,000 x g for 10 min, 2,000 x g for 20 min, 10,000 x g for 30 min, for each of which the supernatant was retained, and finally, 100,000 x g for 2 h, after which the pellet was resuspended in PBS and collected. This resuspension was washed 2x using Nanosep 300-kDa MWCO spin columns (OD300C35; Pall, Port Washington, NY, USA). The washed EVs were resuspended in PBS and filtered using an 0.2-μm syringe filter. EV size distribution and concentration were determined by nanoparticle tracking analysis (NTA) via a NanoSight LM10. Each sample was analyzed in triplicate using consistent acquisition settings. Total EV protein was determined via bicinchoninic acid assay (BCA) following manufacturer's protocol. Relative levels of relevant protein components were determined via western blotting. Alix (ab186429; Abcam, Cambridge, MA, USA), TSG101 (ab125011; Abcam), GAPDH (2118L; Cell Signaling Technology) and CD63 (25682-1-AP; Thermo Fisher). Primary antibodies were added at a 1:1000 dilution, except for GAPDH (1:2000). Secondary antibody IRDye 800CW anti-Mouse and anti-Rabbit (926-32210 and 926-32211; LI-COR Biosciences, Lincoln, NE, USA) were added at 1:10000 dilution, and membranes were imaged on a LI-COR Odyssey CLX Imager.

miRNA reporter system

miR-146a-5p and miR-126-3p activity was detected using a reporter system developed by Gam *et al* [280]. Briefly, each plasmid expresses two fluorescent proteins: mKate2 (Red), which

contains multiple miRNA complementary sequences in its 3' UTR, and EBFP2 (Blue), which

expresses constitutively as a normalization control. For this assay, HEK293T cells were seeded

in a 96-well black-walled plate at 1,200 cells per well. Two days later, each well was transfected

with 15 ng of the plasmid of interest and 15 ng of reporter plasmid, along with necessary control

wells. Two days later, images of each well were taken on an inverted microscope (Nikon Eclipse

Ti2) and automatically analyzed in MATLAB (MathWorks, Inc.). Briefly, images were first

segmented to only analyze the area comprising the well and ignore the outside region. Then, the

image was binarized based on blue fluorescence intensity using an iterative thresholding method

that finds the lowest threshold that does not include background fluorescence. Next, cells were

segmented by the *regionprops* function that provides location data for each fluorescent cell.

Finally, the Red/Blue fluorescence ratio was found for each cell and averaged across all cells

detected in that well. GFP fluorescence intensity was measured by averaging the total

fluorescence in the well after removing non-fluorescent pixels.

RT-PCR

EVs were resuspended in 700 µL Qiazol spiked with 2 fmol cel-miR-39 (Norgen Biotek) per

sample. RNA was isolated using miRNeasy Kit (Qiagen) and cDNA was produced using

miScript RT II Kit (Qiagen) using the same amount of starting RNA according to manufacturer's

protocol. 2 µL cDNA product along with primers and water was added to Ssoadvanced Universal

SYBR Green Supermix (Biorad) according to manufacturer's protocol. A QuantStudio 7 Flex

qPCR System was used to detect the signal from each well. The reaction cycle consisted of 98°C

(1 min), and 40 cycles of 98°C (10 s) and 60°C (20 s). The primers used were miR-146a fwd:

(5'-GAGAACTGAATTACATGGGT-3'), miR-146a rev: (5'-

CAGGTCCAGTTTTTTTTTTTTTTT-3'), pre-miR-146a fwd: (5'-

GTGTCAGTGTCAGACCTCT-3'), pre-miR-146a rev: (5'-

CAGGTCCAGTTTTTTTTTTTTTTT-3'), cel-miR-39 fwd: (5'-

GTCACCGGGTGTAAATCAG-3'), cel-miR-39 rev: (5'-

GGTCCAGTTTTTTTTTTTTTTTCAAG-3'), actin fwd: (5'-

ACTTAGTTGCGTTACACCCTT-3'), actin rev: (5'- GTCACCTTCACCGTTCCA-3'). As an

RNA standard for absolute quantification, 40 pmol miR-146a-5p miRNA mimic was reverse

transcribed including spike-in, and serially diluted 10-fold six times.

Statistical analysis

Data are presented as mean ± SD. One-way ANOVAs with Dunnett's multiple comparison test

or two-way ANOVAs with Tukey's multiple comparison test were used to determine statistical

significance ($p < 0.05$) in RT-PCR experiments and plasmid/reporter fluorescence experiments.

All statistical analysis was performed with Prism 8 (GraphPad Software, La Jolla, CA). Notation

for significance in figures were as follows: ns = $p > 0.05$, * = $p \leq 0.05$; ** = $p \leq 0.01$; *** = $p \leq$

0.001; **** = $p \leq 0.0001$.

Results

Overexpression of miR-146a-5p in HEK293T cells

In order to overexpress miR-146a-5p in HEK293T cells, which express a low level of native

miR-146a, we constructed four homologous plasmids (and a scramble control) that placed the

mature sequence (5'-ugagaacugaauuccauggguu-3') within four distinct miRNA precursor

scaffolds (Fig. 13a). These scaffolds are based on the primary (pri-) or precursor (pre-) sequences of miR-146a and miR-451. Therefore, the constructs are variably independent of miRNA biogenesis proteins Drosha and Dicer, which may improve or inhibit their processing and secretion into EVs. These scaffolds were cloned into the pCMV-GFP plasmid immediately upstream of a five-thymine "T5" RNA polymerase III (Pol III) terminator and immediately downstream of a U6 promoter preceded by a cytomegalovirus (CMV) enhancer, given reports that the CMV enhancer increases U6 expression [281]–[283], as well as that of other RNA Polymerase III promoters [284]–[287].

Given the array of RNA secondary structures involved, it is likely that detection by RT-PCR will be biased against sequences with tighter structures, especially pre451 precursors which have much lower ensemble diversity and Gibbs free energy according to RNAfold software [288], [289]. A comparison of the RNA minimum free energy (MFE) structures and positional entropy are shown in Figure 13b. More stable structures are less likely to degrade during RNA handling, however.
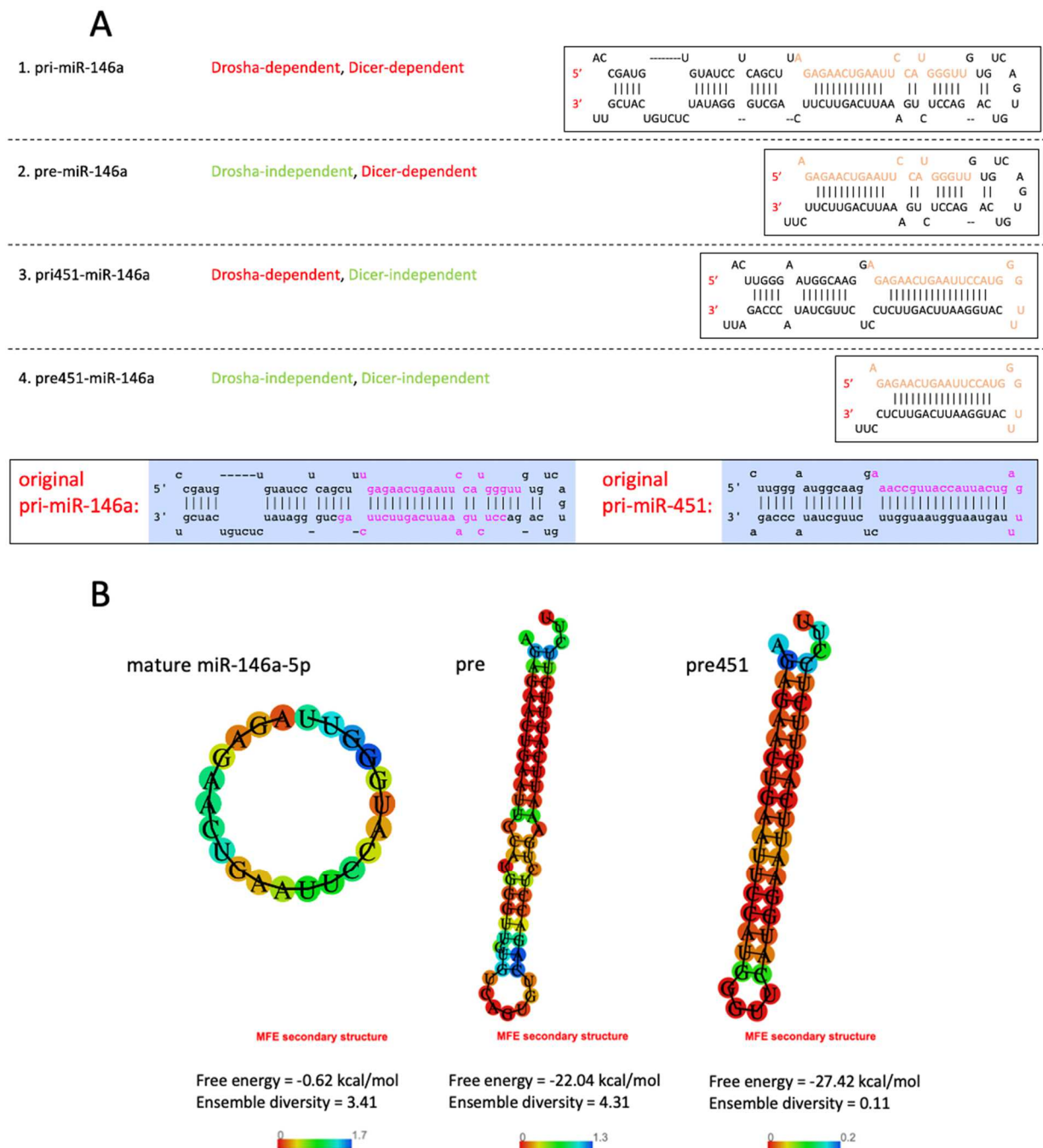
Figure 13. miR-146a overexpression sequences and predicted structures. (A) miR-146a derived sequences and expected base-pairing. Orange highlighted sequence is the mature miR-146a sequence. (B) Predicted minimum free energy (MFE) structure, Gibbs free energy, ensemble diversity, and positional entropy as shown by color bar. Calculations and illustrations produced by RNAfold software.

In order to determine the miR-146a activity from our overexpression systems, we co-transfected the constructs into HEK293T cells along with a fluorescence-based miR-146a reporter system, along with a miR-126 reporter system as a control. These cells were then imaged and analyzed using image analysis software in MATLAB and normalized to a No Plasmid control. The results showed a wide divergence of miR-146a activity based on the construct (Fig. 14a). Compared to No Plasmid, scr and pri451 showed no decrease in signal. Following this, pre, pri, and pre451 constructs had increasing activity, respectively. When we doubled the transfecting dose of pri, we saw a concomitant decrease in signal. We also saw no change in signal in the miR-126 control reporter system, except, strangely, from pri451.

Next we expressed each construct in HEK293T cells and collected EVs via differential ultracentrifugation once cells reaches confluency. RNA isolation was then performed on cellular and EV lysates and RT-PCR was performed using two primers: one for the consensus mature miR-146a ("all miR-146") and one for the stem-loop on the pri and pre constructs ("pre-146"). In the cellular fraction we saw incredible miR-146a enrichment in the pri and pre groups, especially the pre group which had a 777-fold increase in all miR-146 compared to No Plasmid ($p < 0.0001$) (Fig. 14b). We saw no increase in the pri451 group, and intriguingly, only a 19-fold increase in pre451 group, despite the high level of knockdown in the prior experiment. In the EV fraction, most of the groups were not detected due to low sensitivity of the qPCR (Fig. 14c). However, we saw a significant enrichment favoring pre over pri in terms of secretion into EVs, normalized for EV number. Due to the lack of expression or knockdown from the pri451 construct, we stopped including this plasmid in our experiments.
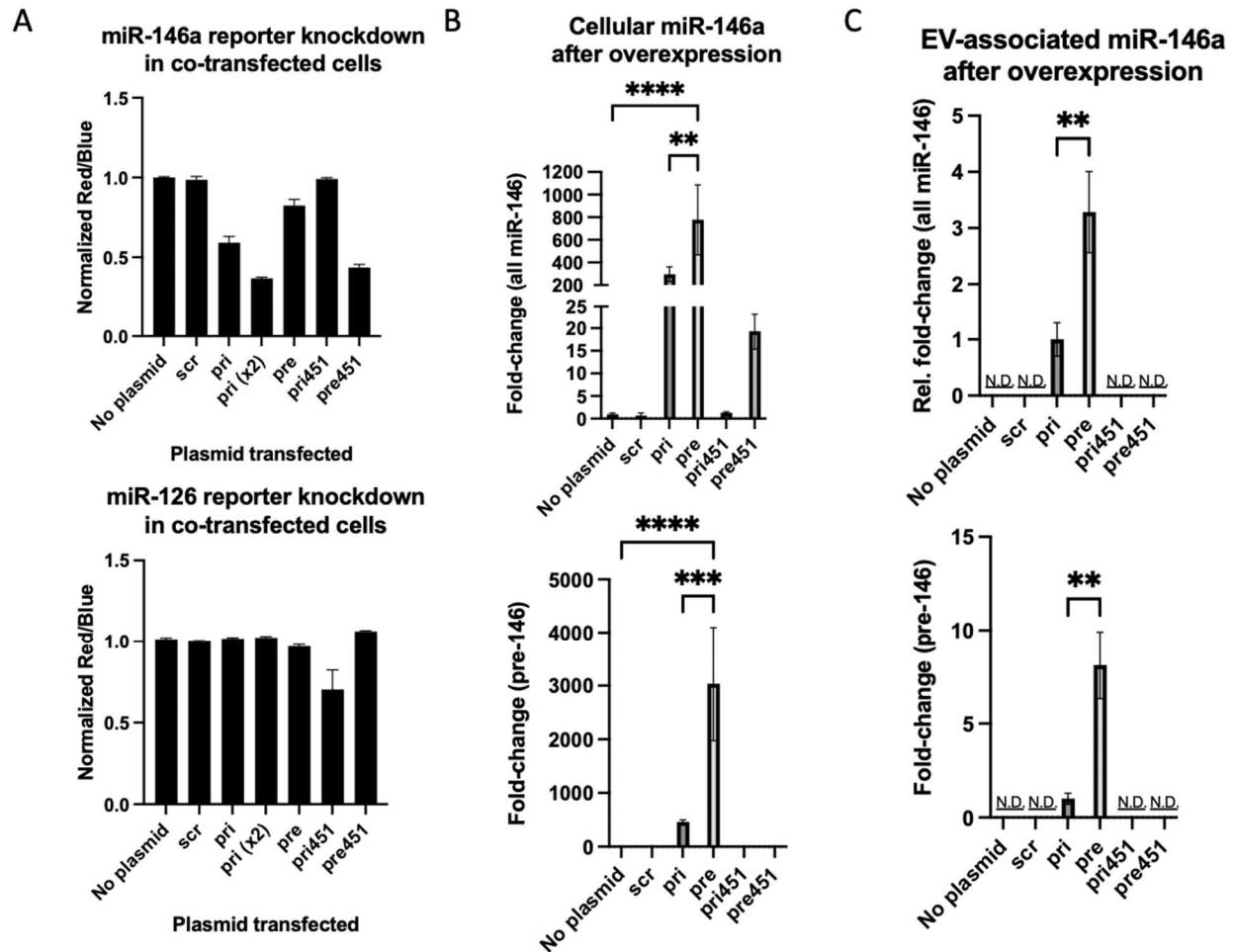
Figure 14. Bioactivity and miR-146a content after overexpression. (A) Target knockdown in cells co-transfected with miR-146a-expressing plasmid and miR-146a reporter plasmid or miR-126 reporter plasmid. Red fluorescent protein expression is targeted by the corresponding miRNA, while blue fluorescent protein is constitutive. (B) Cellular miR-146a as measured by RT-PCR with either a primer for mature miR-146a or pre-miR-146 hairpin. (C) EV-associated miR-146a as measured by RT-PCR with either a primer for mature miR-146a or pre-miR-146 hairpin, normalized by EV particle count. (N.D. = Not Detected). (ns = $p > 0.05$, * = $p \leq 0.05$; ** = $p \leq 0.01$; *** = $p \leq 0.001$; **** = $p \leq 0.0001$).

Overexpression in Dicer-knockout cells

Given the possibility for greater RNA stability in the absence of the Dicer enzyme, we examined

miRNA secretion in Dicer-knockout HEK293T (NoDice) cells, originally developed by the

Cullen lab [279]. In this cell line, pre-miRNAs accumulate and very little RNA is incorporated

into RISC. Analysis of basal level expression in these cells indicates that the total level of mature

68

miR-146a sequence is similar between the WT and KO cells, with 3.5-fold increase in the amount of pre-146a, however this difference was nonsignificant (Fig. 15a).

Overexpression of the constructs yielded an similarly increased expression in the cellular fraction in the pri and pre groups (Fig. 15b). Surprisingly, we saw a massive enrichment of pre451 in comparison to the other groups, potentially due to Ago2 vacancy in Dicer-knockout cells. In the EV fraction, pri and pre451 had similar levels in EVs, and were both more highly secreted than the pre construct (Fig. 15c).
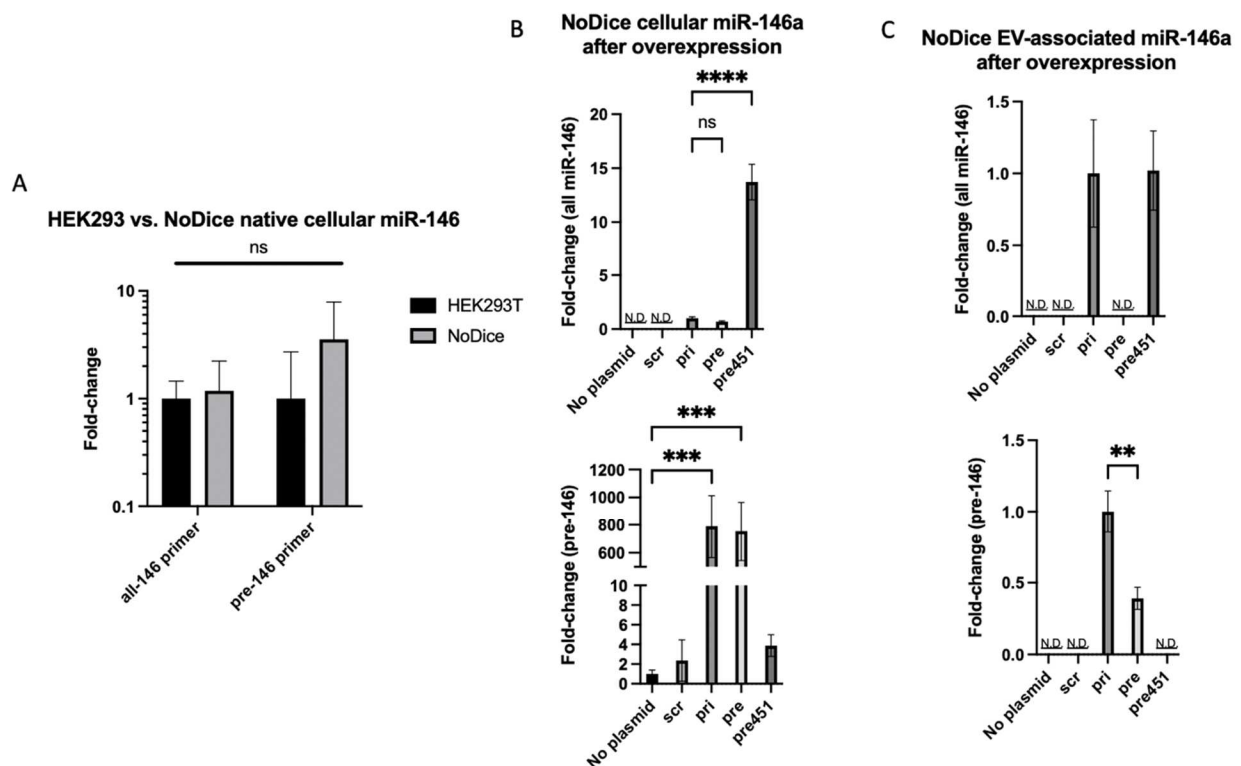
Figure 15. miR-146a content after overexpression in NoDice cells. (A) miR-146a content in nontransfected NoDice cells as measured by RT-PCR with either a primer for mature miR-146a or pre-miR-146 hairpin (B) Cellular miR-146a as measured by RT-PCR with either a primer for mature miR-146a or pre-miR-146 hairpin. (C) EV-associated miR-146a as measured by RT-PCR with either a primer for mature miR-146a or pre-miR-146 hairpin, normalized by EV particle count. (N.D. = Not Detected). (ns = $p > 0.05$, * = $p \le 0.05$; ** = $p \le 0.01$; *** = $p \le 0.001$; **** = $p \le 0.0001$).

Exportin-5 overexpression leads to increased RNA secretion

A previous study showed that Exportin-5 overexpression increased cytoplasmic concentration of miRNAs and improved knockdown in cells [290]. Therefore, we postulated that overexpression of Exportin-5 could also lead to increased secretion of an overexpressed miRNA into EVs. Transfecting HEK293T cells with the pKmyc-XPO5 plasmid resulted in a 5-fold increase in Exportin-5 protein when compared to No Treatment and pKmyc backbone via western blot (Fig. 16a). In the cellular fraction, co-transfecting Exportin-5 interestingly led to a decrease in cellular miR-146a, when normalized to the pKmyc backbone control (Fig. 16b). This trend held true in the scramble control, implying an effect independent of miRNA overexpression. Even more surprisingly, in the EV fraction, pri was significantly enriched by Exportin-5 overexpression when compared to the pKmyc backbone control (Fig. 16c). This inverse effect may result from any number of causes. For example, it is possible that nuclear miR-146a is more stable than cytoplasmic miR-146a, and thus facilitating nuclear export leads to lower total cellular miR-146a even while causing higher cytoplasmic concentrations. It is also possible that Exportin-5 expression leads to greater Actin mRNA levels in the cell, and thus the normalization control would be unreliable. Indeed, we found that in cells that overexpressed Exportin-5, there was a decrease in the Ct value during qPCR (indicating a higher concentration) compared to cells expressing the pKmyc backbone (Fig. 16d). While Exportin-5 has been shown to export some mRNA species [291], [292], this conclusion is unreliable and requires further study.
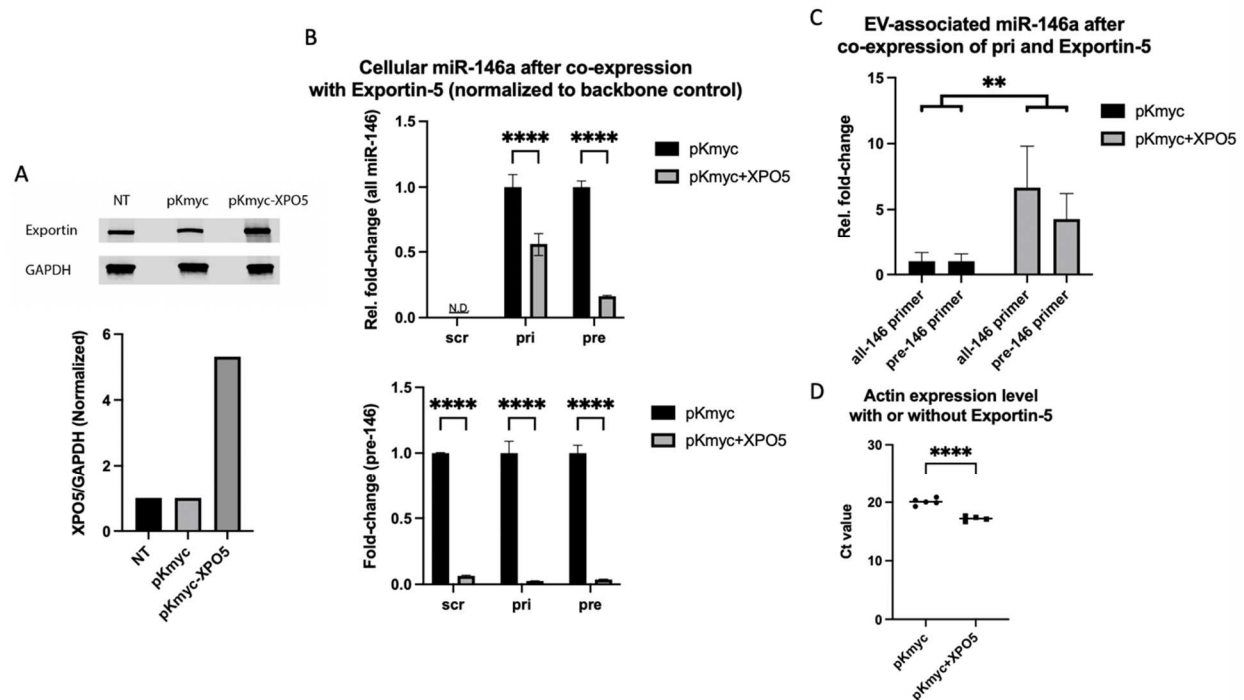
Figure 16. miR-146a content after overexpression in Exportin-5 overexpressing cells. (A) Exportin-5 protein content after overexpression as measured by western blot and quantified by pixel intensity. (B) Cellular miR-146a as measured by RT-PCR with either a primer for mature miR-146a or pre-miR-146 hairpin, normalized independently for each miR-146a plasmid to its pKmyc control. (C) EV-associated miR-146a after overexpression of pri as measured by RT-PCR with either a primer for mature miR-146a or pre-miR-146 hairpin, normalized by EV particle count. (D) Ct value from RT-PCR on cellular RNA using Actin-specific primer. (N.D. = Not Detected). (ns = p > 0.05, * = $p \leq 0.05$; ** = $p \leq 0.01$; *** = $p \leq 0.001$; **** = $p \leq 0.0001$).

Plasmid design affects miRNA expression and activity

To determine the effect of various plasmid features on expression and activity of our miR-146a

constructs, we built three new plasmid constructs, shown in Figure 17a. To the original plasmid

referred to from now on as "CMV-U6", we either removed the CMV enhancer or added a

hepatitis delta virus (HDV) self-cleaving ribozyme immediately downstream of the miR-146a

sequence, or both. The HDV ribozyme cleaves itself at its own 5' end, leaving a uniform 3' end

of the preceding RNA sequence. The inclusion of this sequence would ensure a uniform 3' UU

tail of the transcribed miR-146a scaffold, similar to a synthetically produced miRNA mimic, as

71

opposed to the variable 1-5 U tail produced by the T5 termination sequence [293]. The Drosha enzyme is expected to provide a mostly uniform 3' end during pri biogenesis, but for pre and pre451, this step does not occur. A uridine tail longer than 2 nt may target an miRNA for degradation [294], reduce Exportin-5 export [295], or impair Ago2 binding [296]. On the other hand, miRNAs with greater 3' uridylation are overrepresented in exosomes [76]. Lastly, addition of the HDV ribozyme downstream of shRNA has been demonstrated to improve activity in previous studies [297], [298].

To determine the activity of these new plasmids, we co-transfected them into HEK293T cells along with a fluorescence-based miR-146a reporter system, as well as a miR-126 control reporter system (Fig. 17b). The reporter system showed a great decrease in signal by deletion of the CMV enhancer ($p<0.0001$) and also an additionally decrease in signal by adding the HDV ribozyme to both the CMV-U6 plasmid and the U6 plasmid ($p=0.0002$ and $p=0.026$, respectively). Once the CMV enhancer was removed, variability between pri, pre, and pre451 was much reduced. The miR-126 reporter system registered no change in fluorescence.

To look more closely at the molecular processing of each RNA transcript, we analyzed the GFP fluorescence expressed by each plasmid (Fig. 17c-d). In groups without the HDV ribozyme, we saw variable fluorescence, with decreasing signal in pre, pri, pre451, and scr, respectively. Addition of the HDV ribozyme diminishes the fluorescence to a very low level and abolishes most of the variability. GFP signal does not correlate with Red/Blue signal, as seen with the U6 plasmids, which display both variable GFP signal and uniform target knockdown. However, the fluorescence may act as a reporter for both overall transcription and undesired termination

72

sequence read-through during RNA transcription. Removal of the CMV enhancer increases GFP fluorescence, indicating that the enhancer may interfere with U6 transcription initiation. Additionally, the T5 termination sequence has been shown to incompletely terminate transcription, and may be vulnerable to variable termination based on the sequence or secondary structure of the upstream sequence [293], [299]. The reduction in GFP fluorescence in plasmids containing HDV ribozyme is likely due to the 5' hydroxyl product caused by self-cleavage [300].

Figure 17. miR-146a bioactivity depending on plasmid design. (A) Layout of variable plasmid designs. (B) Target knockdown in cells co-transfected with miR-146a-expressing plasmid and miR-146a reporter plasmid or miR-126 reporter plasmid. Red fluorescent protein expression is targeted by the corresponding miRNA, while blue fluorescent protein is constitutive. (C) Quantified cellular GFP expression after transfection of indicated plasmid. (D) Fluorescent images of cells after transfection of indicated plasmid at indicated image exposure. (ns = $p > 0.05$, * = $p \leq 0.05$; ** = $p \leq 0.01$; *** = $p \leq 0.001$; **** = $p \leq 0.0001$).

Overexpression of optimized miR-146a scaffolds

The U6 plasmids were overexpressed in HEK293T cells and EVs were collected for analysis. In the cellular fraction, U6-pri showed greater enrichment than other constructs (Fig. 18a). In the

EV fraction, U6-pri showed greater enrichment than U6-pre, including a 31.6-fold increase of the precursor sequence over the No plasmid group (Fig. 18b). Against a standard curve, we quantified the amount of miR-146a as 0.243 (SEM = 0.096) copies/EV (Fig. 18c).
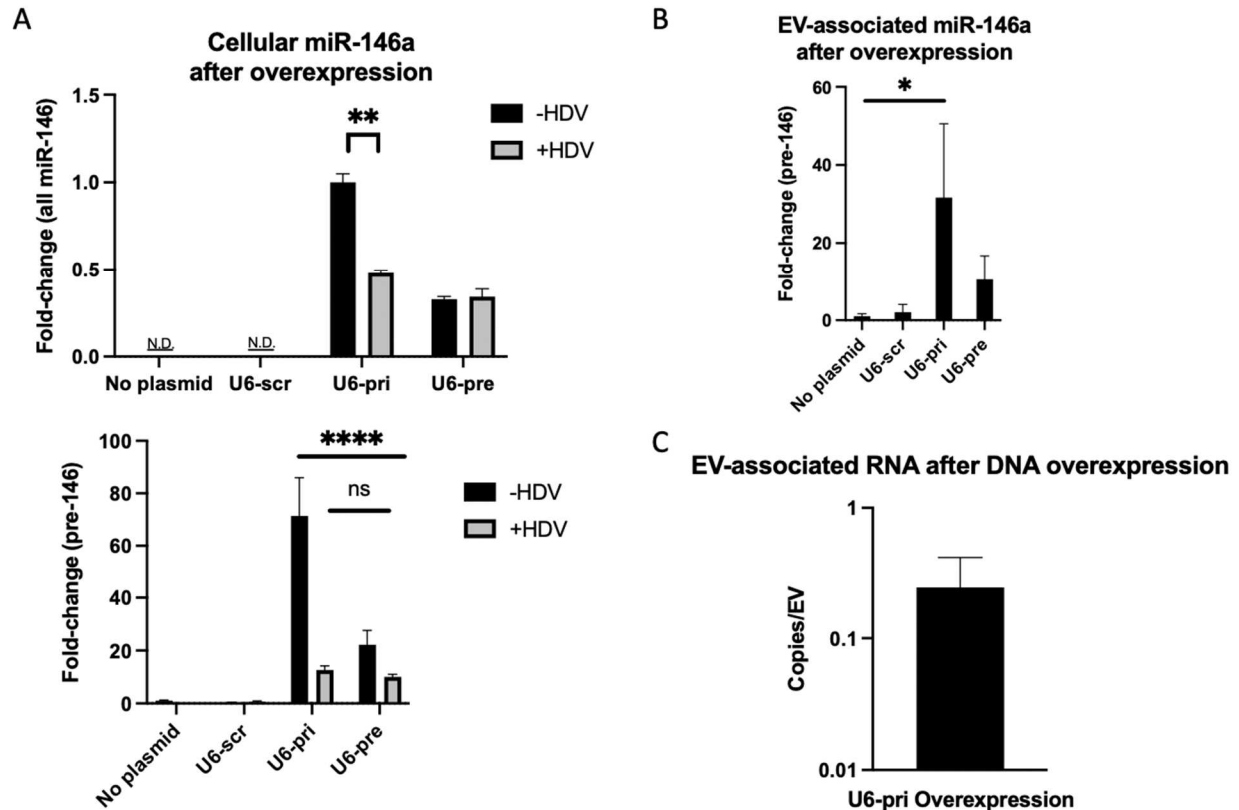
Figure 18. miR-146a content after overexpression using "U6" plasmids. (A) Cellular miR-146a as measured by RT-PCR with either a primer for mature miR-146a or pre-miR-146 hairpin. (B) EV-associated miR-146a as measured by RT-PCR with a primer pre-miR-146 hairpin, normalized by EV particle count. (C) Quantification of EV-associated miR-146a as measured by RT-PCR and NTA. (N.D. = Not Detected). (ns = $p > 0.05$, * = $p \leq 0.05$; ** = $p \leq 0.01$; *** = $p \leq 0.001$; **** = $p \leq 0.0001$).

Discussion

RNA secretion into EVs is an active area of research with ramifications in understanding intercellular communication and therapeutic design. This study sought to elucidate the effects of design choices that could potentially improve RNA loading into EVs, including engineering the

producer cell, DNA expression vector, and RNA secondary structure. However, no alterations were made to the mature miRNA sequence. Our findings showed that miR-146a-5p bioactivity and secretion can be promoted or restricted by tweaking its interactions with the miRNA biogenesis enzymes Drosha, Exportin-5, Dicer, Ago2, and RNA Polymerase.

Initial overexpression of miR-146a-5p demonstrated a large increase in cellular enrichment when placed inside the pri and especially pre RNA scaffold when analyzed via RT-PCR. In isolated EVs, pre was enriched greater than pri, implying that requiring interaction with Drosha may be a bottleneck for RNA maturation. However, functional knockdown in overexpressing cells was seen to be greater in pri over pre, and highest in pre451, even though cellular levels of miR-146a were significantly inverted. We discontinued pri451, which exhibited no expression or knockdown for an unknown reason.

Overexpression of our constructs in Dicer-knockout HEK293T cells led to similar expression levels for pri and pre, but an asymmetric increase in cellular expression for pre451. This is likely the result of the depletion of competing miRNAs that lead to Ago2 vacancy, which would grant miR-146a complete occupancy of cellular Ago2. Upon entering Ago2, miR-451 is progressively trimmed on its 3' end into the mature sequence, as has been described previously [26]–[30], and this mature sequence is likely more easily detected than the pre451 precursor. In the EV fraction, previously undetectable pre451 was found to be exported at a similar level to pri. If the hypothesis regarding Ago2 vacancy is correct, it would follow that association with Ago2 does not prevent miRNA secretion into EVs and may perhaps facilitate it. Further study on this extremely unusual system could provide results that a) show vastly increased RNA secretion,

and/or b) illuminate the debate on miRNA secretion. Additionally, employing this system could streamline the production of miRNA-loaded Ago2. Unfortunately, we cannot pursue this line of inquiry with our current RT-PCR method.

Overexpression of Exportin-5 decreased the level of cellular miR-146a. We hypothesize that this phenomenon could be explained as either: a) cytoplasmic miRNA is degraded or exported at a faster rate than in the nucleus, leading to lower total miRNA but greater cytoplasmic and extracellular RNA, or b) the level of Actin mRNA (the normalization control) is increased by Exportin-5 and therefore the cellular miR-146a result is unreliable. Either way, overexpression of Exportin-5 led to a significant increase in EV-associated miR-146a.

Removal of the CMV enhancer and addition of a 3' HDV ribozyme additively increased the bioactivity of the miRNA constructs. Variability in the bioactivity between pri, pre, and pre451 constructs was also much reduced by removing the CMV enhancer, for unknown reasons. Given the native role of CMV enhancer in recruiting Pol II, combined with modest inherent Pol II activity of the U6 promoter [301], it is possible that undesired Pol II activity is causing transcriptional read-through of the T5 termination sequence. However, removal of the CMV enhancer actually diminished GFP expression, indicating that the enhancer most likely inhibited transcription, possibly through transcriptional interference [302]. It is clear that read-through is occurring in the U6 system, either due to modest inherent Pol II activity [301], or leaky T5 termination, since it has been shown that T5 only terminates 95% of sequences [293]. Upstream hairpins have also been shown to modulate termination efficiency [299], which may explain the variability in GFP expression depending on the RNA scaffold used. Concerns over variable

length of uridine tail and read-through are good reasons to use Drosha-dependent scaffolds like pri, which will process the RNA into a mostly uniform pre-miRNA, or a self-cleaving ribozyme like the HDV ribozyme, which gives exquisite control over the 3' terminus. The use of this ribozyme could also be used for simplified overexpression of therapeutic small RNA in lower organisms such as *E. coli*. Concerns that may arise from the use of a ribozyme are potential inclusion of the 3' ribozyme product into extracellular vesicles meant for human treatment with unknown consequences, and the addition of a 2',3'-cyclic monophosphate on the 3' product, as opposed to the 3' hydroxyl that remains after Drosha cleavage. The effect of this modification does not appear to inhibit pre-miRNA bioactivity, but should be examined further to determine the effect conclusively.

The U6 and U6-HDV plasmids showed more modest increases in cellular RNA compared to previous iterations, with U6-pri exhibiting the highest expression levels. Likewise, U6-pri showed higher expression in EVs compared to U6-pre. Expressing miR-146a in a U6-pri scaffold produced 0.243 (SEM = 0.096) copies/EV. This concentration of loaded miRNA is certainly an enrichment, but does not reach the concentrations seen in other endogenous loading techniques such as electroporation or cationic transfection. By including Exportin-5 overexpression and probing pre451 expression further, in addition to other techniques such as further refinement of the secondary structure, stable cell line production, or knockdown of RNA-degrading proteins, it may be possible to match or exceed other endogenous loading techniques. While pursuing these cellular engineering techniques, however, it is critical to ensure that inherent EV integrity and bioactivity is not degraded.

Conclusion

Current frames of understanding RNA secretion position a "active, selective" process against "passive, nonselective" process with persuasive evidence for both mechanisms. In this work, we sought to improve RNA loading into EVs by leveraging the second mechanism, without requiring changes in RNA sequence or overexpression of any specific RBP. By focusing on sequence-agnostic changes, these engineering techniques could theoretically be applied towards enhanced RNA loading into EVs for (almost) any sequence.

Chapter 5: Combinatorial microRNA loading into extracellular vesicles for anti-inflammatory therapy[5]

Introduction

Endogenous loading strategies have some advantages over exogenous, however, a significant limitation of endogenous loading strategies is total RNA loading. The maximum that we achieved for endogenous loading was approximately one copy/EV, while some exogenous loading strategies have been shown to load thousands of copies/EV, including a sonication method previously developed by our lab [107]. While it is unknown what percentage of miRNA is intravesicularly loaded using this method, the enrichment vastly exceeds that of endogenous methods. Our goal in this chapter is to examine if the utility of exogenous approaches could be expanded and applied for a therapeutically relevant application.

Inflammation-related diseases are responsible for millions of deaths every year [139], [303]. While inflammation is a critical part of an effective response to harmful stimuli, inappropriate acute or chronic inflammatory signaling can cause harm to the body. Widespread adoption of inflammation management protocols has helped lower death rates, but there are still many inflammatory disorders for which there are no specific approved treatments.

As a result, new therapeutic approaches are being pursued. An emerging strategy involves microRNAs (miRNAs), which have been shown to play significant roles in inflammation in

---

5 **A. E. Pottash**, D. Levy, L. Kuo, S. M. Kronstadt, W. Chao, S. M. Jay, "Combinatorial microRNA loading into extracellular vesicles for anti-inflammatory therapy," Submitted.

general and in specific inflammatory conditions such as sepsis, both in promoting pathogenesis and recovery [33], [132], [213], [215], [304]–[312]. For example, miRNAs such as miR-146a and miR-223 have been shown to be downregulated in both septic vs. healthy patients and in non-surviving vs. surviving patients [215]. Thus, the concept of therapeutic miRNA delivery is intriguing as a possible novel anti-inflammatory treatment.

When considering potential vehicles for miRNA delivery, extracellular vesicles (EVs) have been implicated as promising based on their reported natural ability to facilitate intercellular RNA transfer [313]. While the physiological significance of EV-mediated miRNA transfer is still controversial [5]–[7], the capabilities of specifically-loaded EVs for small RNA delivery (siRNA and miRNA) have been clearly established [102], [104], [314]. Further, direct comparisons of EVs and other potential miRNA delivery vehicles such as liposomes have indicated the potential superiority of EVs [94], [315], [316]. Thus, EV-mediated miRNA delivery to treat inflammation is worthy of focused investigation.

Here, we built on previous work from our group using a sonication-based miRNA loading strategy to package miRNA into EVs without any chemical modifications [17]. Our prior study, like many in the field to date, investigated delivery of only a single miRNA species. In this work, we sought to exploit the potential synergy of regulating multiple anti-inflammatory pathways by loading multiple miRNA species into a single EV population. Combinations of miRNAs were tested in an *in vitro* macrophage inflammation model, which was previously shown to correlate with *in vivo* outcomes for EVs [317]. Finally, the most effective combination was tested in an *in vivo* endotoxemia model.

Methods

Cell culture

Human embryonic kidney HEK293T cells and RAW264.7 mouse macrophage cells were cultured in Dulbecco's modified Eagle's medium (DMEM) (Corning 10-013-CV; Corning, NY, USA) supplemented with 10% EV-depleted fetal bovine serum (FBS) and 1% penicillin/streptomycin in T175 tissue culture polystyrene flasks. FBS was EV-depleted via 100,000 x g centrifugation at 4°C for 16 h where the supernatant was retained.

Extracellular vesicle isolation

Conditioned media was collected and subjected to differential centrifugation. Briefly, the supernatant was centrifuged at 1,000 x g for 10 min, 2,000 x g for 20 min, 10,000 x g for 30 min, for each of which the supernatant was retained, and finally, 100,000 x g for 2h, after which the pellet was resuspended in PBS and collected. This resuspension was washed 2x using Nanosep 300-kDa MWCO spin columns (OD300C35; Pall, Port Washington, NY, USA). The washed EVs were resuspended in PBS and filtered using an 0.2-μm syringe filter. EV size distribution and concentration were determined by nanoparticle tracking analysis (NTA) via a NanoSight LM10. Each sample was analyzed in triplicate using consistent acquisition settings. Total EV protein was determined via bicinchoninic acid assay (BCA) following manufacturer's protocol. Relative levels of relevant protein components were determined via western blotting. Alix (ab186429; Abcam), TSG101 (ab125011; Abcam), GAPDH (2118L; Cell Signaling Technology) and CD63 (25682-1-AP; Thermo Fisher). Primary antibodies were added at a 1:1000 dilution, except for GAPDH (1:2000). Secondary antibody IRDye 800CW anti-Rabbit

(926-32211; LI-COR Biosciences, Lincoln, NE, USA) were added at 1:10000 dilution, and membranes were imaged on a LI-COR Odyssey CLX Imager.

Extracellular vesicle loading

100 µg EVs, corresponding to ~3e9 particles detected by NTA, were mixed with 1nmol miRNA mimic (Dharmacon) and the volume was brought up to 100 µL with PBS. This mixture was incubated for 30 min at room temperature, before being sonicated at in a water bath sonicator (VWR® symphony™; cat# 97043-964, 2.8 L capacity, dimensions 24L × 14W × 10D cm) at 35 kHz for 15 s, placed on ice for 1 min, and sonicated for a second 15 s. The mixture was placed back on ice briefly, then washed 3x using Nanosep 300-kDa MWCO spin columns and resuspended by PBS. The miRNA mimics used were: has-miR146a-5p (C-300630-03); hsa-miR-155-5p (C-310430-07); hsa-miR-223-3p (C-300580-07); hsa-miR-126-3p (C- 300626-07); hsa-miR-124-3p (C-310391-05); Negative Control #1 (C-310391-05).

Transmission electron microscopy (TEM)

EVs were negatively stained using a protocol as previously described [318]. Briefly, 4% paraformaldehyde (10 µL) was added to EVs (10 µL) and incubated for 30 min. A carbon film grid was placed on the paraformaldehyde/EV droplet for 20 min, and washed with PBS. Then, the grid was placed on 1% glutaraldehyde (50 µL) for 5 min, and washed eight times with water. Finally, the grid was placed on uranyl acetate replacement stain (50 µL) for 10 min, and left to dry for 10 min.

Fluorescently labeled RNA co-loading test

Cy3-labeled miR-93 and Cy5-labeled miR-126 (Dharmacon) were loaded at indicated ratios according to the normal sonication protocol. After washing, fluorescence readings were taken and normalized to total fluorescence.

In vitro RAW264.7 inflammatory assay

RAW264.7 cells were seeded in DMEM supplemented with 5% FBS in a 48-well plate at 100,000 cells per well. All EVs were prepared by sonication and doses were normalized by protein content after sonication and washing. All treatments were diluted in DMEM supplemented with 5% FBS. The timing of doses depends on the treatment regime which is depicted in Figure 20a. In the "Pre-treat" regime, cells were treated with EVs or PBS alone for 24 hours, when supernatant was replaced by media with 10 ng/mL LPS for 4 h. In the "Co-treat" regime, both EV treatments and 10 ng/mL LPS were added concomitantly for 24 hours. In the "Post-treat" regime, cells were treated with 10ng/mL LPS for 24 hours, and then 10ng/mL LPS with EV treatments for another 24 hours. After all final treatments, media was collected and stored at -80C. IL-6 concentration was determined using the Mouse IL-6 DuoSet ELISA Kit (R&D Systems; DY406). Cell transfection was achieved using HiPerfect (Qiagen) according to manufacturer's protocol. For the "Co-treat" regime, phagocytosis was measured after the removal of the media, following the Vybrant Phagocytosis Assay Kit (Invitrogen) manufacturer's protocol. All tests were performed in biological triplicate.

ELISA

Samples were diluted as needed and cytokine concentrations were determined via DuoSet ELISA

Kits (R&D Systems): IL-6 (DY406), TNFa (DY410), MIP-2 (DY452), and CCL22 (DY439).

Proteome array

An antibody-based protein array was performed on cell supernatants after a "Pre-treat" regime,

using Proteome Profiler Mouse XL Cytokine Array (R&D Systems) according to manufacturer's

protocol. Expression was normalized between membranes.

In vivo endotoxemia study

Male C57BL/6J mice (Jackson Labs), 8 to 12 weeks of age, were used in this study. The animals

were kept at a constant temperature (25°C) under a 12h light/dark cycle with free access to food

and water. On the first and second day, animals received a 200 μL intraperitoneal injection of

PBS or sonicated EVs at a concentration of 2.1e10 particles/mL (by NTA). On the third day,

animals received an intraperitoneal injection of 5 mg/kg LPS. Three hours later, animals were

anesthetized and sacrificed via cardiac blood collection. Blood was collected into EDTA-coated

tubes (450480; Greiner Bio-One) and spun at 1,000 x g for 15min to produce plasma. All animal

work was carried out in accordance with the NIH guidelines and approved by the Institutional

Animal Care and Use Committee (IACUC) at the University of Maryland College Park.

RT-PCR

EVs were resuspended in 700ul Qiazol spiked with 2 fmol cel-miR-39 (Norgen Biotek) per

sample. RNA was isolated using miRNeasy Kit (Qiagen) and cDNA was produced using

miScript RT II Kit (Qiagen) according to manufacturer's protocol. 2ul cDNA product along with

primers and water was added to Ssoadvanced Universal SYBR Green Supermix (Biorad)

according to manufacturer's protocol. A QuantStudio 7 Flex qPCR System was used to detect

the signal from each well. The reaction cycle consisted of 98°C (1m), and 40 cycles of 98°C

(10s) and 60°C (20s). The primers used were miR-146a fwd: (5'-

GAGAACTGAATTACATGGGT-3'), miR-146a rev: (5'-

CAGGTCCAGTTTTTTTTTTTTTTT-3'), cel-miR-39 fwd: (5'-

GTCACCGGGTGTAAATCAG-3'), cel-miR-39 rev: (5'-

GGTCCAGTTTTTTTTTTTTTTTCAAG-3'). As an RNA standard for absolute quantification,

40 pmol miR-146a-5p miRNA mimic was reverse transcribed including spike-in, and serially

diluted 10-fold six times.

Statistical analysis

Data are presented as mean ± SD. One-way ANOVAs with Dunnett's multiple comparison test

to determine statistical significance (p < 0.05) in *in vitro* inflammatory assay, and *in vivo*

endotoxemia experiments. All statistical analysis was performed with Prism 8 (GraphPad

Software, La Jolla, CA). Notation for significance in figures were as follows: ns = p > 0.05, * = p

≤ 0.05; ** = p ≤ 0.01; *** = p ≤ 0.001; **** = p ≤ 0.0001.

Results

<u>EV loading and characterization</u>

In order to test multiple different combinations of miRNAs, a method of sonication-mediated EV loading previously developed by our lab was employed [107]. The sonication method is an exogenous loading technique in which pre-synthesized siRNA or miRNA mimics can be mixed in any combination to EVs and loaded. EVs derived from HEK293T cells were collected and characterized via western blot (Fig. 19a). The EVs were then sonicated in the presence of miR-146-5p double-stranded mimic and washed extensively. These sonicated EVs were then analyzed via NTA to detect any changes in size (Fig. 19b). Sonicated and unsonicated EVs were imaged using transmission electron microscopy (TEM) (Fig. 19c). Visually, we did not detect any changes in EV morphology or aggregation in the sonicated EVs. The ability to controllably co-load two different miRNA cargos into a single EV population was determined by mixing and sonicating Cy3-labeled miR-93 and Cy5-labeled miR-126 in varying proportions (Fig. 19d).

<u>Screening for anti-inflammatory miRNA</u>

EVs were loaded with five different double-stranded miRNA mimics (miR-126a-3p, miR-146a-5p, miR-124-3p, miR-155-5p, and miR-223-3p) that were found in literature to be deficient in septic patients or to modulate immune responses [215], [319]–[321]. These miRNAs were loaded either individually, in combination with all others save one, or as the complete group. In this way, each miRNA could be compared with others both as a lone treatment and when left out of the complete group. These EV treatments were applied to RAW264.7 murine macrophage cells 24 hours in advance of LPS treatment for 4 hours, in a "Pre-treat" regime (Fig. 20a). At the end of the LPS treatment, supernatants were collected and assessed using an IL-6 ELISA (Fig. 20b).
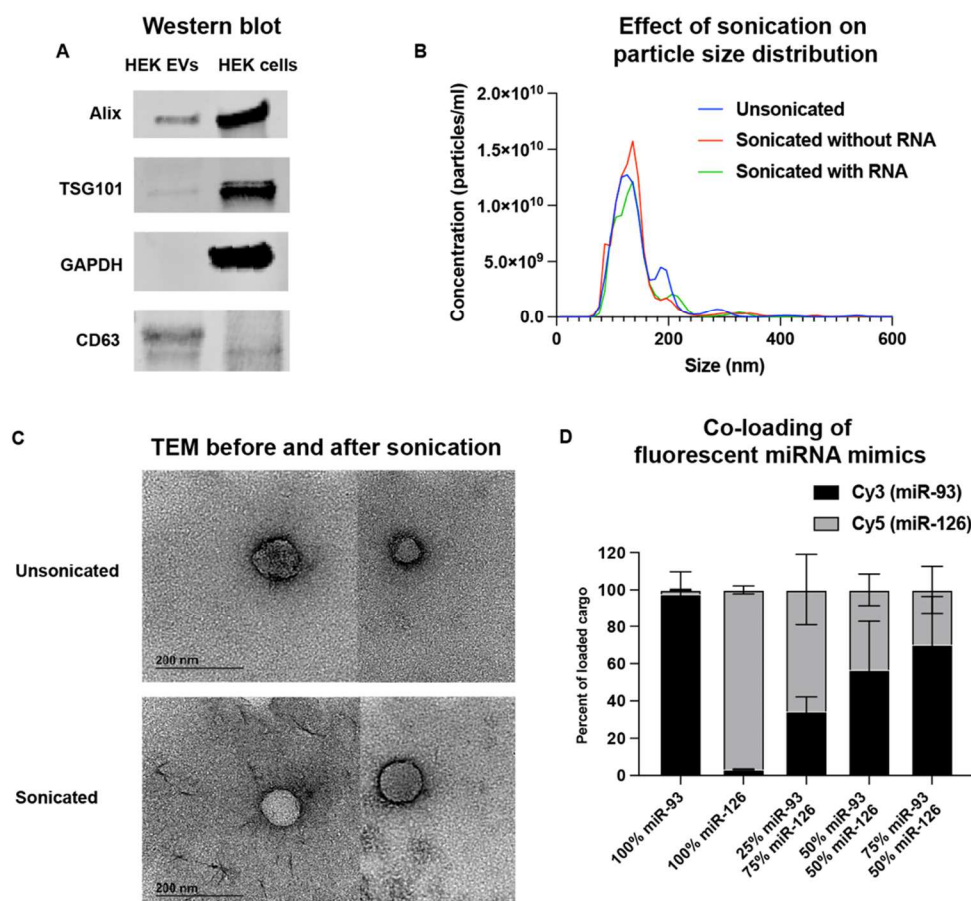
Figure 19. EV characterization and sonication loading quantification. (A) Nanoparticle Tracking Analysis (NTA) performed on EVs unsonicated, sonicated, and sonicated with miRNA. (B) Western blot of EVs vs parental cells. (C) Transmission Electron Microscopy (TEM) for unsonicated and sonicated EVs (D) Relative quantification of co-loaded fluorescently-tagged miRNA mimics.

Results indicated that EVs loaded with all miRNA resulted in downregulated IL-6 secretion. There was no detected difference between groups with miRNA mixed before sonication ("All") or individually loaded EV-miRNAs mixed after sonication ("All, Sonicated Separately"). Positive controls of Dexamethasone (Dex) (1 µg/mL) and transfection of all miRNAs showed significant anti-inflammatory effect. Among the individual miRNAs, miR-146 had a nonsignificant anti-inflammatory effect alone, and a nonsignificant effect in combination. miR-155 had no effect alone, but a significant effect in combination. miR-223 had no effect alone and no effect in combination, surprising in light of previous research [322], [323]. These miRNAs

were included for additional testing. miR-126 had an anti-inflammatory effect alone, but in combination had no additional effect. miR-124 had a nonsignificant pro-inflammatory effect alone and a significant pro-inflammatory effect in combination. Due to these results, we continued with miR-146a, miR-155, and miR-223 for further experiments.

All possible combinations of these three miRNAs were tested in a "Pre-treat" regime (Fig. 20c). All treatment groups led to significant anti-inflammatory effects, with dose-dependence evident. Interestingly, the No miRNA group (unmodified HEK293T EVs) showed an anti-inflammatory effect on par with Dex, reflecting prior data showing benefits of HEK293T EVs in a sepsis model via an unknown mechanism [324]. Cell phagocytic behavior was tested after LPS treatment to see if EV-mediated miRNA treatment impaired phagocytosis (Fig. 20d). No significant changes were detected. Due to the effectiveness of each miRNA combination, a more challenging regime was employed to differentiate between combinations.

All groups were tested in a "Co-treat" regime, wherein LPS and EV treatments were both applied concurrently to RAW264.7 cells for 24 hours (Fig. 20d). miR-146a alone had a significant anti-inflammatory effect, while miR-223 alone and miR-155 alone had no effect. In contrast, strikingly, the 155/223 combination significantly reduced IL-6 secretion. The 146a/223 treatment was not significantly effective, while the 146a/155 and 146a/155/223 treatments significantly reduced IL-6 secretion. Once again, a more challenging regime was employed to further differentiate between groups.

This time, all groups were tested in a "Post-treat" regime, wherein LPS was applied concurrently to RAW264.7 cells for 24 hours, and then LPS and EV treatments were concurrently applied for 24 hours (Fig. 20e). In this regime, no significant effects were detected except for with the complete combination of 146a/155/223, from now on referred to as "EV-TRI", which showed a small but significant effect.
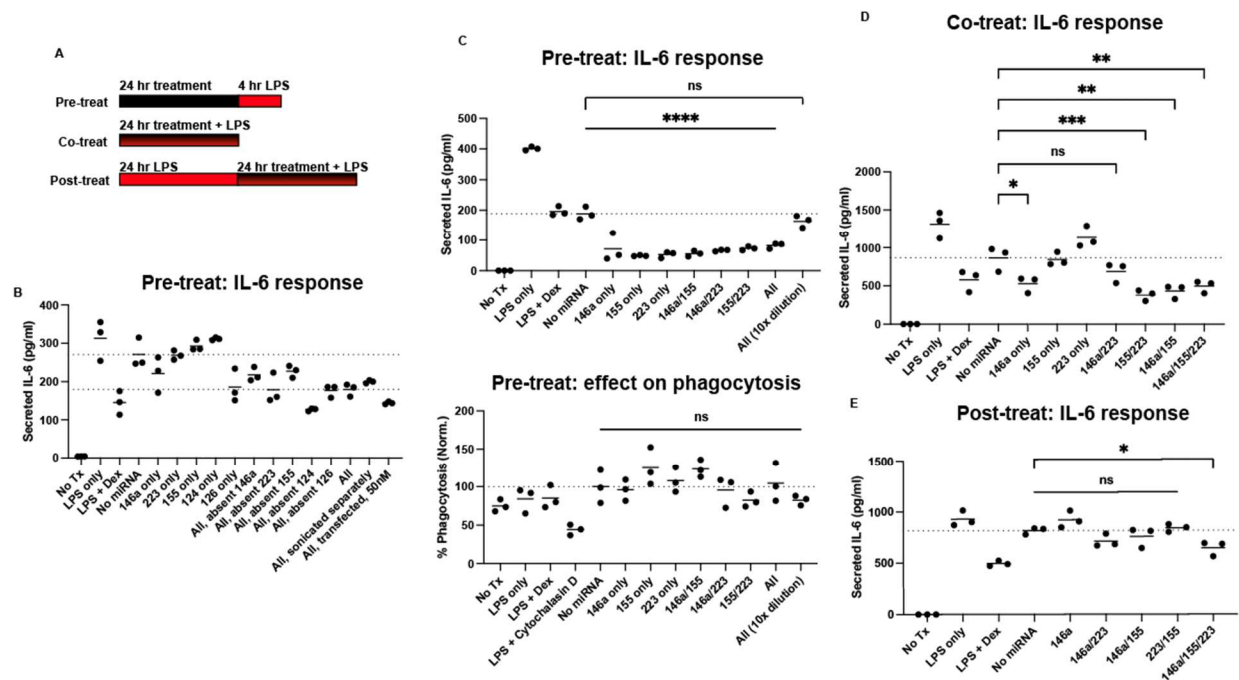
Figure 20. Screening of miRNA for anti-inflammatory combination. (A) Timelines for different treatment regimes. (B) Secreted IL-6 in response to LPS in a pre-treatment regime. "All" refers to all miRNA listed; "All, sonicated separately" refers to all miRNAs sonicated alone and combined for treatment; "All, transfected, 50nM" refers to all miRNAs transfected using HiPerfect (Qiagen). (C and D) Secreted IL-6 and subsequent phagocytosis in response to LPS in a pre-treatment regime. Phagocytosis as measured by the Vybrant Phagocytosis Assay Kit (Invitrogen). (E) Secreted IL-6 in response to LPS in a co-treatment regime. (F) Secreted IL-6 in response to LPS in a post-treatment regime. Results were analyzed via one-way ANOVA (ns = $p > 0.05$, * = $p \leq 0.05$; ** = $p \leq 0.01$; *** = $p \leq 0.001$; **** = $p \leq 0.0001$).

miR-TRI has broad anti-inflammatory effect

Given the effectiveness of EV-TRI in suppressing IL-6 secretion, we screened to see if other relevant secreted cytokine were also regulated using an antibody-based cytokine array. Pre-

89

treatment of RAW264.7 cells with EV-TRI or EV-NC (HEK EVs loaded with cel-miR-67 Negative Control miRNA mimic) showed differential protein expression after LPS treatment for 4 hours (Fig. 21a). In comparison to EV-NC, EV-TRI showed a downregulation of IL-6, IL-10, CCL22, CCL17, CXCL10, CXCL13 and CXCL16 (Fig. 21b). CCL22 downregulation was verified via ELISA (Fig. 21c).
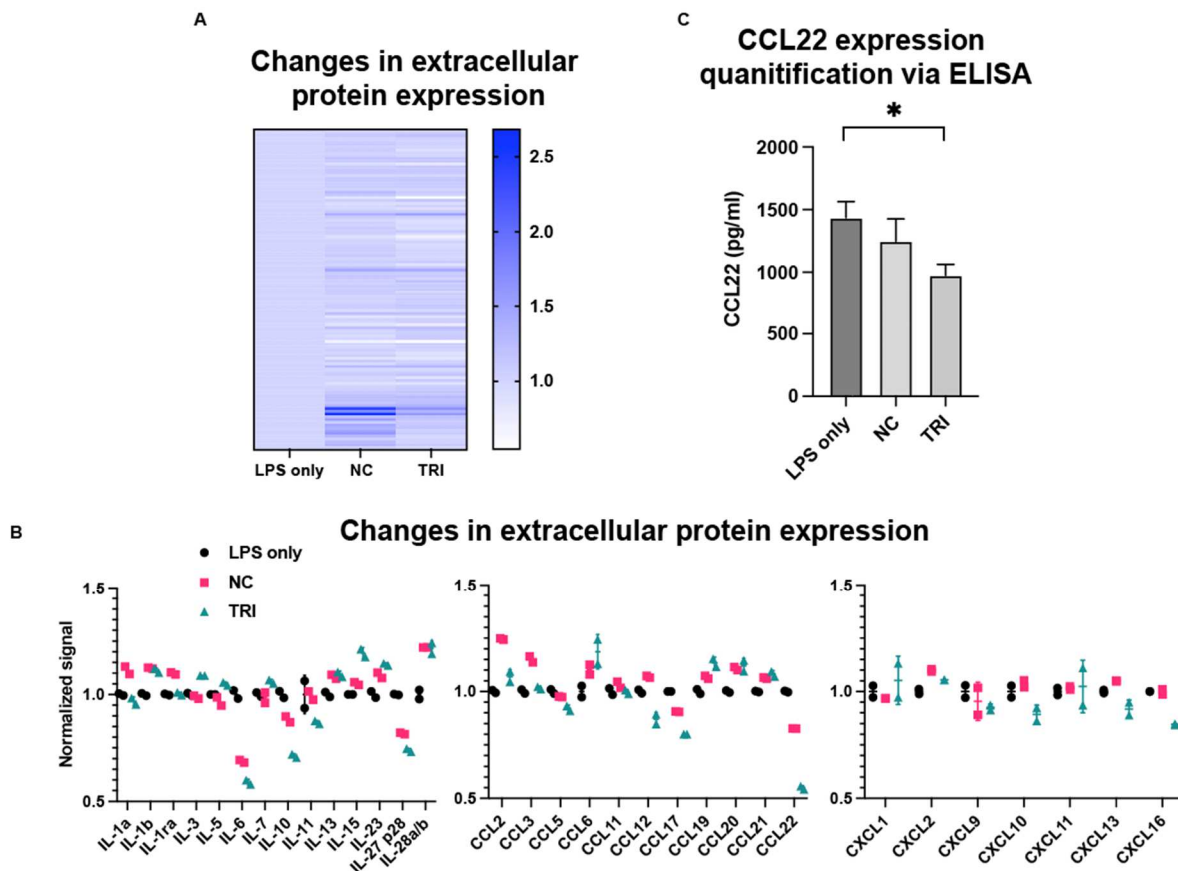
Figure 21. Screen for extracellular protein targets of EV-TRI. (A) Relative expression for all targets. (B) Relative expression for IL, CCL, CXCL cytokines. Expression as measured by the Proteome Profiler Mouse XL Cytokine Array (R&D Systems). (C) CCL22 expression was quantified via ELISA. Results were analyzed via one-way ANOVA (* = p ≤ 0.05).

miR-TRI has no effect on murine endotoxemia model

A murine endotoxemia model was employed to test the efficacy of intervention on systemic inflammation (Fig. 22a). EVs sonicated or unsonicated in the presence or absence of miR-NC

failed to significantly alter the IL-6 response to LPS (Fig. 22b). Similarly, EV-TRI failed to show

any improvement in this model, as no significant difference in IL-6, CCL22, TNFa, MIP-2, or

IL-1β cytokine concentration was detected, though a possible trend was detected for IL-6, with a

23% reduction in cytokine plasma concentration (p=0.07) (Fig. 22c).
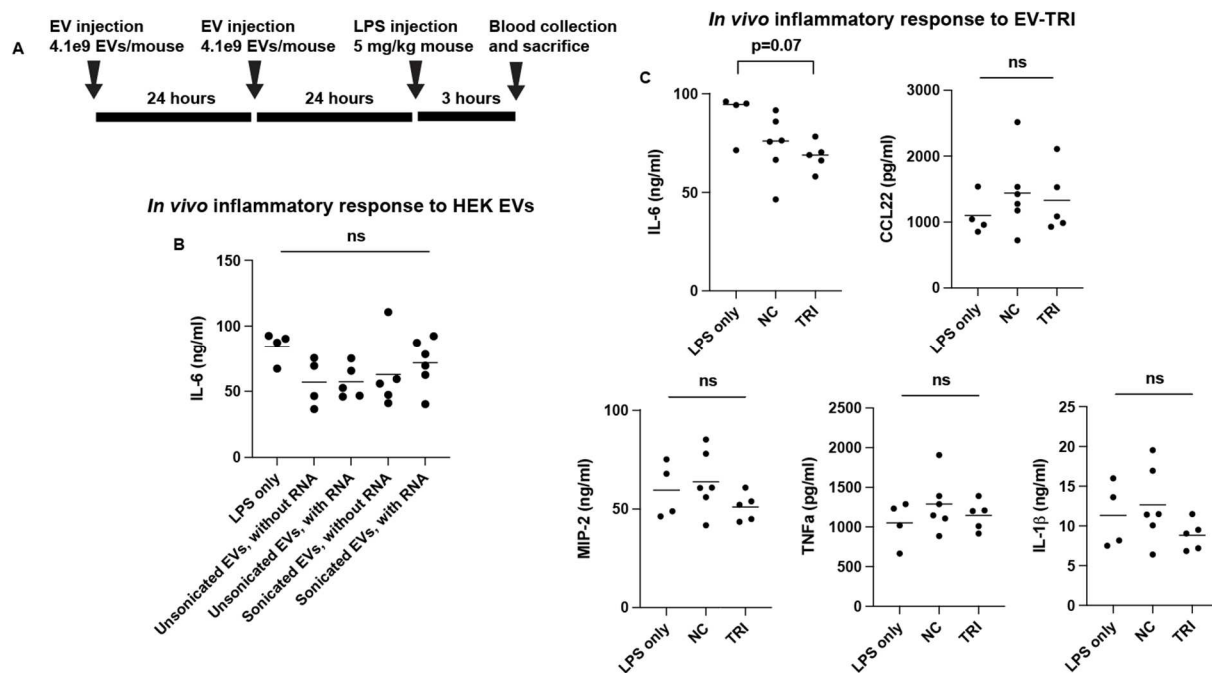
Figure 22. Response of endotoxemic mice pre-treated with EV-TRI. (A) Diagram of treatment schedule. (B) IL-6 response to EVs sonicated/unsonicated with/without RNA. (C) Cytokine response to treatment by NC and TRI. Results were analyzed via one-way ANOVA (ns = p > 0.05).

Discussion

We had previously established [107] that sonication enables the loading of thousands of copies

of miRNA into EVs, with only slight diminishment of *in vitro* EV uptake compared to

unmodified EVs. In this study, we quantify the loading of unlabeled small RNA to be thousands

of copies per EV. We also showed that the loading of multiple small RNA sequences by

sonication is predictable based on the proportion of their concentration in solution. This

91

technique may thus allow several advantages over competing EV loading strategies. We are able to co-load any mixture of miRNA sequences into a single EV population with a reproducible loading efficiency. As opposed to mixtures of individually loaded EVs, the pre-mixing of miRNA allows for loading multiple miRNAs into a single vesicle, guaranteeing proportional delivery to a recipient cell. This exogenous loading technique also is also adaptable for any small RNA cargo and does not require any manipulation of the cargo or producer cells.

To take advantage of this system, we performed a screen for anti-inflammatory miRNA combinations using a limited number of miRNAs selected from the literature. These miRNA combinations were passed through progressively more rigorous LPS challenges *in vitro* in order to determine if any specific combination of miRNAs is superior in reducing inflammation. That process identified the combination of miR-146a, miR-155, and miR-223 as being the most efficacious in reducing IL-6 production by RAW264.7 macrophages in response to LPS. This finding echoes work by Bhaskaran *et al.* that found that overexpression of three miRNAs in glioblastoma had a combinatorial anti-cancer effect [325], as well as a clinical study by Marik *et al.* which found that a combination of hydrocortisone, ascorbic acid, and thiamine worked synergistically as an anti-inflammatory against sepsis [326], [327].

miR-146a, miR-155, and miR-223 have been studied as anti-inflammatory miRNAs that change expression levels in response to LPS and target proteins in the TLR4 pathway [328]–[331]. Interestingly, these miRNA targets are largely non-overlapping, perhaps indicating that when attempting to downregulate a cellular pathway, greater effect may be achieved by targeting different proteins in that pathway rather than focusing on one protein. Work by *Schulte et al.*

described the tiered response by macrophages to LPS, in which miR-146 expression saturates at even sub-inflammatory LPS concentrations in order to protect against hyper-sensitivity, whereas miR-155 is expressed proportionally over a broad range of LPS concentrations in order to respond appropriately to the level of stimulation [332]. This indicates that both miRNAs seem to work in tandem to prevent an extreme cellular response. However, in other contexts, introducing miR-155 has been shown to be pro-inflammatory [333], [334]. For example, EVs from wild-type bone marrow-derived dendritic cells (BMDCs) increased IL-6 production in response to LPS in miR-155$^{-/-}$ BMDCs and mice, compared to EVs from miR-155$^{-/-}$ BMDCs [335]. These seemingly contradictory results indicate that miR-155 activity is nuanced and likely very context dependent. Concurrent introduction of other anti-inflammatory miRNAs like miR-146a and miR-223 may tilt the RNA network towards an environment in which miR-155 suppresses inflammation. Indeed, while miR-155 and miR-223 had no effect on IL-6 secretion on their own, in combination they were highly suppressive (Fig. 20d).

The results of our protein array showed a downregulation of IL-6, as expected. CCL22 and CCL17, the two CCR4 ligands, which are involved in T-cell chemotaxis, are also downregulated by the TRI treatment. Interestingly, in an LPS challenge model, CCR4$^{-/-}$ mice had decreased cytokine release and higher survival rate when compared to wild-type mice [336]. In another study, CCR4$^{-/-}$ mice had reduced immune response and greater survival after cecal ligation and puncture (CLP), and greater responsiveness and survival to a secondary fungal challenge [337]. These previous results indicated that, in addition to inhibition of IL-6, inhibition of the CCR4 ligands CCL22 and CCL17 may lead to an improved outcome *in vivo*.

Despite these encouraging signs, we saw no significant decrease in pro-inflammatory cytokines in response to EV-TRI *in vivo*. There are multiple reasons why this may be the case. Firstly, since cell source plays a role in EV biodistribution and delivery [338], the choice of HEK293T-derived EVs may limit an *in vivo* effect. A recent study showed that HEK293T EVs have a short half-life in healthy mice; in one hour, 80% of EVs were cleared from circulation [339]. It is possible that cargo packaged within EVs from mesenchymal stromal cells or another cell source could have a greater chance of functional delivery. Additionally, while sonication may inhibit EV delivery only slightly *in vitro*, this effect may be increased under more challenging delivery conditions i*n vivo*. Finally, the *in vitro* model used to screen for anti-inflammatory effects may be insufficiently representative of *in vivo* dynamics, despite prior correlation noted in the literature [317]. For example, the RAW264.7 macrophage model may be insufficiently representative of native macrophage behavior and is certainly insufficiently representative of other cell types affected by LPS injection.

Conclusion

Sonication is an effective method for loading multiple miRNAs into EVs in predictable proportions. Given the vast number of targets that are regulated by any one miRNA sequence (usually numbered in the hundreds), it would be difficult to fully map or predict the changes in the transcriptome, proteome, or phenotype of a cell that takes up one miRNA, let alone three. In this way, while literature can guide selection of therapeutic miRNA, empirical combinatorial testing of multiple miRNAs may be necessary when seeking to design a miRNA-based therapeutic. This work, which by no means exhausts the possible space of miRNA combinations, is nonetheless our attempt to illuminate the strengths of such an approach.

Chapter 6: Conclusions and outlook

EVs are an exciting platform for small RNA delivery that could solve current obstacles in RNA therapeutic development. However, there are technical challenges in EV cargo loading that need to be addressed before this method can truly be applied. In this work, we examined current small RNA loading techniques and attempted to innovate new refinements and opportunities for these techniques. In this chapter, we will review the results of the prior chapters and discuss further opportunities to reach the goal of developing EV-based small RNA therapies and our contributions to the field.

Summary of results

In **Chapter 3**, we optimized protocols for the endogenous loading techniques of electroporation and cationic transfection. Here, we discovered that using certain transfection reagents leads to enrichment within EVs, but also contamination in the final EV product. Likewise, we saw RNA aggregation as a result of electroporation, which could possibly impact cell health and contaminate the EV product. We also quantified miR-146a loading into EVs with each technique and found that they each result in approximately one copy per one EV. This finding leads us to consider if one copy per one EV is approaching the limit for endogenous loading techniques, and supplies the field with specific values to reference.

In **Chapter 4**, we developed a number of different miR-146a DNA expression plasmids that differed in RNA secondary sequence and compared them in HEK293T cells in their cellular bioactivity and EV export. While the miR-146a packaged within a pre-miR-451 backbone posed

difficulties for detection, we found that overexpression in a Dicer-knockout cell line led to an interestingly high level of cellular expression and export. Additionally, we co-expressed miR-146a and Exportin-5 and saw an increase in miR-146a secretion. Next, altering the plasmid promoter and adding a downstream HDV ribozyme improved the bioactivity of our plasmids. Finally, we quantified the miR-146a loading into EVs with this method and found about one copy per four EVs. Figure 23 shows a comparison between all endogenous loading techniques based our studies, including the native level of miR-146a (which was below the limit of our detection; <0.015 copies/EV). While DNA overexpression did lead to lower final miR-146a concentration within EVs, there are still opportunities to improve this technique, including some studied above.

Maximum achieved EV-associated RNA by endogenous loading method
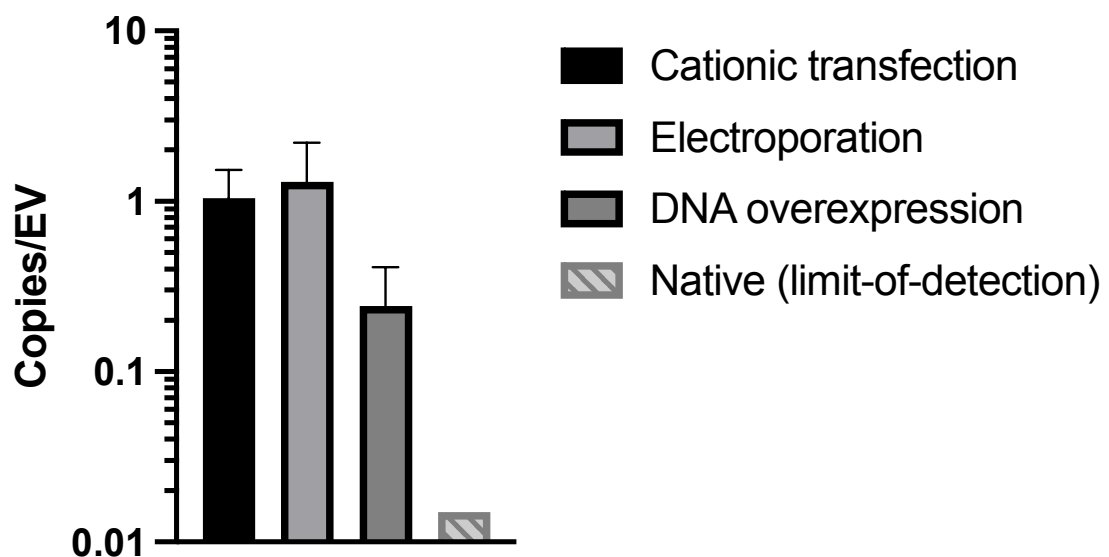
Figure 23. Comparison of different endogenous loading techniques in copies per EV, as measured by RT-PCR and NTA.

In **Chapter 5**, we sought to utilize the exogenous sonication loading technique in order to load multiple RNAs into a single EV population, and we saw no dramatic changes in EV size or morphology as a result of sonication. After demonstrating this, we screened combinations of five miRNAs identified from literature in an *in vitro* macrophage inflammation model and found that the combination of miR-146a-5p, miR-155-5p, and miR-223-3p demonstrated superior anti-inflammatory effects over the single miRNAs alone. Cytokine targets of this combination were also identified *in vitro*. Finally, we applied this EV-loaded combination into a mouse endotoxemia model and found a 23% reduction in IL-6 (p=0.07). This result confirmed that sonication loading is a viable technique for loading any combination of small RNA in relative proportions, and that combining multiple small RNAs may enhance a desired therapeutic effect.

Taken together, these results contributed to the understanding of RNA export from cells, determined important numbers for the wider community to reference, innovated novel techniques for RNA overexpression and bioactivity, and discovered a novel combination therapeutic for fighting inflammatory disease.

Future directions

The research presented here advances knowledge of small RNA loading into EVs, however, much more work needs to be done before these techniques can be implemented in a clinical setting. Figure 24 (an updated version of Figure 7) shows a descriptive comparison of various loading techniques, incorporating findings from this work.
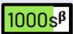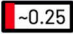
		EV loading efficiency*	EV integrity	Scalability	Optimization still needed
Exogenous	Electroporation	<1[α] (red)	red	red	green
Exogenous	Sonication	1000s[β] (green)	yellow	red	green
Endogenous	Electroporation	~1 (red)	yellow	green	yellow
Endogenous	Cationic transfection	~1 (red)	red	yellow	red
Endogenous	DNA overexpression	~0.25 (red)	green	green	red

Figure 24. Comparison of various exogenous and endogenous loading techniques according to current knowledge including results from this thesis. EV loading efficiency describes the copies RNA/EV. EV integrity describes structural and functional soundness of final product. Scalability describes ability to scale up to a high-throughput industrial process. Optimization still needed describes further research required to optimize this technique. Red, yellow, and green describe how well each technique fulfills each parameter. * copies/EV. [α]Data from [109]. [β] Data from [107].

For cationic transfection, if this technology is to be viable, new reagents would need to be developed that do not contaminate the final EV product or have residual binding. Many chemical reagents are lipid-based or nanoparticle-based, and thus can easily be incorporated into EVs or co-isolate with them. For electroporation, RNA aggregation is an issue that may hamper adoption of this technique. One possible solution could be the use of cuvettes with polymer-based electrodes instead of metal electrodes, which would likely abolish aggregation [109]. Impressive advances in high-throughput continuous-flow microfluidic electroporation devices allow for large scale introduction of nucleic acid into cells, including a recent iteration that introduced mRNA into 20 million human T cells per minute at a 95% transfection efficiency [115], [340]. Additionally, cationic transfection and electroporation allow for chemical modification in the RNA strand. For these reasons, we view electroporation as the most promising near-term solution for endogenous loading into EVs.

However, in the long-term, DNA overexpression may possess advantages over electroporation. In terms of cost, DNA overexpression would require no RNA or DNA synthesis or specialized equipment at all, since desired sequences could be stably integrated into the genome. Additionally, producer cells would not undergo any acute stresses like chemical toxicity or physical/electrical forces. However, further understanding of cellular miRNA secretion is required to enable engineering opportunities. Ideally, cellular engineering techniques could be developed that promote the secretion of any sequence, to avoid sequence-dependent cell lines that will complicate manufacturing and production. Relatedly, for all endogenous techniques, strategies to avoid the secondary effects of the therapeutic small RNA on the producer cell should be investigated. This would allow for standardized production of small RNA therapies without concern for negative or complicating effect on final EV product. Of course, this could also remove some positive secondary effects, such as differential protein or RNA secretion.

Finally, our studies on sonication loading indicate that this is a powerful method that needs only some further characterization before use in therapeutic development. This characterization could include reliable quantification of intravesicular RNA, comparison between different cell sources, biodistribution, dosing, and so on. Once these questions are resolved, sonication could be a leading method for small RNA delivery in medicine. Additionally, the specific miRNA combination that we discovered, miR-146a, miR-155, and miR-223, should be studied for why they work so well together. A broader screen of miRNA and siRNA could find further combinations that are synergistic and may outperform this combination.

Appendix A: Additional protein-based vehicles for RNA delivery[6]

<u>Albumin</u>

Human serum albumin (HSA) is the most abundant protein in blood. It is distributed throughout the blood circulation and has exceptionally low immunogenicity and long half-life [341]. Previous success in harnessing HSA as a drug delivery vehicle makes it attractive for RNA delivery. HSA, like RNA, is a negatively charged molecule and the two do not spontaneously interact. However, Sarett *et al.* showed that lipophilic DSPE-PEG-conjugated siRNA was capable of binding endogenous HSA [342]. In a mouse model, HSA-binding reduced renal clearance and improved half-life of modified siRNA, and enhanced delivery to the tumor, achieving a tumor:liver delivery ratio over 40 (in comparison to ~3 for jetPEI, a cationic polymer). Others have modified the charge of the albumin to generate electrostatic attraction with RNA. Han *et al.* modified the isoelectric point of bovine albumin with ethylenediamine, making it positively charged at the pH of blood and able to spontaneously form complexes with negative RNA [343]. In mice, these molecules were distributed primarily to the lungs (5-12:1 lung:liver delivery ratio) and reduced the number of lung cancer metastases by over half. Wen *et al.* made RNA-HSA complexes by mixing unmodified molecules at pH 4, at which HSA is positively charged. Thermal treatment crosslinked the complexes, which remained stable at blood pH [344].

---

6 This section is adapted from [409].

<u>p19</u>

The p19 protein of the Tombusvirus genus has been developed as a siRNA delivery vehicle by a number of groups, but has not shown success in any *in vivo* environments. Originally detected as function-ambiguous subgenomic RNA in the tomato bushy stunt plant (and named for its size), the 19 kiloDalton (kDa) protein was found to greatly enhance systemic invasion of plants [345]–[348]. Voinnet *et al.* showed that p19 was a viral counter-defense to posttranscriptional gene silencing (PTGS), the analogue of RNAi in the plant kingdom [349]. Further studies elucidated that p19 dimers selectively bind to small double-stranded RNA (dsRNA) ~19-21 bp in length with subnanomolar affinity, behaving as a "molecular caliper" [350]–[352]. Engineering of the p19 protein began with Cheng *et al.* enhancing dsRNA affinity by linking two p19 monomers [353]. Choi *et al.* fused the ephrin mimetic peptide YSA to p19 monomers to effectively target siRNA to EphA2-expressing cancer cells *in vitro* [354]. This group saw a ~6- to 36-fold extension of siRNA half-life in 30% serum when first incubated with p19-YSA. Additionally, they saw protein-RNA dissociation at endosomal pH. Danielson *et al.* fused a cell-penetrating Tat peptide to p19 dimers, and saw substantial knockdown *in vitro* only when co-treated with cell-penetrating endosomolytic compound E5-TAT [355]. Yang *et al.* performed yeast-display directed evolution on p19, ultimately finding a double mutant with 160-fold greater binding affinity [356]. The p19 monomers were then fused to an EGFR-targeting domain and added to cells *in vitro*, along with an EGFR-targeting endosomolytic compound. Experiments showed that higher affinity led to greater silencing efficacy. The authors attributed this to increased uptake as well as enhanced intracellular pharmacodynamics.

Some designs have utilized antibodies as targeting moieties for specific delivery, but others have conjugated RNA directly to antibodies themselves [357]. Cuellar *et al.* utilized THIOMAB antibodies covalently bound to siRNA to form antibody-siRNA conjugates [358]. These antibodies are referred to as THIOMABs since they contained an exposed cysteine residue on each heavy chain to which the cargo was attached, allowing for production of homogeneous antibody-drug conjugates [359]. These constructs targeted tumor cells in mice, but were limited by endosomal entrapment and intracellular clearance. Xia *et al.* used streptavidin-conjugated antibodies and biotinylated siRNA to deliver *in vitro*, but also saw issues with endosomal degradation [360]. Sugo *et al.* conjugated thiol-reactive siRNA to a single-chain variable fragment (scFv) antibody for CD71 in order to deliver to mouse heart and skeletal muscle [361]. Remarkably, they observed persistent knockdown (30% and 62%, respectively) even one month later.

PKR

Protein Kinase R (PKR) is an interferon-induced kinase that is a key component in the antiviral innate immune pathway in eukaryotes. PKR is activated by double stranded viral RNAs, a byproduct of transcription in RNA/DNA viruses. Once activated, PKR phosphorylates eukaryotic initiation factor-2, which inhibits translation of viral proteins and subsequent viral spread.

PKR is one of the well-studied proteins with canonical dsRNA binding motifs. The protein contains two dsRNA binding domains (DRBD), one at the N- terminus and one at the C-terminus connected by a long linker [362]. The DRBDs consist of two tandem binding motifs, dsRBM1

and dsRBM2 joined by a 20-residue linker to form the αββα fold. It is thought that dsRNA

binds to PKR in a sequence independent manner. The crystal structure shows the protein

spanning 16 bp of the dsRNA and primarily interacting with 2′-hydroxyls and the phosphate

backbone of the dsRNA [363].

Eguchi *et al.* developed the fusion protein PTD-DRBD, now commercially known as

Transductin, comprised of the PKR binding domains and a Tat peptide that showed effective

siRNA delivery in various cell lines. However, *in vivo* studies showed an observed non-specific

cell uptake, which caused several side effects [364]. It was therefore thought that replacing the

Tat sequence with a receptor ligand would allow for specific targeting. Geoghegan *et al.* replaced

the Tat peptide with B2 peptide sequence that binds to a recombinant transferrin receptor. The

fusion protein was shown to effectively knockdown HPRT in HeLa cells and showed TfR

mediated uptake. It was also noted that knockdown was enhanced with chloroquine suggesting

the endosomal entrapment of the complexed protein [365]. In 2014, Lui *et al.* developed a

multiagent siRNA delivery system consisting of the dsRBD domain, an EGFR clustering

domain, and a pore-forming protein Perfringolysin O (PFO) domain to induce endosomal escape.

The delivery system showed efficient silencing in vitro but did not achieve delivery in vivo due

to the dissociation of the siRNA from the protein [366].

Viral vectors and virus-like particles

~70% of gene therapy clinical trials have utilized modified viruses, starting in 1989, before the

discovery of RNAi [367]. Some viruses deliver genetic material for transient expression, while

others integrate into the genome, allowing for long-term expression. Long-term expression is

usually preferred, though when coupled with broad tropism (which many viruses exhibit) can be dangerous [368]. Additionally, genome integration can be carcinogenic [369]. Furthermore, in one case, extended genomic expression of exogenous shRNA in the liver consistently led to fatality in mice due to saturation of RNAi machinery [370]. Other concerns that have cooled interest in viral delivery are potential immunogenicity, viral sequence mutation, and difficulty in large-scale manufacture [371], [372]. However, there are also advantages to using viral vectors. Viruses have been evolutionarily honed for delivery to the mammalian cell cytoplasm (and nucleus), and they do so extremely efficiently and in low doses. Additionally, viruses have recently been approved by the FDA for multiple diseases: the treatment of inoperable melanoma, as an ocular gene delivery vehicle for hereditary retinal dystrophy, and for the transfection of chimeric antigen receptor T-cells. There are many reviews that focus on viral vectors for gene delivery [373]–[375]. There have been strategies to improve viral molecules for targeting, including pseudotyping and introducing adaptor and binding domains [368], [376]. Other attempts to optimize viral vectors as drug delivery vehicles are ongoing as well [377], [378].

Heterologous expression of the major structural proteins of viruses leads to the self-assembly of virus-like particles (VLPs). VLPs have similar structural formation of the parental virus without any secondary proteins or genomic data, and thereby forego some of the concerns with viral delivery discussed above. Unlike viruses, VLPs can be produced in high-yield expression systems such as *E. coli* or insect cells and are more easily manipulable. All VLPs discussed here are ~24-40 nm in diameter. A common strategy available with some VLPs is encapsulation of cargo via disassembly-reassembly, whereby reduction of disulfide bonds leads to VLP dissociation and dialysis into a oxidizing environment in the presence of nucleic acids leads to

packaging [379]. Bousarghin *et al.* utilized this strategy with a VLP based on human papillomavirus virus (HPV) capsid protein L1, and encapsulated plasmid DNA that expressed shRNA [380]. This shRNA targeted p53-inhibiting proteins, and halved tumor weight in a mouse model of HPV-caused cervical cancer. The same disassembly-reassembly strategy was used in VLPs based on JC virus by two different groups [381], [382]. Chou *et al.* injected VLPs containing IL-10 shRNA into mice along with immunogenic LPS, and saw a massive reduction of IL-10 and TNF-α in the bloodstream, by 93% and 81%, respectively, and improved mouse survival. Hoffmann *et al.* performed extensive *in vivo* studies looking at delivery of VLP-siRNA to the tibia and lumbar vertebrae in mice. They observed up to a 40% decrease in RANKL mRNA that was dose-dependent and sustained with multiple injections.

A second strategy is to encapsulate the RNA through binding to the internal face of a capsid. Often, as in the case of the coat protein from bacteriophage MS2, the VLP will only form when stabilized by the presence of specific RNA sequences. Ashley *et al.* co-packaged four different siRNA molecules (~84 molecules/VLP) into MS2 VLPs, finding that a specific sequence was not required for them [383]. They also conjugated a peptide for targeting and saw a remarkable increase in endocytic specificity *in vitro*. Pan *et al.* packaged pre-miR-146a into MS2 VLPs using a specific sequence called a *pac* site and then conjugated a TAT peptide [384]. In mice, they saw almost equal concentration of the miRNA in plasma, lung, spleen, and kidney. Galaway *et al.* packaged siRNA into MS2 VLPs using a specific "TR" sequence, and later conjugated transferrin for targeting [385]. Fang *et al.* used a specific hairpin to load miR-30 into a VLP derived from the bacteriophage Qβ [386]. A third strategy was employed by Choi *et al.*, wherein they made a chimera of truncated Hepatitus B Virus (HBV) capsid protein, RGD peptide (for

targeting), and p19 (for RNA binding) [387], [388]. This construct greatly reduced tumor size in a mouse model. A fourth strategy involves nano-scale self-assembled protein structures that are not virally derived: nanocages. In work by Lee *et al.*, each ferritin-based nanocage was designed to display 24 polypeptides with the following constitution: lysosome-exclusive cleavable peptide – cationic protamine-derived peptide (which associated with siRNA) – EGFR-targeting affibody – cell-penetrating Tat peptide [389]. Likewise, Guan *et al.* designed a heat shock protein-based nanocage that displayed an arginine-rich peptide for cell penetration (see below) [390].

Naturally occurring cationic peptides

Cationic peptides that have been used for small RNA delivery have been covered by Shukla *et al.* [391]. In general, vehicles that display a high concentration of positive charge often suffer due to high retention in all tissues, including those that are not being targeted [392], [393]. Here we briefly discuss naturally occurring cationic peptides. Protamine is a naturally-occuring peptide with a high percentage of arginine (67%) that is FDA approved. In nature, protamine condenses DNA of fish sperm for delivery to the nucleus of an egg. This property has led to research into its potential as an siRNA carrier. In one attempt, siRNA as well as cholesterol were condensed by protamine into a nanocomplex that showed preferential endocytosis into liver cells *in vitro* [394], [395]. Protamine has also been fused to antibodies and antibody fragments for targeted siRNA delivery to tumors, and shown inhibition of tumor genes in mouse models [357], [396]–[398]. Some groups have also utilized atelocollagen, which is collagen treated with pepsin, as a small RNA delivery vehicle [399]–[402]. Other groups have used gelatin, another collagen derivative.

Cell-penetrating and endosomolytic peptides

Much focus has been directed at devising simple peptides for cytoplasmic delivery of siRNA. Cell-penetrating and endosomolytic peptides interact with the plasma membrane or the endosome membrane, respectively, in a biophysical manner in order to pass through the bilayer. These peptides are most effectively used in conjunction with targeting moieties since they are nonspecific and will interact with any cell type. This promiscuity contributes to their overall toxicity [403]. There have been a number of reviews on these peptides in the context of siRNA delivery [404]–[406]. Briefly, cationic arginine-rich peptides, such as the Tat peptide, interact with negatively charged phospholipids on the cell surface and can create transient pores in the membrane. Amphipathic peptides insert themselves into the lipid bilayer and can traverse the plasma membrane in this manner. These mechanisms are also related to endocytosis, however, and can lead to accumulation in the endosome [403]. Endosomolytic peptides are specifically designed to be reactive to the low pH environment. Fusogenic peptides change confirmation to become amphipathic helices which fuse to and disrupt the endosome. Some peptides have masked reactive moieties that are revealed through a pH-sensitive chemical reaction. Proton buffering peptides have weak bases and act as a proton sponge, accumulating protons and causing osmotic swelling and/or rupture. Some light-activated peptides have even been developed for endosomolytic escape. There are ongoing attempts to design peptides that exhibit both cell-penetrating and endosomolytic capabilities [407].

Bibliography

[1]   S. Y. Wu, G. Lopez-Berestein, G. a Calin, and A. K. Sood, "RNAi therapies: drugging the undruggable.," *Sci. Transl. Med.*, vol. 6, no. 240, p. 240ps7, 2014.

[2]   L. Alvarez-Erviti, Y. Seow, H. Yin, C. Betts, S. Lakhal, and M. J. A. Wood, "Delivery of siRNA to the mouse brain by systemic injection of targeted exosomes," *Nat. Biotechnol.*, vol. 29, no. 4, pp. 341–345, 2011.

[3]   L. Stevanato, L. Thanabalasundaram, N. Vysokov, and J. D. Sinden, "Investigation of content, stoichiometry and transfer of miRNA from human neural stem cell line derived exosomes," *PLoS One*, vol. 11, no. 1, p. e0146353, Jan. 2016.

[4]   R. Reshke *et al.*, "Reduction of the therapeutic dose of silencing RNA by packaging it in extracellular vesicles via a pre-microRNA backbone," *Nat. Biomed. Eng.*, 2020.

[5]   M. Piffoux, J. Volatron, A. K. A. Silva, and F. Gazeau, "Thinking quantitatively of rna-based information transfer via extracellular vesicles: Lessons to learn for the design of rna-loaded evs," *Pharmaceutics*, vol. 13, no. 11. Multidisciplinary Digital Publishing Institute, p. 1931, 15-Nov-2021.

[6]   J. R. Chevillet *et al.*, "Quantitative and stoichiometric analysis of the microRNA content of exosomes," *Proc. Natl. Acad. Sci. U. S. A.*, vol. 111, no. 41, pp. 14888–14893, Oct. 2014.

[7]   M. Albanese *et al.*, "MicroRNAs are minor constituents of extracellular vesicles that are rarely delivered to target cells," *PLoS Genet.*, vol. 17, no. 12, p. e1009951, Dec. 2021.

[8]   J. C. Akers *et al.*, "miRNA contents of cerebrospinal fluid extracellular vesicles in glioblastoma patients," *J. Neurooncol.*, vol. 123, no. 2, pp. 205–216, Jun. 2015.

[9]   A. Fire, S. Xu, M. K. Montgomery, S. A. Kostas, S. E. Driver, and C. C. Mello, "Potent

and specific genetic interference by double-stranded RNA in Caenorhabditis elegans," *Nature*, vol. 391, no. 6669, pp. 806–811, 1998.

[10] A. Fire, S. Xu, M. K. Montgomery, S. A. Kostas, S. E. Driver, and C. C. Mello, "Potent and specific genetic interference by double-stranded RNA in caenorhabditis elegans," *Nature*, 1998.

[11] S. M. Hammond, E. Bernstein, D. Beach, and G. J. Hannon, "An RNA-directed nuclease mediates post-transcriptional gene silencing in Drosophila cells," *Nature*, vol. 404, no. 6775, pp. 293–296, Mar. 2000.

[12] P. D. Zamore, T. Tuschl, P. A. Sharp, and D. P. Bartel, "RNAi: Double-stranded RNA directs the ATP-dependent cleavage of mRNA at 21 to 23 nucleotide intervals," *Cell*, vol. 101, no. 1, pp. 25–33, Mar. 2000.

[13] S. M. Elbashir, W. Lendeckel, and T. Tuschl, "RNA interference is mediated by 21- and 22-nucleotide RNAs," *Genes Dev.*, vol. 15, no. 2, pp. 188–200, Jan. 2001.

[14] S. M. Elbashir, J. Harborth, W. Lendeckel, A. Yalcin, K. Weber, and T. Tuschl, "Duplexes of 21-nucleotide RNAs mediate RNA interference in cultured mammalian cells," *Nature*, vol. 411, no. 6836, pp. 494–498, May 2001.

[15] E. Bernstein, A. A. Caudy, S. M. Hammond, and G. J. Hannon, "Role for a bidentate ribonuclease in the initiation step of RNA interference," *Nature*, vol. 409, no. 6818, pp. 363–366, Jan. 2001.

[16] J. J. Song, S. K. Smith, G. J. Hannon, and L. Joshua-Tor, "Crystal structure of argonaute and its implications for RISC slicer activity," *Science (80-.).*, vol. 305, no. 5689, pp. 1434–1437, Sep. 2004.

[17] J. Liu *et al.*, "Argonaute2 is the catalytic engine of mammalian RNAi," *Science (80-.).*,

vol. 305, no. 5689, pp. 1437–1441, Sep. 2004.

[18]   J. O'Brien, H. Hayder, Y. Zayed, and C. Peng, "Overview of microRNA biogenesis, mechanisms of actions, and circulation," *Frontiers in Endocrinology*, vol. 9, no. AUG. Frontiers Media S.A., p. 402, 03-Aug-2018.

[19]   M. Ha and V. N. Kim, "Regulation of microRNA biogenesis," *Nat. Rev. Mol. Cell Biol. 2014 158*, vol. 15, no. 8, pp. 509–524, Jul. 2014.

[20]   Y. K. Kim, B. Kim, and V. N. Kim, "Re-evaluation of the roles of DROSHA, Exportin 5, and DICER in microRNA biogenesis," *Proc. Natl. Acad. Sci. U. S. A.*, vol. 113, no. 13, pp. E1881–E1889, Mar. 2016.

[21]   D. Völler *et al.*, "Argonaute Family Protein Expression in Normal Tissue and Cancer Entities," *PLoS One*, vol. 11, no. 8, p. e0161165, Aug. 2016.

[22]   P. H. Patel, S. A. Barbee, and J. T. Blankenship, "GW-bodies and P-bodies constitute two separate pools of sequestered non-translating RNAs," *PLoS One*, vol. 11, no. 3, Mar. 2016.

[23]   A. Jakymiw *et al.*, "The role of GW/P-bodies in RNA processing and silencing," *J. Cell Sci.*, vol. 120, no. 8, pp. 1317–1323, Apr. 2007.

[24]   A. Eulalio, I. Behm-Ansmant, D. Schweizer, and E. Izaurralde, "P-Body Formation Is a Consequence, Not the Cause, of RNA-Mediated Gene Silencing," *Mol. Cell. Biol.*, vol. 27, no. 11, pp. 3970–3981, Jun. 2007.

[25]   C. J. Stavast and S. J. Erkeland, "The Non-Canonical Aspects of MicroRNAs: Many Roads to Gene Regulation," *Cells*, vol. 8, no. 11. Multidisciplinary Digital Publishing Institute (MDPI), 19-Nov-2019.

[26]   P. T. Nelson *et al.*, "A novel monoclonal antibody against human Argonaute proteins

reveals unexpected characteristics of miRNAs in human blood cells," *RNA*, vol. 13, no. 10, pp. 1787–1792, Oct. 2007.

[27] D. Cifuentes *et al.*, "A novel miRNA processing pathway independent of dicer requires argonaute2 catalytic activity," *Science (80-.).*, vol. 328, no. 5986, pp. 1694–1698, Jun. 2010.

[28] S. Cheloufi, C. O. Dos Santos, M. M. W. Chong, and G. J. Hannon, "A dicer-independent miRNA biogenesis pathway that requires Ago catalysis," *Nature*, vol. 465, no. 7298, pp. 584–589, Apr. 2010.

[29] S. Yang *et al.*, "Conserved vertebrate mir-451 provides a platform for Dicer-independent, Ago2-mediated microRNA biogenesis," *Proc. Natl. Acad. Sci. U. S. A.*, vol. 107, no. 34, pp. 15163–15168, Aug. 2010.

[30] M. Yoda *et al.*, "Poly(A)-specific ribonuclease mediates 3'-end trimming of argonaute2-cleaved precursor micrornas," *Cell Rep.*, vol. 5, no. 3, pp. 715–726, 2013.

[31] M. Xie *et al.*, "Mammalian 5′-capped microRNA precursors that generate a single microRNA," *Cell*, vol. 155, no. 7, pp. 1568–1580, Dec. 2013.

[32] I. Heo *et al.*, "Mono-uridylation of pre-microRNA as a key step in the biogenesis of group II let-7 microRNAs," *Cell*, vol. 151, no. 3, pp. 521–532, Oct. 2012.

[33] J. Xu, Y. Feng, A. Jeyaram, S. M. Jay, L. Zou, and W. Chao, "Circulating Plasma Extracellular Vesicles from Septic Mice Induce Inflammation via MicroRNA- and TLR7-Dependent Mechanisms," *J. Immunol.*, 2018.

[34] J. Winter, S. Jung, S. Keller, R. I. Gregory, and S. Diederichs, "Many roads to maturity: MicroRNA biogenesis pathways and their regulation," *Nature Cell Biology*, vol. 11, no. 3. Nature Publishing Group, pp. 228–234, 2009.

[35] D. E. Kuhn, M. M. Martin, D. S. Feldman, A. V. Terry, G. J. Nuovo, and T. S. Elton, "Experimental validation of miRNA targets," *Methods*, vol. 44, no. 1, pp. 47–54, Jan. 2008.

[36] V. Agarwal, G. W. Bell, J. W. Nam, and D. P. Bartel, "Predicting effective microRNA target sites in mammalian mRNAs," *Elife*, vol. 4, no. AUGUST2015, Aug. 2015.

[37] M. E. Peter, "Targeting of mRNAs by multiple miRNAs: The next step," *Oncogene*, vol. 29, no. 15. Nature Publishing Group, pp. 2161–2164, 01-Mar-2010.

[38] L. Salmena, L. Poliseno, Y. Tay, L. Kats, and P. P. Pandolfi, "A ceRNA hypothesis: The rosetta stone of a hidden RNA language?," *Cell*, vol. 146, no. 3. Elsevier, pp. 353–358, 05-Aug-2011.

[39] S. Yonezawa, H. Koide, and T. Asai, "Recent advances in siRNA delivery mediated by lipid-based nanoparticles," *Advanced Drug Delivery Reviews*, vol. 154–155. Elsevier, pp. 64–78, 01-Jan-2020.

[40] A. D. Springer and S. F. Dowdy, "GalNAc-siRNA Conjugates: Leading the Way for Delivery of RNAi Therapeutics," *Nucleic Acid Therapeutics*, vol. 28, no. 3. Mary Ann Liebert Inc., pp. 109–118, 01-Jun-2018.

[41] I. V. Chernikov, V. V. Vlassov, and E. L. Chernolovskaya, "Current development of siRNA bioconjugates: From research to the clinic," *Frontiers in Pharmacology*, vol. 10, no. APR. Frontiers Media S.A., p. 444, 2019.

[42] H. Valadi, K. Ekström, A. Bossios, M. Sjöstrand, J. J. Lee, and J. O. Lötvall, "Exosome-mediated transfer of mRNAs and microRNAs is a novel mechanism of genetic exchange between cells," *Nat. Cell Biol.*, 2007.

[43] J. P. Nederveen, G. Warnier, A. Di Carlo, M. I. Nilsson, and M. A. Tarnopolsky,

"Extracellular Vesicles and Exosomes: Insights From Exercise Science," *Frontiers in Physiology*, vol. 11. Frontiers Media S.A., p. 1757, 01-Feb-2021.

[44]   C. A. Murphy *et al.*, "A review of the role of extracellular vesicles in neonatal physiology and pathology," *Pediatr. Res. 2020 902*, vol. 90, no. 2, pp. 289–299, Nov. 2020.

[45]   N. H. Pirolli, W. E. Bentley, and S. M. Jay, "Bacterial Extracellular Vesicles and the Gut-Microbiota Brain Axis: Emerging Roles in Communication and Potential as Therapeutics," *Advanced Biology*, vol. 5, no. 7. Adv Biol (Weinh), 01-Jul-2021.

[46]   G. Schiera, C. M. Di Liegro, and I. Di Liegro, "Extracellular Membrane Vesicles as Vehicles for Brain Cell-to-Cell Interactions in Physiological as well as Pathological Conditions," *Biomed Res. Int.*, vol. 2015, 2015.

[47]   M. Hassanpour, J. Rezaie, M. Nouri, and Y. Panahi, "The role of extracellular vesicles in COVID-19 virus infection," *Infect. Genet. Evol.*, vol. 85, p. 104422, Nov. 2020.

[48]   S. Fu, Y. Zhang, Y. Li, L. Luo, Y. Zhao, and Y. Yao, "Extracellular vesicles in cardiovascular diseases," *Cell Death Discovery*, vol. 6, no. 1. Nature Publishing Group, pp. 1–9, 30-Jul-2020.

[49]   P. pei Hou and H. zi Chen, "Extracellular vesicles in the tumor immune microenvironment," *Cancer Letters*, vol. 516. Elsevier, pp. 48–56, 28-Sep-2021.

[50]   E. R. Abels and X. O. Breakefield, "Introduction to Extracellular Vesicles: Biogenesis, RNA Cargo Selection, Content, Release, and Uptake," *Cellular and Molecular Neurobiology*, vol. 36, no. 3. NIH Public Access, pp. 301–312, 01-Apr-2016.

[51]   E. M. Veziroglu and G. I. Mias, "Characterizing Extracellular Vesicles and Their Diverse RNA Contents," *Frontiers in Genetics*, vol. 11. Frontiers Media S.A., p. 700, 17-Jul-2020.

[52]   M. Mathieu, L. Martin-Jaular, G. Lavieu, and C. Théry, "Specificities of secretion and

uptake of exosomes and other extracellular vesicles for cell-to-cell communication," *Nature Cell Biology*, vol. 21, no. 1. Nature Publishing Group, pp. 9–17, 02-Jan-2019.

[53] D. Fitzner *et al.*, "Selective transfer of exosomes from oligodendrocytes to microglia by macropinocytosis," *J. Cell Sci.*, vol. 124, no. 3, pp. 447–458, Feb. 2011.

[54] M. Chivet, C. Javalet, K. Laulagnier, B. Blot, F. J. Hemming, and R. Sadoul, "Exosomes secreted by cortical neurons upon glutamatergic synapse activation specifically interact with neurons," *J. Extracell. Vesicles*, vol. 3, no. 1, 2014.

[55] S. Kamerkar *et al.*, "Exosomes facilitate therapeutic targeting of oncogenic KRAS in pancreatic cancer," *Nature*, vol. 546, no. 7659, pp. 498–503, Jun. 2017.

[56] A. Matsumoto *et al.*, "Phosphatidylserine-deficient small extracellular vesicle is a major somatic cell-derived sEV subpopulation in blood," *iScience*, vol. 24, no. 8, p. 102839, Aug. 2021.

[57] D. J. Gibbings, C. Ciaudo, M. Erhardt, and O. Voinnet, "Multivesicular bodies associate with components of miRNA effector complexes and modulate miRNA activity," *Nat. Cell Biol. 2009 119*, vol. 11, no. 9, pp. 1143–1149, Aug. 2009.

[58] Y. S. Lee *et al.*, "Silencing by small RNAs is linked to endosomal trafficking," *Nat. Cell Biol.*, vol. 11, no. 9, pp. 1150–1156, Aug. 2009.

[59] A. Iavello, V. S. L. Frech, C. Gai, M. C. Deregibus, P. J. Quesenberry, and G. Camussi, "Role of Alix in miRNA packaging during extracellular vesicle biogenesis," *Int. J. Mol. Med.*, vol. 37, no. 4, pp. 958–966, Apr. 2016.

[60] M. L. Squadrito *et al.*, "Endogenous RNAs Modulate MicroRNA Sorting to Exosomes and Transfer to Acceptor Cells," *Cell Rep.*, vol. 8, no. 5, pp. 1432–1446, 2014.

[61] S. Ghosh, K. Mukherjee, Y. Chakrabarty, S. Chatterjee, B. Ghoshal, and S. N.

Bhattacharyya, "GW182 Proteins Restrict Extracellular Vesicle-Mediated Export of MicroRNAs in Mammalian Cancer Cells," *Mol. Cell. Biol.*, vol. 41, no. 5, Apr. 2021.

[62] A. Turchinovich, L. Weiz, A. Langheinz, and B. Burwinkel, "Characterization of extracellular circulating microRNA," *Nucleic Acids Res.*, vol. 39, no. 16, pp. 7223–7233, 2011.

[63] J. P. Tosar, F. Gámbaro, J. Sanguinetti, B. Bonilla, K. W. Witwer, and A. Cayota, "Assessment of small RNA sorting into different extracellular fractions revealed by high-throughput sequencing of breast cell lines," *Nucleic Acids Res.*, vol. 43, no. 11, pp. 5601–5616, Jun. 2015.

[64] M. Mittelbrunn *et al.*, "Unidirectional transfer of microRNA-loaded exosomes from T cells to antigen-presenting cells," *Nat. Commun.*, vol. 2, no. 1, pp. 1–10, Apr. 2011.

[65] Y. Li *et al.*, "Circular RNA is enriched and stable in exosomes: A promising biomarker for cancer diagnosis," *Cell Research*, vol. 25, no. 8. Nature Publishing Group, pp. 981–984, 03-Jul-2015.

[66] D. M. Pegtel *et al.*, "Functional delivery of viral miRNAs via exosomes," *Proc. Natl. Acad. Sci. U. S. A.*, vol. 107, no. 14, pp. 6328–6333, Apr. 2010.

[67] A. Montecalvo *et al.*, "Mechanism of transfer of functional microRNAs between mouse dendritic cells via exosomes," *Blood*, vol. 119, no. 3, pp. 756–766, Jan. 2012.

[68] C. Villarroya-Beltri *et al.*, "Sumoylated hnRNPA2B1 controls the sorting of miRNAs into exosomes through binding to specific motifs," *Nat. Commun.*, vol. 4, no. 1, pp. 1–10, Dec. 2013.

[69] L. Santangelo, G. Giurato, C. Cicchini, T. Alonzi, A. Weisz, and M. T. Correspondence, "The RNA-Binding Protein SYNCRIP Is a Component of the Hepatocyte Exosomal

Machinery Controlling MicroRNA Sorting," *CellReports*, vol. 17, pp. 799–808, 2016.

[70]   D. K. Jeppesen *et al.*, "Reassessment of Exosome Composition," *Cell*, vol. 177, no. 2, pp. 428-445.e18, 2019.

[71]   M. M. Temoche-Diaz *et al.*, "Distinct mechanisms of microrna sorting into cancer cell-derived extracellular vesicle subtypes," *Elife*, vol. 8, Aug. 2019.

[72]   R. Garcia-Martin *et al.*, "MicroRNA sequence codes for small extracellular vesicle release and cellular retention," *Nature*, vol. 601, no. 7893, pp. 446–451, Dec. 2022.

[73]   K. Mukherjee *et al.*, "Reversible HuR□micro RNA binding controls extracellular export of miR□122 and augments stress response," *EMBO Rep.*, vol. 17, no. 8, pp. 1184–1203, Aug. 2016.

[74]   Y. Teng *et al.*, "MVP-mediated exosomal sorting of miR-193a promotes colon cancer progression," *Nat. Commun.*, vol. 8, no. 1, pp. 1–16, Feb. 2017.

[75]   L. Statello *et al.*, "Identification of RNA-binding proteins in exosomes capable of interacting with different types of RNA: RBP-facilitated transport of RNAs into exosomes," *PLoS One*, 2018.

[76]   D. Koppers-Lalic *et al.*, "Nontemplated nucleotide additions distinguish the small RNA composition in cells from exosomes," *Cell Rep.*, vol. 8, no. 6, pp. 1649–1658, Sep. 2014.

[77]   J. P. Tosar, F. Gámbaro, J. Sanguinetti, B. Bonilla, K. W. Witwer, and A. Cayota, "Assessment of small RNA sorting into different extracellular fractions revealed by high-throughput sequencing of breast cell lines," *Nucleic Acids Res.*, vol. 43, no. 11, pp. 5601–5616, Apr. 2015.

[78]   E. E. Snell, P. D. Boyer, A. Meister, and C. C. Richardson, "Annual Review of Biochemistry," *Soil Sci.*, vol. 129, no. 5, pp. 325–326, 1980.

[79]   B. Mateescu *et al.*, "Obstacles and opportunities in the functional analysis of extracellular vesicle RNA - An ISEV position paper," *J. Extracell. Vesicles*, vol. 6, no. 1, 2017.

[80]   J. P. Tosar, K. Witwer, and A. Cayota, "Revisiting Extracellular RNA Release, Processing, and Function," *Trends in Biochemical Sciences*, vol. 46, no. 6. Trends Biochem Sci, pp. 438–445, 01-Jun-2021.

[81]   T. S. Chen, R. C. Lai, M. M. Lee, A. B. H. Choo, C. N. Lee, and S. K. Lim, "Mesenchymal stem cell secretes microparticles enriched in pre-microRNAs," *Nucleic Acids Res.*, vol. 38, no. 1, pp. 215–224, Oct. 2009.

[82]   H. Sork *et al.*, "Heterogeneity and interplay of the extracellular vesicle small RNA transcriptome and proteome," *Sci. Rep.*, vol. 8, no. 1, pp. 1–12, Jul. 2018.

[83]   F. Gámbaro *et al.*, "Stable tRNA halves can be sorted into extracellular vesicles and delivered to recipient cells in a concentration-dependent manner," *RNA Biol.*, 2019.

[84]   W. S. Toh, R. C. Lai, B. Zhang, and S. K. Lim, "MSC exosome works through a protein-based mechanism of action," *Biochemical Society Transactions*, vol. 46, no. 4. Portland Press Ltd, pp. 843–853, 09-Jul-2018.

[85]   A. Wittrup *et al.*, "Visualizing lipid-formulated siRNA release from endosomes and target gene knockdown," *Nat. Biotechnol.*, vol. 33, no. 8, pp. 870–876, Aug. 2015.

[86]   Y. Pei *et al.*, "Quantitative evaluation of siRNA delivery in vivo," *RNA*, vol. 16, no. 12, pp. 2553–2563, Dec. 2010.

[87]   S. Veldhoen, S. D. Laufer, A. Trampe, and T. Restle, "Cellular delivery of small interfering RNA by a non-covalently attached cell-penetrating peptide: Quantitative analysis of uptake and biological effect," *Nucleic Acids Res.*, vol. 34, no. 22, pp. 6561–6573, Dec. 2006.

[88]   K. R. Vrijsen *et al.*, "Cardiomyocyte progenitor cell-derived exosomes stimulate migration of endothelial cells," *Journal of Cellular and Molecular Medicine*. 2010.

[89]   S. Sahoo *et al.*, "Exosomes from human CD34+ stem cells mediate their proangiogenic paracrine activity," *Circ. Res.*, 2011.

[90]   R. C. Lai *et al.*, "Exosome secreted by MSC reduces myocardial ischemia/reperfusion injury," *Stem Cell Res.*, 2010.

[91]   O. P. B. Wiklander, M. Brennan, J. Lötvall, X. O. Breakefield, and S. E. L. Andaloussi, "Advances in therapeutic applications of extracellular vesicles," *Science Translational Medicine*. 2019.

[92]   I. K. Herrmann, M. J. A. Wood, and G. Fuhrmann, "Extracellular vesicles as a next-generation drug delivery platform," *Nature Nanotechnology*, vol. 16, no. 7. Nature Research, pp. 748–759, 01-Jul-2021.

[93]   X. Zhu *et al.*, "Comprehensive toxicity and immunogenicity studies reveal minimal effects in mice following sustained dosing of extracellular vesicles derived from HEK293T cells," *J. Extracell. Vesicles*, vol. 6, no. 1, Dec. 2017.

[94]   D. E. Murphy, O. G. de Jong, M. J. W. Evers, M. Nurazizah, R. M. Schiffelers, and P. Vader, "Natural or synthetic RNA delivery: A stoichiometric comparison of extracellular vesicles and synthetic nanoparticles," *Nano Lett.*, vol. 21, no. 4, pp. 1888–1895, Feb. 2021.

[95]   K. Bryniarski *et al.*, "Antigen-specific, antibody-coated, exosome-like nanovesicles deliver suppressor T-cell microRNA-150 to effector T cells to inhibit contact sensitivity," *J. Allergy Clin. Immunol.*, vol. 132, no. 1, pp. 170-181.e9, Jul. 2013.

[96]   S. Stremersch, R. E. Vandenbroucke, E. Van Wonterghem, A. Hendrix, S. C. De Smedt,

and K. Raemdonck, "Comparing exosome-like vesicles with liposomes for the functional cellular delivery of small RNAs," *J. Control. Release*, 2016.

[97]   S. Clejan and R. Bittman, "Kinetics of cholesterol and phospholipid exchange between Mycoplasma gallisepticum cells and lipid vesicles. Alterations in membrane cholesterol and protein content.," *J. Biol. Chem.*, vol. 259, no. 1, pp. 441–448, 1984.

[98]   F. R. Maxfield and G. van Meer, "Cholesterol, the central lipid of mammalian cells," *Curr. Opin. Cell Biol.*, vol. 22, no. 4, p. 422, Aug. 2010.

[99]   J. L. Richens *et al.*, "Spontaneous charged lipid transfer between lipid vesicles," *Sci. Rep.*, vol. 7, no. 1, pp. 1–10, Oct. 2017.

[100] P. D. Thomas and M. J. Poznansky, "Cholesterol transfer between lipid vesicles. Effect of phospholipids and gangliosides.," *Biochem. J.*, vol. 251, no. 1, p. 55, 1988.

[101] S. M. Elvington and J. W. Nichols, "Spontaneous, intervesicular transfer rates of fluorescent, acyl chain-labeled phosphatidylcholine analogs," *Biochim. Biophys. Acta - Biomembr.*, vol. 1768, no. 3, pp. 502–508, Mar. 2007.

[102] S. Guo *et al.*, "Intranasal Delivery of Mesenchymal Stem Cell Derived Exosomes Loaded with Phosphatase and Tensin Homolog siRNA Repairs Complete Spinal Cord Injury," *ACS Nano*, vol. 13, no. 9, pp. 10015–10028, Sep. 2019.

[103] A. J. O'Loughlin *et al.*, "Functional Delivery of Lipid-Conjugated siRNA by Extracellular Vesicles," *Mol. Ther.*, vol. 25, no. 7, pp. 1580–1587, Jul. 2017.

[104] M. C. Didiot *et al.*, "Exosome-mediated delivery of hydrophobically modified siRNA for huntingtin mRNA silencing," *Mol. Ther.*, vol. 24, no. 10, pp. 1836–1847, Oct. 2016.

[105] R. A. Haraszti *et al.*, "Optimized Cholesterol-siRNA Chemistry Improves Productive Loading onto Extracellular Vesicles," *Mol. Ther.*, vol. 26, no. 8, pp. 1973–1982, Aug.

2018.

[106] A. Biscans *et al.*, "Hydrophobicity of Lipid-Conjugated siRNAs Predicts Productive Loading to Small Extracellular Vesicles," *Mol. Ther.*, vol. 26, no. 6, pp. 1520–1528, Jun. 2018.

[107] T. N. Lamichhane *et al.*, "Oncogene Knockdown via Active Loading of Small RNAs into Extracellular Vesicles by Sonication," *Cell. Mol. Bioeng.*, 2016.

[108] D. S. Sutaria, M. Badawi, M. A. Phelps, and T. D. Schmittgen, "Achieving the Promise of Therapeutic Extracellular Vesicles: The Devil is in Details of Therapeutic Loading," *Pharmaceutical Research*. 2017.

[109] S. A. A. Kooijmans *et al.*, "Electroporation-induced siRNA precipitation obscures the efficiency of siRNA loading into extracellular vesicles," *J. Control. Release*, vol. 172, no. 1, pp. 229–238, Nov. 2013.

[110] T. N. Lamichhane, R. S. Raiker, and S. M. Jay, "Exogenous DNA loading into extracellular vesicles via electroporation is size-dependent and enables limited gene delivery," *Mol. Pharm.*, vol. 12, no. 10, pp. 3650–3657, Oct. 2015.

[111] G. Fuhrmann, A. Serio, M. Mazo, R. Nair, and M. M. Stevens, "Active loading into extracellular vesicles significantly improves the cellular uptake and photodynamic effect of porphyrins," *J. Control. Release*, 2015.

[112] R. C. de Abreu *et al.*, "Exogenous loading of miRNAs into small extracellular vesicles," *J. Extracell. Vesicles*, vol. 10, no. 10, p. e12111, Aug. 2021.

[113] D. Zhang, H. Lee, Z. Zhu, J. K. Minhas, and Y. Jin, "Enrichment of selective miRNAs in exosomes and delivery of exosomal miRNAs in vitro and in vivo," *Am. J. Physiol. - Lung Cell. Mol. Physiol.*, vol. 312, no. 1, pp. L110–L121, Nov. 2016.

[114] A. Jeyaram *et al.*, "Enhanced Loading of Functional miRNA Cargo via pH Gradient Modification of Extracellular Vesicles," *Mol. Ther.*, vol. 28, no. 3, pp. 975–985, Mar. 2020.

[115] J. Brooks *et al.*, "High Throughput and Highly Controllable Methods for In Vitro Intracellular Delivery," *Small*, vol. 16, no. 51. John Wiley & Sons, Ltd, p. 2004917, 01-Dec-2020.

[116] C. Luft and R. Ketteler, "Electroporation Knows No Boundaries: The Use of Electrostimulation for siRNA Delivery in Cells and Tissues," *Journal of Biomolecular Screening*, vol. 20, no. 8. SAGE Publications, pp. 932–942, 24-Sep-2015.

[117] C. Rosazza, A. Buntz, T. Rieß, D. Wöll, A. Zumbusch, and M. P. Rols, "Intracellular tracking of single-plasmid DNA particles after delivery by electroporation," *Mol. Ther.*, vol. 21, no. 12, pp. 2217–2226, Dec. 2013.

[118] C. Rosazza, E. Phez, J. M. Escoffre, L. Cézanne, A. Zumbusch, and M. P. Rols, "Cholesterol implications in plasmid DNA electrotransfer: Evidence for the involvement of endocytotic pathways," in *International Journal of Pharmaceutics*, 2012, vol. 423, no. 1, pp. 134–143.

[119] A. Paganin-Gioanni, E. Bellard, J. M. Escoffre, M. P. Rols, J. Teissié, and M. Golzio, "Direct visualization at the single-cell level of siRNA electrotransfer into cancer cells," *Proc. Natl. Acad. Sci. U. S. A.*, vol. 108, no. 26, pp. 10443–10447, Jun. 2011.

[120] S. Sachdev, S. Feijoo Moreira, Y. Keehnen, L. Rems, M. T. Kreutzer, and P. E. Boukany, "DNA-membrane complex formation during electroporation is DNA size-dependent," *Biochim. Biophys. Acta - Biomembr.*, vol. 1862, no. 2, p. 183089, Feb. 2020.

[121] E. Dauty and A. S. Verkman, "Actin cytoskeleton as the principal determinant of size-

dependent DNA mobility in cytoplasm: A new barrier for non-viral gene delivery," *J. Biol. Chem.*, vol. 280, no. 9, pp. 7823–7828, Mar. 2005.

[122] G. L. Lukacs, P. Haggie, O. Seksek, D. Lechardeur, N. Freedman, and A. S. Verkman, "Size-dependent DNA mobility in cytoplasm and nucleus," *J. Biol. Chem.*, vol. 275, no. 3, pp. 1625–1629, Jan. 2000.

[123] J. Wang *et al.*, "MiR-101a loaded extracellular nanovesicles as bioactive carriers for cardiac repair," *Nanomedicine Nanotechnology, Biol. Med.*, vol. 27, p. 102201, Jul. 2020.

[124] L. Chen *et al.*, "Epigenetic regulation of connective tissue growth factor by MicroRNA-214 delivery in exosomes from mouse or human hepatic stellate cells," *Hepatology*, vol. 59, no. 3, pp. 1118–1129, Mar. 2014.

[125] Q. Chen *et al.*, "Bone marrow mesenchymal stem cell-secreted exosomes carrying microRNA-125b protect against myocardial ischemia reperfusion injury via targeting SIRT7," *Mol. Cell. Biochem.*, vol. 465, no. 1–2, pp. 103–114, Feb. 2020.

[126] Z. Wei *et al.*, "miRNA-181a over-expression in mesenchymal stem cell-derived exosomes influenced inflammatory response after myocardial ischemia-reperfusion injury," *Life Sci.*, vol. 232, p. 116632, Sep. 2019.

[127] G. Lou *et al.*, "Exosomes derived from miR-122-modified adipose tissue-derived MSCs increase chemosensitivity of hepatocellular carcinoma," *J. Hematol. Oncol.*, vol. 8, no. 1, Oct. 2015.

[128] A. Stamatikos *et al.*, "Exosome-Mediated Transfer of Anti-miR-33a-5p from Transduced Endothelial Cells Enhances Macrophage and Vascular Smooth Muscle Cell Cholesterol Efflux," *Hum. Gene Ther.*, vol. 31, no. 3–4, p. 219, Feb. 2020.

[129] S. Baldari, G. Di Rocco, A. Magenta, M. Picozza, and G. Toietta, "Extracellular Vesicles–

Encapsulated MicroRNA-125b Produced in Genetically Modified Mesenchymal Stromal Cells Inhibits Hepatocellular Carcinoma Cell Proliferation," *Cells*, vol. 8, no. 12, Dec. 2019.

[130] N. Kosaka, H. Iguchi, Y. Yoshioka, K. Hagiwara, F. Takeshita, and T. Ochiya, "Competitive interactions of cancer cells and normal cells via secretory microRNAs," *J. Biol. Chem.*, vol. 287, no. 2, pp. 1397–1405, Jan. 2012.

[131] M. Katakowski *et al.*, "Exosomes from marrow stromal cells expressing miR-146b inhibit glioma growth," *Cancer Lett.*, vol. 335, no. 1, pp. 201–204, 2013.

[132] B. K. Shimada *et al.*, "Extracellular miR-146a-5p Induces Cardiac Innate Immune Response and Cardiomyocyte Dysfunction," *ImmunoHorizons*, vol. 4, no. 9, pp. 561–572, 2020.

[133] S. Wang *et al.*, "Role of extracellular microRNA-146a-5p in host innate immunity and bacterial sepsis," *iScience*, vol. 24, no. 12, p. 103441, Dec. 2021.

[134] T. Van Der Poll, F. L. Van De Veerdonk, B. P. Scicluna, and M. G. Netea, "The immunopathology of sepsis and potential therapeutic targets," *Nature Reviews Immunology*, vol. 17, no. 7. Nature Publishing Group, pp. 407–420, 24-Apr-2017.

[135] S. M. Opal and T. van der Poll, "Endothelial barrier dysfunction in septic shock," *Journal of Internal Medicine*. 2015.

[136] J. C. Mira *et al.*, "Sepsis pathophysiology, chronic critical illness, and persistent inflammation-immunosuppression and catabolism syndrome," *Crit. Care Med.*, vol. 45, no. 2, pp. 253–262, Feb. 2017.

[137] J. S. Boomer, J. M. Green, and R. S. Hotchkiss, "The changing immune system in sepsis is individualized immuno-modulatory therapy the answer?," *Virulence*, vol. 5, no. 1.

Taylor & Francis, pp. 45–56, 2014.

[138] A. Rhodes *et al.*, "Surviving Sepsis Campaign: International Guidelines for Management of Sepsis and Septic Shock: 2016," *Intensive Care Med.*, vol. 43, no. 3, pp. 304–377, Jan. 2017.

[139] K. E. Rudd *et al.*, "Global, regional, and national sepsis incidence and mortality, 1990–2017: analysis for the Global Burden of Disease Study," *Lancet*, vol. 395, no. 10219, pp. 200–211, Jan. 2020.

[140] J. Cohen, S. Opal, and T. Calandra, "Sepsis studies need new direction," *The Lancet Infectious Diseases*, vol. 12, no. 7. Elsevier, pp. 503–505, 01-Jul-2012.

[141] R. C. Bone *et al.*, "Definitions for sepsis and organ failure and guidelines for the use of innovative therapies in sepsis," in *Chest*, 1992.

[142] W.-T. Hsu *et al.*, "Effect of Renin-Angiotensin-Aldosterone System Inhibitors on Short-Term Mortality After Sepsis," *Hypertension*, vol. 75, no. 2, pp. 483–491, 2020.

[143] L. Margolis and Y. Sadovsky, "The biology of extracellular vesicles: The known unknowns," *PLoS Biol.*, vol. 17, no. 7, pp. e3000363–e3000363, Jul. 2019.

[144] F. Meziani, X. Delabranche, P. Asfar, and F. Toti, "Bench-to-bedside review: circulating microparticles--a new player in sepsis?," *Crit. Care*, vol. 14, no. 5, p. 236, 2010.

[145] G. Woth, M. Tőkés-Füzesi, T. Magyarlaki, G. L. Kovács, I. Vermes, and D. Mühl, "Activated platelet-derived microparticle numbers are elevated in patients with severe fungal (Candida albicans) sepsis," *Ann. Clin. Biochem. Int. J. Lab. Med.*, vol. 49, no. 6, pp. 554–560, 2012.

[146] A. Dickhout and R. R. Koenen, "Extracellular Vesicles as Biomarkers in Cardiovascular Disease; Chances and Risks," *Front. Cardiovasc. Med.*, vol. 5, p. 113, Aug. 2018.

[147] E. Woith, G. Fuhrmann, and M. F. Melzig, "Extracellular Vesicles-Connecting Kingdoms," *Int. J. Mol. Sci.*, vol. 20, no. 22, p. 5695, Nov. 2019.

[148] M. L. Mastronardi, H. A. Mostefai, F. Meziani, M. C. Martínez, P. Asfar, and R. Andriantsitohaina, "Circulating microparticles from septic shock patients exert differential tissue expression of enzymes related to inflammation and oxidative stress*," *Crit. Care Med.*, vol. 39, no. 7, pp. 1739–1748, 2011.

[149] P. S. Prakash, C. C. Caldwell, A. B. Lentsch, T. A. Pritts, and B. R. H. Robinson, "Human microparticles generated during sepsis in patients with critical illness are neutrophil-derived and modulate the immune response," *J. Trauma Acute Care Surg.*, vol. 73, no. 2, pp. 401–407, Aug. 2012.

[150] S. Balusu *et al.*, "Identification of a novel mechanism of blood-brain communication during peripheral inflammation via choroid plexus-derived extracellular vesicles," *EMBO Mol. Med.*, vol. 8, no. 10, pp. 1162–1183, Oct. 2016.

[151] B. L. Johnson *et al.*, "Neutrophil derived microparticles increase mortality and the counter-inflammatory response in a murine model of sepsis," *Biochim. Biophys. Acta - Mol. Basis Dis.*, 2017.

[152] M. Kojima *et al.*, "Exosomes in postshock mesenteric lymph are key mediators of acute lung injury triggering the macrophage activation via Toll□like receptor 4," *FASEB J.*, vol. 32, no. 1, pp. 97–110, 2017.

[153] Z. Yuan, B. Bedi, and R. T. Sadikot, "Bronchoalveolar Lavage Exosomes in Lipopolysaccharide-induced Septic Lung Injury," *J. Vis. Exp.*, no. 135, p. 57737, May 2018.

[154] K. Jiang, J. Yang, S. Guo, G. Zhao, H. Wu, and G. Deng, "Peripheral Circulating

Exosome-Mediated Delivery of miR-155 as a Novel Mechanism for Acute Lung Inflammation," *Mol. Ther.*, vol. 27, no. 10, pp. 1758–1771, Oct. 2019.

[155] J. R. Wisler, K. Singh, A. R. Mccarty, A. S. E. Abouhashem, J. W. Christman, and C. K. Sen, "Proteomic Pathway Analysis of Monocyte-Derived Exosomes during Surgical Sepsis Identifies Immunoregulatory Functions," *Surg. Infect. (Larchmt).*, vol. 21, no. 2, pp. 101–111, Mar. 2020.

[156] J. J. Li *et al.*, "In vivo evidence for the contribution of peripheral circulating inflammatory exosomes to neuroinflammation," *J. Neuroinflammation*, vol. 15, no. 1, p. 8, Jan. 2018.

[157] Z.-G. Li *et al.*, "Lung epithelial cell-derived IL-25 negatively regulates LPS-induced exosome release from macrophages," *Mil. Med. Res.*, vol. 5, no. 1, p. 24, Jul. 2018.

[158] R. Nieuwland *et al.*, "Cellular origin and procoagulant properties of microparticles in meningococcal sepsis," *Blood*, 2000.

[159] X. Delabranche *et al.*, "Microparticles are new biomarkers of septic shock-induced disseminated intravascular coagulopathy," *Intensive Care Med.*, vol. 39, no. 10, pp. 1695–1703, 2013.

[160] H. Matsumoto, K. Yamakawa, H. Ogura, T. Koh, N. Matsumoto, and T. Shimazu, "Enhanced expression of cell-specific surface antigens on endothelial microparticles in sepsis-induced disseminated intravascular coagulation," *Shock*, vol. 43, no. 5, pp. 443–449, May 2015.

[161] M. J. Mooberry, R. Bradford, E. L. Hobl, F. C. Lin, B. Jilma, and N. S. Key, "Procoagulant microparticles promote coagulation in a factor XI-dependent manner in human endotoxemia," *J. Thromb. Haemost.*, vol. 14, no. 5, pp. 1031–1042, May 2016.

[162] Y. Wang, L. Luo, M. Mörgelin, and H. Thorlacius, "Rac1 regulates sepsis-induced

formation of platelet-derived microparticles and thrombin generation," *Biochem. Biophys. Res. Commun.*, vol. 487, no. 4, pp. 887–891, 2017.

[163] C. Tripisciano *et al.*, "Different Potential of Extracellular Vesicles to Support Thrombin Generation: Contributions of Phosphatidylserine, Tissue Factor, and Cellular Origin," *Sci. Rep.*, vol. 7, no. 1, p. 6522, Jul. 2017.

[164] T. Iba and H. Ogura, "Role of extracellular vesicles in the development of sepsis-induced coagulopathy," *J. intensive care*, vol. 6, p. 68, Oct. 2018.

[165] Y. Wang *et al.*, "Platelet□derived microparticles regulates thrombin generation via phophatidylserine in abdominal sepsis," *J. Cell. Physiol.*, vol. 233, no. 2, pp. 1051–1060, 2017.

[166] C. Tripisciano, R. Weiss, S. Karuthedom George, M. B. Fischer, and V. Weber, "Extracellular Vesicles Derived From Platelets, Red Blood Cells, and Monocyte-Like Cells Differ Regarding Their Ability to Induce Factor XII-Dependent Thrombin Generation," *Front. cell Dev. Biol.*, vol. 8, p. 298, May 2020.

[167] J. Deng *et al.*, "Exosomes derived from plasma of septic patients inhibit apoptosis of T lymphocytes by down-regulating bad via hsa-miR-7-5p," *Biochem. Biophys. Res. Commun.*, vol. 513, no. 4, pp. 958–966, 2019.

[168] M. Janiszewski, A. O. Do Carmo, M. A. Pedro, E. Silva, E. Knobel, and F. R. M. Laurindo, "Platelet-derived exosomes of septic individuals possess proapoptotic NAD(P)H oxidase activity: A novel vascular redox pathway," *Crit. Care Med.*, vol. 32, no. 3, pp. 818–825, Mar. 2004.

[169] M. H. Gambim, A. de O. do Carmo, L. Marti, S. Veríssimo-Filho, L. R. Lopes, and M. Janiszewski, "Platelet-derived exosomes induce endothelial cell apoptosis through

peroxynitrite generation: experimental evidence for a novel mechanism of septic vascular dysfunction," *Crit. Care*, vol. 11, no. 5, pp. R107–R107, 2007.

[170] H. A. Mostefai *et al.*, "Interleukin-10 controls the protective effects of circulating microparticles from patients with septic shock on tissue-engineered vascular media," *Clin. Sci.*, vol. 125, no. 2, pp. 77–85, 2013.

[171] X. Mu *et al.*, "Circulating Exosomes Isolated from Septic Mice Induce Cardiovascular Hyperpermeability Through Promoting Podosome Cluster Formation," *Shock*, vol. 49, no. 4, pp. 429–441, Apr. 2018.

[172] V. Chatterjee *et al.*, "Endothelial microvesicles carrying Src-rich cargo impair adherens junction integrity and cytoskeleton homeostasis," *Cardiovasc. Res.*, vol. 116, no. 8, pp. 1525–1538, Jul. 2020.

[173] P. D. Robbins and A. E. Morelli, "Regulation of immune responses by extracellular vesicles," *Nat. Rev. Immunol.*, vol. 14, no. 3, pp. 195–208, Mar. 2014.

[174] D. W. Greening, S. K. Gopal, R. Xu, R. J. Simpson, and W. Chen, "Exosomes and their roles in immune regulation and cancer," *Semin. Cell Dev. Biol.*, vol. 40, pp. 72–81, 2015.

[175] W. Jian, L. Gu, B. Williams, Y. Feng, W. Chao, and L. Zou, "Toll-like Receptor 7 Contributes to Inflammation, Organ Injury, and Mortality in Murine Sepsis," *Anesthesiology*, vol. 131, no. 1, pp. 105–118, Jul. 2019.

[176] K. Essandoh *et al.*, "Blockade of exosome generation with GW4869 dampens the sepsis-induced inflammation and cardiac dysfunction," *Biochim. Biophys. Acta*, vol. 1852, no. 11, pp. 2362–2371, Nov. 2015.

[177] J. Dalli *et al.*, "Heterogeneity in neutrophil microparticles reveals distinct proteome and functional properties," *Mol. Cell. Proteomics*, vol. 12, no. 8, pp. 2205–2219, Aug. 2013.

[178] J. Dalli *et al.*, "Microparticle alpha-2-macroglobulin enhances pro-resolving responses and promotes survival in sepsis," *EMBO Mol. Med.*, vol. 6, no. 1, pp. 27–42, Jan. 2014.

[179] K. Gao *et al.*, "Exosomes Derived From Septic Mouse Serum Modulate Immune Responses via Exosome-Associated Cytokines," *Front. Immunol.*, vol. 10, p. 1560, Jul. 2019.

[180] M. Ticlea, L. M. Bratu, F. Bodog, O. H. Bedreag, A. F. Rogobete, and Z. P. Crainiceanu, "The Use of Exosomes as Biomarkers for Evaluating and Monitoring Critically Ill Polytrauma Patients with Sepsis," *Biochem. Genet.*, vol. 55, no. 1, pp. 1–9, 2016.

[181] D. A. Dakhlallah *et al.*, "Circulating extracellular vesicle content reveals de novo DNA methyltransferase expression as a molecular method to predict septic shock," *J. Extracell. vesicles*, vol. 8, no. 1, p. 1669881, Sep. 2019.

[182] S.-C. Wu *et al.*, "Profiling circulating microRNA expression in experimental sepsis using cecal ligation and puncture," *PLoS One*, vol. 8, no. 10, pp. e77936–e77936, Oct. 2013.

[183] A. J. Goodwin, C. Guo, J. A. Cook, B. Wolf, P. V Halushka, and H. Fan, "Plasma levels of microRNA are altered with the development of shock in human sepsis: an observational study," *Crit. Care*, vol. 19, p. 440, Dec. 2015.

[184] M. Reithmair *et al.*, "Cellular and extracellular miRNAs are blood-compartment-specific diagnostic targets in sepsis," *J. Cell. Mol. Med.*, vol. 21, no. 10, pp. 2403–2411, Oct. 2017.

[185] J. Wang *et al.*, "Serum miR-146a and miR-223 as potential new biomarkers for sepsis," *Biochem. Biophys. Res. Commun.*, vol. 394, no. 1, pp. 184–188, 2010.

[186] T. Panich, W. Chancharoenthana, P. Somparn, J. Issara-Amphorn, N. Hirankarn, and A. Leelahavanichkul, "Urinary exosomal activating transcriptional factor 3 as the early

diagnostic biomarker for sepsis-induced acute kidney injury," *BMC Nephrol.*, vol. 18, no. 1, p. 10, Jan. 2017.

[187] R. R. Nair, D. Mazza, F. Brambilla, A. Gorzanelli, A. Agresti, and M. E. Bianchi, "LPS-Challenged Macrophages Release Microvesicles Coated With Histones," *Front. Immunol.*, vol. 9, p. 1463, Jun. 2018.

[188] K. Subramani *et al.*, "Effect of plasma-derived extracellular vesicles on erythrocyte deformability in polymicrobial sepsis," *Int. Immunopharmacol.*, vol. 65, pp. 244–247, 2018.

[189] Y. Xu, X. Ku, C. Wu, C. Cai, J. Tang, and W. Yan, "Exosomal proteome analysis of human plasma to monitor sepsis progression," *Biochem. Biophys. Res. Commun.*, vol. 499, no. 4, pp. 856–861, 2018.

[190] W. Li *et al.*, "LPS Induces Active HMGB1 Release From Hepatocytes Into Exosomes Through the Coordinated Activities of TLR4 and Caspase-11/GSDMD Signaling," *Front. Immunol.*, vol. 11, p. 229, Apr. 2020.

[191] R. Zhang *et al.*, "Human umbilical cord mesenchymal stem cell exosomes alleviate sepsis-associated acute kidney injury via regulating microRNA-146b expression," *Biotechnol. Lett.*, vol. 42, no. 4, pp. 669–679, 2020.

[192] M. Eriksson, D. Nelson, A. Nordgren, and A. Larsson, "Increased platelet microvesicle formation is associated with mortality in a porcine model of endotoxemia," *Acta Anaesthesiol. Scand.*, vol. 42, no. 5, pp. 551–557, 1998.

[193] S. Mortaza *et al.*, "Detrimental hemodynamic and inflammatory effects of microparticles originating from septic rats*," *Crit. Care Med.*, vol. 37, no. 6, pp. 2045–2050, 2009.

[194] L. C. P. Azevedo *et al.*, "Platelet-derived exosomes from septic shock patients induce

myocardial dysfunction," *Crit. Care*, vol. 11, no. 6, pp. R120–R120, 2007.

[195] H. A. Mostefai *et al.*, "Circulating Microparticles from Patients with Septic Shock Exert Protective Role in Vascular Function," *Am. J. Respir. Crit. Care Med.*, vol. 178, no. 11, pp. 1148–1155, 2008.

[196] M. Pérez-Casal *et al.*, "The clinical and functional relevance of microparticles induced by activated protein C treatment in sepsis," *Crit. Care*, vol. 15, no. 4, pp. R195–R195, Aug. 2011.

[197] M. Tőkés-Füzesi *et al.*, "Microparticles and acute renal dysfunction in septic patients," *J. Crit. Care*, vol. 28, no. 2, pp. 141–147, 2013.

[198] M. C. Exline *et al.*, "Microvesicular caspase-1 mediates lymphocyte apoptosis in sepsis," *PLoS One*, vol. 9, no. 3, pp. e90968–e90968, Mar. 2014.

[199] M. Hellum, R. Øvstebø, B. S. Brusletto, J. P. Berg, P. Brandtzaeg, and C. E. Henriksson, "Microparticle-associated tissue factor activity correlates with plasma levels of bacterial lipopolysaccharides in meningococcal septic shock," *Thromb. Res.*, vol. 133, no. 3, pp. 507–514, 2014.

[200] G. F. Lehner *et al.*, "Characterization of Microvesicles in Septic Shock Using High-Sensitivity Flow Cytometry," *Shock*, vol. 46, no. 4, pp. 373–381, 2016.

[201] H. Jaurila *et al.*, "Inhibitory effects of serum from sepsis patients on epithelial cell migration in vitro: a case control study," *J. Transl. Med.*, vol. 15, no. 1, p. 11, Jan. 2017.

[202] H. Matsumoto, K. Yamakawa, H. Ogura, T. Koh, N. Matsumoto, and T. Shimazu, "Clinical Significance of Tissue Factor and CD13 Double-Positive Microparticles in Sirs Patients with Trauma and Severe Sepsis," *Shock*, vol. 47, no. 4, pp. 409–415, 2017.

[203] C. M. Shaver *et al.*, "Circulating microparticle levels are reduced in patients with ARDS,"

Crit. Care, vol. 21, no. 1, p. 120, May 2017.

[204] H. M. S. Lashin *et al.*, "Microvesicle Subsets in Sepsis Due to Community Acquired Pneumonia Compared to Faecal Peritonitis," *Shock*, vol. 49, no. 4, pp. 393–401, 2018.

[205] M. A. Puskarich *et al.*, "Phosphatidylserine expressing platelet microparticle levels at hospital presentation are decreased in sepsis non-survivors and correlate with thrombocytopenia," *Thromb. Res.*, vol. 168, pp. 138–144, Aug. 2018.

[206] J. M. Real *et al.*, "Exosomes from patients with septic shock convey miRNAs related to inflammation and cell cycle regulation: new signaling pathways in sepsis?," *Crit. Care*, vol. 22, no. 1, p. 68, Mar. 2018.

[207] A. Boscolo *et al.*, "Levels of circulating microparticles in septic shock and sepsis-related complications: a case-control study," *Minerva Anestesiol.*, vol. 85, no. 6, 2019.

[208] E. Homsy *et al.*, "Circulating Gasdermin-D in Critically Ill Patients," *Crit. care Explor.*, vol. 1, no. 9, pp. e0039–e0039, Sep. 2019.

[209] E. Kawamoto *et al.*, "Integrin and PD-1 Ligand Expression on Circulating Extracellular Vesicles in Systemic Inflammatory Response Syndrome and Sepsis," *Shock*, vol. 52, no. 1, pp. 13–22, 2019.

[210] H. Ogura *et al.*, "Activated Platelets Enhance Microparticle Formation and Platelet-Leukocyte Interaction in Severe Trauma and Sepsis," *J. Trauma Inj. Infect. Crit. Care*, vol. 50, no. 5, pp. 801–809, 2001.

[211] K. Joop *et al.*, "Microparticles from Patients with Multiple Organ Dysfunction Syndrome and Sepsis Support Coagulation through Multiple Mechanisms," *Thromb. Haemost.*, vol. 85, no. 05, pp. 810–820, 2001.

[212] A. O. Soriano *et al.*, "Levels of endothelial and platelet microparticles and their

interactions with leukocytes negatively correlate with organ dysfunction and predict mortality in severe sepsis," *Crit. Care Med.*, vol. 33, no. 11, pp. 2540–2546, 2005.

[213] L. Zou, Y. Feng, G. Xu, W. Jian, and W. Chao, "Splenic RNA and MicroRNA Mimics Promote Complement Factor B Production and Alternative Pathway Activation via Innate Immune Signaling," *J. Immunol.*, 2016.

[214] C. Kannemeier *et al.*, "Extracellular RNA constitutes a natural procoagulant cofactor in blood coagulation," *Proc. Natl. Acad. Sci. U. S. A.*, 2007.

[215] B. Szilágyi, Z. Fejes, M. Pócsi, J. Kappelmayer, and B. Nagy Jr, "Role of sepsis modulated circulating microRNAs," *EJIFCC*, vol. 30, no. 2, pp. 128–145, Jun. 2019.

[216] F. Tabet *et al.*, "HDL-transferred microRNA-223 regulates ICAM-1 expression in endothelial cells," *Nat. Commun.*, 2014.

[217] M. P. Boldin *et al.*, "miR-146a is a significant brake on autoimmunity, myeloproliferation, and cancer in mice," *J. Exp. Med.*, 2011.

[218] W. R. Strohl, "Fusion Proteins for Half-Life Extension of Biologics as a Strategy to Make Biobetters," *BioDrugs*. 2015.

[219] M. M. Schmidt and K. D. Wittrup, "A modeling analysis of the effects of molecular size and binding affinity on tumor targeting," *Mol. Cancer Ther.*, 2009.

[220] K. C. Vickers, B. T. Palmisano, B. M. Shoucri, R. D. Shamburek, and A. T. Remaley, "MicroRNAs are transported in plasma and delivered to recipient cells by high-density lipoproteins," *Nat. Cell Biol.*, 2011.

[221] J. Wagner *et al.*, "Characterization of levels and cellular transfer of circulating lipoprotein-bound microRNAs," *Arterioscler. Thromb. Vasc. Biol.*, 2013.

[222] D. L. Michell and K. C. Vickers, "Lipoprotein carriers of microRNAs," *Biochim. Biophys.*

Acta - Mol. Cell Biol. Lipids, vol. 1861, no. 12 (Part B), pp. 2069–2074, 2016.

[223] R. M. Allen *et al.*, "Bioinformatic analysis of endogenous and exogenous small RNAs on lipoproteins," *J. Extracell. Vesicles*, vol. 7, no. 1, p. 1506198, 2018.

[224] H. Wang and R. H. Eckel, "What are lipoproteins doing in the brain?," *Trends Endocrinol. Metab.*, vol. 25, no. 1, pp. 8–14, 2014.

[225] W. Shen, S. Asthana, F. Kraemer, and S. Azhar, "Scavenger receptor B type 1 : Expression, Molecular Regulation, and Cholesterol Transport Function," *J Lipid Res*, 2018.

[226] M. M. K. Shahzad *et al.*, "Targeted Delivery of Small Interfering RNA Using Reconstituted High-Density Lipoprotein Nanoparticles," *Neoplasia*, 2011.

[227] C. Röhrl and H. Stangl, "HDL endocytosis and resecretion," *Biochimica et Biophysica Acta - Molecular and Cell Biology of Lipids*. 2013.

[228] A. Kontush, "HDL particle number and size as predictors of cardiovascular disease," *Front. Pharmacol.*, 2015.

[229] C. B. Blum, R. I. Levy, S. Eisenberg, M. Hall, R. H. Goebel, and M. Berman, "High Density Lipoprotein Metabolism in Man," *J. Clin. Invest.*, vol. 60, no. 4, pp. 795–807, 1977.

[230] A. L. Catapano, A. Pirillo, F. Bonacina, and G. D. Norata, "HDL in innate and adaptive immunity," *Cardiovascular Research*. 2014.

[231] A. Jonas, "Reconstitution of High-Density Lipoproteins," *Methods Enzymol.*, 1986.

[232] C. Lorenz, P. Hadwiger, M. John, H. P. Vornlocher, and C. Unverzagt, "Steroid and lipid conjugates of siRNAs to enhance cellular uptake and gene silencing in liver cells," *Bioorganic Med. Chem. Lett.*, 2004.

[233] J. Desjardins, J. Mata, T. Brown, D. Graham, G. Zon, and P. Iversen, "Cholesteryl-conjugated phosphorothioate oligodeoxynucleotides modulate CYP2b1 expression in vivo," *J. Drug Target.*, 1995.

[234] P. C. De Smidt, T. Le Doan, S. De Falco, and T. J. C. Van Berkel, "Association of antisense oligonucleotides with lipoproteins prolongs the plasma half-life and modifies the tissue distribution," *Nucleic Acids Res.*, 1991.

[235] T. S. Zimmermann *et al.*, "RNAi-mediated gene silencing in non-human primates," *Nature*, 2006.

[236] C. Wolfrum *et al.*, "Mechanisms and optimization of in vivo delivery of lipophilic siRNAs," *Nat. Biotechnol.*, 2007.

[237] T. Nakayama *et al.*, "Harnessing a physiologic mechanism for siRNA delivery with mimetic lipoprotein particles," *Mol. Ther.*, 2012.

[238] Y. Ding *et al.*, "Direct cytosolic siRNA delivery by reconstituted high density lipoprotein for target-specific therapy of tumor angiogenesis," *Biomaterials*, vol. 35, no. 25, pp. 7214–7227, 2014.

[239] Z. Zhang *et al.*, "HDL-mimicking peptide-lipid nanoparticles with improved tumor targeting," *Small*, vol. 6, no. 3, pp. 430–437, 2010.

[240] M. Yang *et al.*, "Efficient cytosolic delivery of siRNA using HDL-mimicking nanoparticles," *Small*, vol. 7, no. 5, pp. 568–573, 2011.

[241] Q. Lin *et al.*, "Efficient systemic delivery of siRNA by using high-density lipoprotein-mimicking peptide lipid nanoparticles," *Nanomedicine*, vol. 7, no. 12, pp. 1813–1825, 2012.

[242] K. M. McMahon *et al.*, "Biomimetic high density lipoprotein nanoparticles for nucleic

acid delivery," *Nano Lett.*, vol. 11, no. 3, pp. 1208–1214, 2011.

[243] S. Tripathy, E. Vinokour, K. M. McMahon, O. V. Volpert, and C. S. Thaxton, "High-Density lipoprotein nanoparticles deliver RNAi to endothelial cells to inhibit angiogenesis," *Part. Part. Syst. Charact.*, vol. 31, no. 11, pp. 1141–1150, 2014.

[244] H. Lee *et al.*, "Hepatic siRNA delivery using recombinant human apolipoprotein A-I in mice," *Biochem. Biophys. Res. Commun.*, vol. 378, no. 2, pp. 192–196, 2009.

[245] S. I. Kim *et al.*, "Systemic and specific delivery of small interfering RNAs to the liver mediated by apolipoprotein A-I," *Mol. Ther.*, vol. 15, no. 6, pp. 1145–1152, 2007.

[246] Y. Ding *et al.*, "Rerouting Native HDL to Predetermined Receptors for Improved Tumor-Targeted Gene Silencing Therapy," *ACS Appl. Mater. Interfaces*, vol. 9, no. 36, pp. 30488–30501, 2017.

[247] Y. Ding *et al.*, "A biomimetic nanovector-mediated targeted cholesterol-conjugated siRNA delivery for tumor gene therapy," *Biomaterials*, vol. 33, no. 34, pp. 8893–8905, 2012.

[248] P. C. N. Rensen, S. H. Van Leeuwen, L. A. J. M. Sliedregt, T. J. C. Van Berkel, and E. A. L. Biessen, "Design and synthesis of novel N-acetylgalactosamine-terminated glycolipids for targeting of lipoproteins to the hepatic asialoglycoprotein receptor," *J. Med. Chem.*, vol. 47, no. 23, pp. 5798–5808, 2004.

[249] I. R. Corbin, J. Chen, W. Cao, H. Li, S. Lund-Katz, and G. Zheng, "Enhanced cancer-targeted delivery using engineered high-density lipoprotein-based nanocarriers," *J. Biomed. Nanotechnol.*, vol. 3, no. 4, pp. 367–376, 2007.

[250] S. Sabnis, N. A. Sabnis, S. Raut, and A. G. Lacko, "Superparamagnetic reconstituted high-density lipoprotein nanocarriers for magnetically guided drug delivery," *Int. J.*

Nanomedicine, vol. 12, pp. 1453–1464, 2017.

[251] A. G. Lacko, M. Nair, S. Paranjape, S. Johnson, and W. J. McConathy, "High density lipoprotein complexes as delivery vehicles for anticancer drugs," *Anticancer Res.*, vol. 22, no. 4, pp. 2045–2049, 2002.

[252] Y. Yuan, W. Wang, B. Wang, H. Zhu, B. Zhang, and M. Feng, "Delivery of hydrophilic drug doxorubicin hydrochloride-targeted liver using apoAI as carrier," *J. Drug Target.*, vol. 21, no. 4, pp. 367–374, 2013.

[253] W. J. McConathy, M. P. Nair, S. Paranjape, L. Mooberry, and A. G. Lacko, "Evaluation of synthetic/reconstituted high-density lipoproteins as delivery vehicles for paclitaxel," *Anticancer. Drugs*, vol. 19, no. 2, pp. 183–188, 2008.

[254] A. Hrzenjak *et al.*, "Inhibition of lung carcinoma cell growth by high density lipoprotein-associated alpha-tocopheryl-succinate," *Cell. Mol. Life Sci.*, vol. 61, no. 12, pp. 1520–1531, 2004.

[255] G. Franceschini, G. Vecchio, and G. Gianfranceschi, "Apolipoprotein AI(Milano). Accelerated binding and dissociation from lipids of a human apolipoprotein variant," *J. Biol. Chem.*, vol. 260, no. 30, pp. 16321–16325, 1985.

[256] E. Bruckert *et al.*, "The replacement of arginine by cysteine at residue 151 in apolipoprotein A-I produces a phenotype similar to that of apolipoprotein A-I(Milano)," *Atherosclerosis*, vol. 128, no. 1, pp. 121–8, 1997.

[257] J. D. Arroyo *et al.*, "Argonaute2 complexes carry a population of circulating microRNAs independent of vesicles in human plasma.," *Proc. Natl. Acad. Sci. U. S. A.*, vol. 108, no. 12, pp. 5003–5008, 2011.

[258] G. J. Prud'homme, Y. Glinka, Z. Lichner, and G. M. Yousef, "Neuropilin-1 is a receptor

for extracellular miRNA and AGO2/miRNA complexes and mediates the internalization of miRNAs that modulate cell function," *Oncotarget.*, p. 10, 2016.

[259] S. Soker, S. Takashima, # Hua, Q. Miao, G. Neufeld, and M. Klagsbrun, "Neuropilin-1 Is Expressed by Endothelial and Tumor Cells as an Isoform-Specific Receptor for Vascular Endothelial Growth Factor," *Cell*, vol. 92, pp. 735–745, 1998.

[260] C. Gu *et al.*, "Neuropilin-1 conveys semaphorin and VEGF signaling during neural and cardiovascular development," *Dev. Cell*, 2003.

[261] K. Roya *et al.*, "Stable association of RNAi machinery is conserved between the cytoplasm and nucleus of human cells," *RNA*, vol. 22, no. 7, pp. 1085–1098, 2016.

[262] J. D. Shepherd and M. F. Bear, "New views of Arc, a master regulator of synaptic plasticity," *Nature Neuroscience*. 2011.

[263] S. Chowdhury *et al.*, "Arc/Arg3.1 Interacts with the Endocytic Machinery to Regulate AMPA Receptor Trafficking," *Neuron*, 2006.

[264] E. D. Pastuzyn *et al.*, "The Neuronal Gene Arc Encodes a Repurposed Retrotransposon Gag Protein that Mediates Intercellular RNA Transfer," *Cell*, 2018.

[265] J. Ashley, B. Cordy, D. Lucia, L. G. Fradkin, V. Budnik, and T. Thomson, "Retrovirus-like Gag Protein Arc1 Binds RNA and Traffics across Synaptic Boutons," *Cell*, 2018.

[266] M. Segel *et al.*, "Mammalian retrovirus-like protein PEG10 packages its own mRNA and can be pseudotyped for mRNA delivery," *Science (80-.).*, vol. 373, no. 6557, pp. 882–889, Aug. 2021.

[267] P. Wang, Y. Zhou, and A. M. Richards, "Effective tools for RNA-derived therapeutics: siRNA interference or miRNA mimicry," *Theranostics*, vol. 11, no. 18. Ivyspring International Publisher, pp. 8771–8796, 2021.

[268] B. Claridge, J. Lozano, Q. H. Poh, and D. W. Greening, "Development of Extracellular Vesicle Therapeutics: Challenges, Considerations, and Opportunities," *Frontiers in Cell and Developmental Biology*, vol. 9. Frontiers Media S.A., p. 2307, 20-Sep-2021.

[269] S. I. Ohno *et al.*, "Systemically injected exosomes targeted to EGFR deliver antitumor microrna to breast cancer cells," *Mol. Ther.*, vol. 21, no. 1, pp. 185–191, Jan. 2013.

[270] Y. Zhang *et al.*, "Secreted Monocytic miR-150 Enhances Targeted Endothelial Cell Migration," *Mol. Cell*, vol. 39, no. 1, pp. 133–144, Jul. 2010.

[271] M. Yang *et al.*, "Microvesicles secreted by macrophages shuttle invasion-potentiating microRNAs into breast cancer cells," *Mol. Cancer*, vol. 10, no. 1, pp. 1–13, Sep. 2011.

[272] D. Wang *et al.*, "Exosomes from mesenchymal stem cells expressing miR-125b inhibit neointimal hyperplasia via myosin IE," *J. Cell. Mol. Med.*, vol. 23, no. 2, pp. 1528–1540, Feb. 2019.

[273] H. Li, C. Yang, Y. Shi, and L. Zhao, "Exosomes derived from siRNA against GRP78 modified bone-marrow-derived mesenchymal stem cells suppress Sorafenib resistance in hepatocellular carcinoma," *J. Nanobiotechnology*, vol. 16, no. 1, Dec. 2018.

[274] J. L. Munoz, S. A. Bliss, S. J. Greco, S. H. Ramkissoon, K. L. Ligon, and P. Rameshwar, "Delivery of functional anti-miR-9 by mesenchymal stem cell-derived exosomes to glioblastoma multiforme cells conferred chemosensitivity," *Mol. Ther. - Nucleic Acids*, vol. 2, no. OCT, p. e126, 2013.

[275] M. Wirth *et al.*, "A simple and cost-effective method to transfect small interfering RNAs into pancreatic cancer cell lines using polyethylenimine," *Pancreas*, vol. 40, no. 1, pp. 144–150, Jan. 2011.

[276] R. Stapulionis, "Electric pulse-induced precipitation of biological macromolecules in

electroporation," *Bioelectrochemistry Bioenerg.*, vol. 48, no. 1, pp. 249–254, Feb. 1999.

[277] H. Y. Jin *et al.*, "Transfection of microRNA mimics should be used with caution," *Front. Genet.*, vol. 6, no. DEC, p. 340, 2015.

[278] K. O'Brien, K. Breyne, S. Ughetto, L. C. Laurent, and X. O. Breakefield, "RNA delivery by extracellular vesicles in mammalian cells and its applications," *Nature Reviews Molecular Cell Biology*, vol. 21, no. 10. Nature Publishing Group, pp. 585–606, 26-May-2020.

[279] H. P. Bogerd, A. W. Whisnant, E. M. Kennedy, O. Flores, and B. R. Cullen, "Derivation and characterization of Dicer- and microRNA-deficient human cells," *RNA*, vol. 20, no. 6, pp. 923–937, 2014.

[280] J. J. Gam, J. Babb, and R. Weiss, "A mixed antagonistic/synergistic miRNA repression model enables accurate predictions of multi-input miRNA sensor activity," *Nat. Commun.*, vol. 9, no. 1, pp. 1–12, Jun. 2018.

[281] X. G. Xia, H. Zhou, H. Ding, E. B. Affar, Y. Shi, and Z. Xu, "An enhanced U6 promoter for synthesis of short hairpin RNA," *Nucleic Acids Res.*, vol. 31, no. 17, p. e100, 2003.

[282] J. Su, Z. Zhu, F. Xiong, and Y. Wang, "Hybrid cytomegalovirus-U6 promoter-based plasmid vectors improve efficiency of RNA interference in zebrafish," *Mar. Biotechnol. (NY).*, vol. 10, no. 5, pp. 511–517, Sep. 2008.

[283] A. E. Carnes *et al.*, "Critical design criteria for minimal antibiotic-free plasmid vectors necessary to combine robust RNA Pol II and Pol III-mediated eukaryotic expression with high bacterial production yields," *J. Gene Med.*, vol. 12, no. 10, pp. 818–831, Oct. 2010.

[284] Y. Jiang, W. Ma, Z. Xie, F. Liu, and H. Ning, "A significant increase of RNAi efficiency in human cells by the CMV enhancer with a tRNAlys promoter," *J. Biomed. Biotechnol.*,

vol. 2009, 2009.

[285] S. T. Ong, F. Li, J. Du, Y. W. Tan, and S. Wang, "Hybrid Cytomegalovirus Enhancer–H1 Promoter-Based Plasmid and Baculovirus Vectors Mediate Effective RNA Interference," *https://home.liebertpub.com/hum*, vol. 16, no. 12, pp. 1404–1412, Jan. 2006.

[286] Z. Hassani *et al.*, "A hybrid CMV-H1 construct improves efficiency of PEI-delivered shRNA in the mouse brain," *Nucleic Acids Res.*, vol. 35, no. 9, pp. e65–e65, May 2007.

[287] L. Yang, F. Wang, X. Lu, M. Zhou, C. Ye, and Y. Sun, "The influence of a chimeric insulator on the stabilization of shRNA expression transfected by lentivirus," *Life Sci. J.*, vol. 16, no. 5, pp. 1097–8135, 2019.

[288] A. R. Gruber, R. Lorenz, S. H. Bernhart, R. Neuböck, and I. L. Hofacker, "The Vienna RNA websuite.," *Nucleic Acids Res.*, vol. 36, no. Web Server issue, pp. W70–W74, Jul. 2008.

[289] R. Lorenz *et al.*, "ViennaRNA Package 2.0," *Algorithms Mol. Biol.*, vol. 6, no. 1, pp. 1–14, Nov. 2011.

[290] R. Yi, B. P. Doehle, Y. Qin, I. G. Macara, and B. R. Cullen, "Overexpression of Exportin 5 enhances RNA interference mediated by short hairpin RNAs and microRNAs," *RNA*, vol. 11, no. 2, pp. 220–226, Feb. 2005.

[291] M. T. Bohnsack *et al.*, "Exp5 exports eEF1A via tRNA from nuclei and synergizes with other transport pathways to confine translation to the cytoplasm," *EMBO J.*, vol. 21, no. 22, p. 6205, Nov. 2002.

[292] Y. Bennasser *et al.*, "Competition for XPO5 binding between Dicer mRNA, pre-miRNA and viral RNA regulates human Dicer levels," *Nat. Struct. Mol. Biol. 2011 183*, vol. 18, no. 3, pp. 323–327, Feb. 2011.

[293] Z. Gao, E. Herrera-Carrillo, and B. Berkhout, "Delineation of the Exact Transcription Termination Signal for Type 3 Polymerase III," *Mol. Ther. - Nucleic Acids*, vol. 10, pp. 36–44, Mar. 2018.

[294] D. Zigáčková and Š. Vaňáčová, "The role of 3′ end uridylation in RNA metabolism and cellular physiology," *Philosophical Transactions of the Royal Society B: Biological Sciences*, vol. 373, no. 1762. The Royal Society, 19-Dec-2018.

[295] Y. Zeng and B. R. Cullen, "Structural requirements for pre-microRNA binding and nuclear export by Exportin 5," *Nucleic Acids Res.*, vol. 32, no. 16, pp. 4776–4785, 2004.

[296] G. Sun, S. Y. Yeh, C. W. Y. Yuan, M. J. Y. Chiu, B. S. H. Yung, and Y. Yen, "Molecular Properties, Functional Mechanisms, and Applications of Sliced siRNA," *Mol. Ther. - Nucleic Acids*, vol. 4, no. 1, p. e221, 2015.

[297] R. Shang *et al.*, "Ribozyme-enhanced single-stranded Ago2-processed interfering RNA triggers efficient gene silencing with fewer off-target effects," *Nat. Commun.*, vol. 6, Oct. 2015.

[298] E. Herrera-Carrillo, Z. Gao, and B. Berkhout, "Influence of a 3′ Terminal Ribozyme on AgoshRNA Biogenesis and Activity," *Mol. Ther. - Nucleic Acids*, vol. 16, pp. 452–462, Jun. 2019.

[299] W. M. Chu, R. E. Ballard, and C. W. Schmid, "Palindromic sequences preceding the terminator increase polymerase III template activity," *Nucleic Acids Res.*, vol. 25, no. 11, pp. 2077–2082, 1997.

[300] G. J. Kapral, S. Jain, J. Noeske, J. A. Doudna, D. C. Richardson, and J. S. Richardson, "New tools provide a second look at HDV ribozyme structure, dynamics and cleavage," *Nucleic Acids Res.*, vol. 42, no. 20, pp. 12833–12846, Nov. 2014.

[301] Z. Gao, E. Herrera-Carrillo, and B. Berkhout, "RNA Polymerase II Activity of Type 3 Pol III Promoters," *Mol. Ther. - Nucleic Acids*, vol. 12, pp. 135–145, Sep. 2018.

[302] L. Nie, M. Das Thakur, Y. Wang, Q. Su, Y. Zhao, and Y. Feng, "Regulation of U6 Promoter Activity by Transcriptional Interference in Viral Vector-Based RNAi," *Genomics, Proteomics Bioinforma.*, vol. 8, no. 3, pp. 170–179, Sep. 2010.

[303] D. Furman *et al.*, "Chronic inflammation in the etiology of disease across the life span," *Nat. Med.*, vol. 25, no. 12, pp. 1822–1832, Dec. 2019.

[304] X. Bai *et al.*, "MicroRNA-146a protects against LPS-induced organ damage by inhibiting Notch1 in macrophage," *Int. Immunopharmacol.*, vol. 63, pp. 220–226, Oct. 2018.

[305] X. Wang *et al.*, "Exosomal MIR-223 Contributes to Mesenchymal Stem Cell-Elicited Cardioprotection in Polymicrobial Sepsis," *Sci. Rep.*, vol. 5, no. 1, pp. 1–16, Sep. 2015.

[306] K. Essandoh and G. C. Fan, "Role of extracellular and intracellular microRNAs in sepsis," *Biochimica et Biophysica Acta - Molecular Basis of Disease*, vol. 1842, no. 11. Elsevier, pp. 2155–2162, 01-Nov-2014.

[307] S. M. R. Hashemian, M. H. Pourhanifeh, S. Fadaei, A. A. Velayati, H. Mirzaei, and M. R. Hamblin, "Non-coding RNAs and Exosomes: Their Role in the Pathogenesis of Sepsis," *Molecular Therapy - Nucleic Acids*, vol. 21. Cell Press, pp. 51–74, 04-Sep-2020.

[308] Y. Feng *et al.*, "Extracellular MicroRNAs Induce Potent Innate Immune Responses via TLR7/MyD88-Dependent Mechanisms," *J. Immunol.*, vol. 199, no. 6, pp. 2106–2117, Sep. 2017.

[309] S. D. Gurien *et al.*, "Extracellular micro RNA 130b□3p inhibits eCIRP □induced inflammation," *EMBO Rep.*, vol. 21, no. 1, Jan. 2020.

[310] R. Dumache *et al.*, "Use of miRNAs as Biomarkers in Sepsis," *Analytical Cellular*

Pathology, vol. 2015. Hindawi Publishing Corporation, 2015.

[311] Y. Song *et al.*, "Exosomal miR-146a Contributes to the Enhanced Therapeutic Efficacy of Interleukin-1β-Primed Mesenchymal Stem Cells Against Sepsis," *Stem Cells*, 2017.

[312] L. zhang *et al.*, "miRNA-20a suppressed lipopolysaccharide☐induced HK☐2 cells injury via NFκB and ERK1/2 signaling by targeting CXCL12," *Mol. Immunol.*, vol. 118, pp. 117–123, Feb. 2020.

[313] H. Valadi, K. Ekström, A. Bossios, M. Sjöstrand, J. J. Lee, and J. O. Lötvall, "Exosome-mediated transfer of mRNAs and microRNAs is a novel mechanism of genetic exchange between cells," *Nat. Cell Biol.*, vol. 9, no. 6, pp. 654–659, May 2007.

[314] S. Kamerkar *et al.*, "Exosomes facilitate therapeutic targeting of oncogenic KRAS in pancreatic cancer," *Nature*, vol. 546, no. 7659, pp. 498–503, Jun. 2017.

[315] I. Osorio-Querejeta *et al.*, "MiR-219a-5p enriched extracellular vesicles induce OPC differentiation and EAE improvement more efficiently than liposomes and polymeric nanoparticles," *Pharmaceutics*, vol. 12, no. 2, p. 186, Feb. 2020.

[316] K. W. Witwer and J. Wolfram, "Extracellular vesicles versus synthetic nanoparticles for drug delivery," *Nature Reviews Materials*, vol. 6, no. 2. Nature Publishing Group, pp. 103–106, 07-Jan-2021.

[317] N. Pacienza *et al.*, "In Vitro Macrophage Assay Predicts the In Vivo Anti-inflammatory Potential of Exosomes from Human Mesenchymal Stromal Cells," *Mol. Ther. - Methods Clin. Dev.*, 2019.

[318] L. J. Born *et al.*, "HOTAIR-Loaded Mesenchymal Stem/Stromal Cell Extracellular Vesicles Enhance Angiogenesis and Wound Healing," *Adv. Healthc. Mater.*, vol. 11, no. 5, p. 2002070, 2022.

[319] M. Chen, F. Wang, H. Xia, and S. Yao, "MicroRNA-155: Regulation of Immune Cells in Sepsis," *Mediators of Inflammation*, vol. 2021. Mediators Inflamm, 2021.

[320] C. Chen *et al.*, "Serum miR-126-3p level is down-regulated in sepsis patients," *Int. J. Clin. Exp. Pathol.*, vol. 11, no. 5, p. 2605, 2018.

[321] Z. Qin, P. Y. Wang, D. F. Su, and X. Liu, "miRNA-124 in immune system and immune disorders," *Frontiers in Immunology*, vol. 7, no. OCT. Frontiers Media SA, 04-Oct-2016.

[322] Q. Chen *et al.*, "Inducible microRNA-223 down-regulation promotes TLR-triggered IL-6 and IL-1β production in macrophages by targeting STAT3," *PLoS One*, vol. 7, no. 8, p. e42971, Aug. 2012.

[323] J. Wang *et al.*, "miR-223 inhibits lipid deposition and inflammation by suppressing toll-like receptor 4 signaling in macrophages," *Int. J. Mol. Sci.*, vol. 16, no. 10, pp. 24965–24982, Oct. 2015.

[324] H. Choi *et al.*, "Exosome-based delivery of super-repressor IκBα relieves sepsis-associated organ damage and mortality," *Sci. Adv.*, vol. 6, no. 15, 2020.

[325] V. Bhaskaran *et al.*, "The functional synergism of microRNA clustering provides therapeutically relevant epigenetic interference in glioblastoma," *Nat. Commun.*, vol. 10, no. 1, pp. 1–13, Jan. 2019.

[326] P. E. Marik, V. Khangoora, R. Rivera, M. H. Hooper, and J. Catravas, "Hydrocortisone, Vitamin C, and Thiamine for the Treatment of Severe Sepsis and Septic Shock: A Retrospective Before-After Study," *Chest*, vol. 151, no. 6, pp. 1229–1238, Jun. 2017.

[327] P. E. Marik, "Hydrocortisone, ascorbic acid and thiamine (HAT therapy) for the treatment of sepsis. focus on ascorbic acid," *Nutrients*, vol. 10, no. 11. Multidisciplinary Digital Publishing Institute, p. 1762, 14-Nov-2018.

[328] A. Raza Naqvi and S. Zhong, "Expression Profiling of LPS Responsive miRNA in Primary Human Macrophages," *J. Microb. Biochem. Technol.*, vol. 08, no. 02, p. 136, 2016.

[329] R. Bayraktar, M. T. S. Bertilaccio, and G. A. Calin, "The interaction between two worlds: MicroRNAs and Toll-like receptors," *Frontiers in Immunology*, vol. 10, no. MAY. Frontiers Media S.A., p. 1053, 2019.

[330] M. Arenas-Padilla and V. Mata-Haro, "Regulation of TLR signaling pathways by microRNAs: Implications in inflammatory diseases," *Cent. Eur. J. Immunol.*, vol. 43, no. 4, pp. 482–489, 2018.

[331] Y. Yan, K. Lu, T. Ye, and Z. Zhang, "MicroRNA-223 attenuates LPS-induced inflammation in an acute lung injury model via the NLRP3 inflammasome and TLR4/NF-κB signaling pathway via RHOB," *Int. J. Mol. Med.*, vol. 43, no. 3, pp. 1467–1477, Mar. 2019.

[332] L. N. Schulte, A. J. Westermann, and J. Vogel, "Differential activation and functional specialization of miR-146 and miR-155 in innate immune sensing," *Nucleic Acids Res.*, vol. 41, no. 1, pp. 542–553, Jan. 2013.

[333] R. M. O'Connell, A. A. Chaudhuri, D. S. Rao, and D. Baltimore, "Inositol phosphatase SHIP1 is a primary target of miR-155," *Proc. Natl. Acad. Sci. U. S. A.*, vol. 106, no. 17, pp. 7113–7118, Apr. 2009.

[334] E. Tili *et al.*, "Modulation of miR-155 and miR-125b Levels following Lipopolysaccharide/TNF-α Stimulation and Their Possible Roles in Regulating the Response to Endotoxin Shock," *J. Immunol.*, vol. 179, no. 8, pp. 5082–5089, Oct. 2007.

[335] M. Alexander *et al.*, "Exosome-delivered microRNAs modulate the inflammatory

response to endotoxin," *Nat. Commun.*, 2015.

[336] Y. Chvatchko *et al.*, "A key role for CC chemokine receptor 4 in lipopolysaccharide-induced endotoxic shock," *J. Exp. Med.*, vol. 191, no. 10, pp. 1755–1763, May 2000.

[337] R. Molinaro *et al.*, "CCR4 controls the suppressive effects of regulatory T cells on early and late events during severe sepsis," *PLoS One*, vol. 10, no. 7, Jul. 2015.

[338] O. P. B. Wiklander *et al.*, "Extracellular vesicle in vivo biodistribution is determined by cell source, route of administration and targeting," *J. Extracell. Vesicles*, vol. 4, no. 2015, pp. 1–13, 2015.

[339] A. Mirzaaghasi, Y. Han, S. H. Ahn, C. Choi, and J. H. Park, "Biodistribution and pharmacokinectics of liposomes and exosomes in a mouse model of sepsis," *Pharmaceutics*, vol. 13, no. 3, Mar. 2021.

[340] C. A. Lissandrello *et al.*, "High-throughput continuous-flow microfluidic electroporation of mRNA into primary human T cells for applications in cellular therapy manufacturing," *Sci. Rep.*, vol. 10, no. 1, pp. 1–16, Oct. 2020.

[341] F. F. An and X. H. Zhang, "Strategies for preparing albumin-based nanoparticles for multifunctional bioimaging and drug delivery," *Theranostics*, vol. 7, no. 15, pp. 3667–3689, 2017.

[342] S. M. Sarett *et al.*, "Lipophilic siRNA targets albumin in situ and promotes bioavailability, tumor penetration, and carrier-free gene silencing," *Proc. Natl. Acad. Sci.*, vol. 114, no. 32, pp. E6490–E6497, 2017.

[343] J. Han, Q. Wang, Z. Zhang, T. Gong, and X. Sun, "Cationic bovine serum albumin based self-assembled nanoparticles as siRNA delivery vector for treating lung metastatic cancer," *Small*, vol. 10, no. 3, pp. 524–535, 2014.

[344] H. Wen, Y. Yin, C. Huang, W. Pan, and D. Liang, "Encapsulation of RNA by negatively charged human serum albumin via physical interactions," *Sci. China Chem.*, vol. 60, no. 1, pp. 130–135, 2017.

[345] B. I. Hillman, P. Hearne, D. Rochon, and T. J. Morris, "Organization of tomato bushy stunt virus genome: Characterization of the coat protein gene and the 3′ terminus," *Virology*, vol. 169, no. 1, pp. 42–50, 1989.

[346] D. M. Rochon, "Rapid de novo generation of defective interfering RNA by cucumber necrosis virus mutants that do not express the 20-kDa nonstructural protein.," *Proc. Natl. Acad. Sci. U. S. A.*, vol. 88, no. 24, pp. 11153–11157, 1991.

[347] H. B. Scholthof, K. B. G. Scholthof, and A. O. Jackson, "Identification of Tomato Bushy Stunt Virus Host-Specific Symptom Determinants by Expression of Individual Genes from a Potato Virus X Vector," *Plant Cell*, vol. 7, no. 8, pp. 1157–1172, 1995.

[348] H. B. Scholthof, K. B. G. Scholthof, M. Kikkert, and A. O. Jackson, "Tomato bushy stunt virus spread is regulated by two nested genes that function in cell-to-cell movement and host-dependent systemic invasion," *Virology*, vol. 213, no. 2, pp. 425–438, 1995.

[349] O. Voinnet, Y. M. Pinto, and D. C. Baulcombe, "Suppression of gene silencing: A general strategy used by diverse DNA and RNA viruses of plants," *Proc. Natl. Acad. Sci.*, vol. 96, no. 24, pp. 14147–14152, 1999.

[350] D. Silhavy *et al.*, "A viral protein suppresses RNA silencing and binds silencing-generated, 21- to 25-nucleotide double-stranded RNAs," *EMBO J.*, vol. 21, no. 12, pp. 3070–3080, 2002.

[351] K. Ye, L. Malinina, and D. J. Patel, "Recognition of small interfering RNA by a viral suppressor of RNA silencing," *Nature*, vol. 426, no. 6968, pp. 874–878, 2003.

[352] J. M. Vargason, G. Szittya, J. Burgyán, and T. M. Tanaka Hall, "Size Selective Recognition of siRNA by an RNA Silencing Suppressor," *Cell*, vol. 115, no. 7, pp. 799–811, 2003.

[353] J. Cheng, S. M. Sagan, N. Assem, R. Koukiekolo, N. K. Goto, and J. P. Pezacki, "Stabilized recombinant suppressors of RNA silencing: Functional effects of linking monomers of Carnation Italian Ringspot virus p19," *Biochim. Biophys. Acta - Proteins Proteomics*, vol. 1774, no. 12, pp. 1528–1535, 2007.

[354] K. M. Choi, G. L. Park, K. Y. Hwang, J. W. Lee, and H. J. Ahn, "Efficient siRNA delivery into tumor cells by p19-YSA fusion protein," *Mol. Pharm.*, vol. 10, no. 2, pp. 763–773, 2013.

[355] D. C. Danielson, N. Sachrajda, W. Wang, R. Filip, and J. P. Pezacki, "A Novel p19 Fusion Protein as a Delivery Agent for Short-interfering RNAs," *Mol. Ther. - Nucleic Acids*, vol. 5, 2016.

[356] N. J. Yang *et al.*, "Cytosolic delivery of siRNA by ultra-high affinity dsRNA binding proteins," *Nucleic Acids Res.*, vol. 45, no. 13, pp. 7602–7614, 2017.

[357] N. Bäumer, W. E. Berdel, and S. Bäumer, "Immunoprotein-Mediated siRNA Delivery," *Mol. Pharm.*, vol. 14, no. 5, pp. 1339–1351, 2017.

[358] T. L. Cuellar *et al.*, "Systematic evaluation of antibody-mediated siRNA delivery using an industrial platform of THIOMAB-siRNA conjugates," *Nucleic Acids Res.*, vol. 43, no. 2, pp. 1189–1203, 2015.

[359] X. Chen, M. Nguyen, F. Jacobson, and J. Ouyang, "Charge-based analysis of antibodies with engineered cysteines: From multiple peaks to a single main peak," *MAbs*, vol. 1, no. 6, pp. 563–571, 2009.

[360] C. F. Xia, R. J. Boado, and W. M. Pardridge, "Antibody-mediated targeting of siRNA via the human insulin receptor using avidin-biotin technology," *Mol. Pharm.*, vol. 6, no. 3, pp. 747–751, 2009.

[361] T. Sugo *et al.*, "Development of antibody-siRNA conjugate targeted to cardiac and skeletal muscles," *J. Control. Release*, vol. 237, pp. 1–13, 2016.

[362] S. Nanduri, B. W. Carpick, Y. Yang, B. R. G. Williams, and J. Qin, "Structure of the double-stranded RNA-binding domain of the protein kinase PKR reveals the molecular basis of its dsRNA-mediated activation," *EMBO J.*, vol. 17, no. 18, pp. 5458–5465, 1998.

[363] J. M. Ryter and S. C. Schultz, "Molecular basis of double-stranded RNA-protein interactions: Structure of a dsRNA-binding domain complexed with dsRNA," *EMBO J.*, vol. 17, no. 24, pp. 7505–7513, 1998.

[364] A. Eguchi *et al.*, "Efficient siRNA delivery into primary cells by a peptide transduction domain-dsRNA binding domain fusion protein," *Nat. Biotechnol.*, vol. 27, no. 6, pp. 567–571, 2009.

[365] J. C. Geoghegan, B. L. Gilmore, and B. L. Davidson, "Gene silencing mediated by siRNA-binding fusion proteins is attenuated by double-stranded RNA-binding domain structure," *Mol. Ther. - Nucleic Acids*, vol. 1, p. e53, 2012.

[366] D. V. Liu, N. J. Yang, and K. D. Wittrup, "A nonpolycationic fully proteinaceous multiagent system for potent targeted delivery of siRNA," *Mol. Ther. - Nucleic Acids*, vol. 3, p. e162, 2014.

[367] S. L. Ginn, A. K. Amaya, I. E. Alexander, M. Edelstein, and M. R. Abedi, "Gene therapy clinical trials worldwide to 2017: An update," *J. Gene Med.*, vol. 20, no. 5, p. e3015, Mar. 2018.

[368] R. Waehler, S. J. Russell, and D. T. Curiel, "Engineering targeted viral vectors for gene therapy," *Nat. Rev. Genet.*, vol. 8, no. 8, pp. 573–587, 2007.

[369] C. Baum, O. Kustikova, U. Modlich, Z. Li, and B. Fehse, "Mutagenesis and Oncogenesis by Chromosomal Insertion of Gene Transfer Vectors," *Hum. Gene Ther.*, vol. 17, no. 3, pp. 253–263, 2006.

[370] D. Grimm *et al.*, "Fatality in mice due to oversaturation of cellular microRNA/short hairpin RNA pathways," *Nature*, vol. 441, no. 7092, pp. 537–541, 2006.

[371] N. Bessis, F. J. GarciaCozar, and M. C. Boissier, "Immune responses to gene therapy vectors: Influence on vector function and effector mechanisms," *Gene Ther.*, vol. 11, pp. S10–S17, 2004.

[372] D. Castanotto and J. J. Rossi, "The promises and pitfalls of RNA-interference-based therapeutics," *Nature*, vol. 457, no. 7228, pp. 426–433, 2009.

[373] N. Nayerossadat, P. Ali, and T. Maedeh, "Viral and nonviral delivery systems for gene delivery," *Adv. Biomed. Res.*, vol. 1, p. 27, 2012.

[374] M. A. Kotterman, T. W. Chalberg, and D. V. Schaffer, "Viral Vectors for Gene Therapy: Translational and Clinical Outlook," *Annu. Rev. Biomed. Eng.*, vol. 17, pp. 63–89, 2015.

[375] K. Lundstrom, "Viral Vectors in Gene Therapy," *Dis. (Basel, Switzerland)*, vol. 6, no. 2, p. 42, May 2018.

[376] C. J. Buchholz, T. Friedel, and H. Büning, "Surface-Engineered Viral Vectors for Selective and Cell Type-Specific Gene Delivery," *Trends Biotechnol.*, vol. 33, no. 12, pp. 777–790, 2015.

[377] M. A. Kotterman and D. V. Schaffer, "Engineering adeno-associated viruses for clinical gene therapy," *Nat. Rev. Genet.*, vol. 15, no. 7, pp. 445–451, 2014.

[378] D. V. Schaffer, J. T. Koerber, and K. Lim, "Molecular Engineering of Viral Gene Delivery Vehicles," *Annu. Rev. Biomed. Eng.*, vol. 10, pp. 169–194, 2008.

[379] A. Touze and P. Coursaget, "In vitro gene transfer using human papillomavirus-like particles," *Nucleic Acids Res.*, vol. 26, no. 5, pp. 1317–1323, 1998.

[380] L. Bousarghin *et al.*, "Inhibition of cervical cancer cell growth by human papillomavirus virus-like particles packaged with human papillomavirus oncoprotein short hairpin RNAs," *Mol. Cancer Ther.*, vol. 8, no. 2, pp. 357–365, 2009.

[381] M. I. Chou *et al.*, "In vitro and in vivo targeted delivery of IL-10 interfering RNA by JC virus-like particles," *J. Biomed. Sci.*, vol. 17, p. 51, 2010.

[382] D. B. Hoffmann *et al.*, "In Vivo siRNA Delivery Using JC Virus-like Particles Decreases the Expression of RANKL in Rats," *Mol. Ther. - Nucleic Acids*, vol. 5, p. e298, 2016.

[383] C. E. Ashley *et al.*, "Cell-specific delivery of diverse cargos by bacteriophage MS2 virus-like particles," *ACS Nano*, vol. 5, no. 7, pp. 5729–5745, 2011.

[384] Y. Pan, Y. Zhang, T. Jia, K. Zhang, J. Li, and L. Wang, "Development of a microRNA delivery system based on bacteriophage MS2 virus-like particles," *FEBS J.*, vol. 279, no. 7, pp. 1198–1208, 2012.

[385] F. A. Galaway and P. G. Stockley, "MS2 viruslike particles: A robust, semisynthetic targeted drug delivery platform," *Mol. Pharm.*, vol. 10, no. 1, pp. 59–68, 2013.

[386] P. Y. Fang *et al.*, "Functional RNAs: Combined assembly and packaging in VLPs," *Nucleic Acids Res.*, vol. 45, no. 6, pp. 3519–3527, 2016.

[387] K. M. Choi, S. H. Choi, H. Jeon, I. S. Kim, and H. J. Ahn, "Chimeric capsid protein as a nanocarrier for siRNA delivery: Stability and cellular uptake of encapsulated siRNA," *ACS Nano*, vol. 5, no. 11, pp. 8690–8699, 2011.

[388] K. M. Choi, K. Kim, I. C. Kwon, I. S. Kim, and H. J. Ahn, "Systemic delivery of siRNA by chimeric capsid protein: Tumor targeting and RNAi activity in vivo," *Mol. Pharm.*, vol. 10, no. 1, pp. 18–25, 2013.

[389] E. J. Lee *et al.*, "Engineered proteinticles for targeted delivery of siRNA to cancer cells," *Adv. Funct. Mater.*, vol. 25, no. 8, pp. 1279–1286, 2015.

[390] X. Guan, Y. Chang, J. Sun, J. Song, and Y. Xie, "Engineered Hsp Protein Nanocages for siRNA Delivery," *Macromol. Biosci.*, vol. 18, no. 5, 2018.

[391] R. S. Shukla, B. Qin, and K. Cheng, "Peptides used in the delivery of small noncoding RNA," *Mol. Pharm.*, vol. 11, no. 10, pp. 3395–3408, 2014.

[392] C. A. Boswell, D. B. Tesar, K. Mukhyala, F. P. Theil, P. J. Fielder, and L. A. Khawli, "Effects of charge on antibody tissue distribution and pharmacokinetics," *Bioconjug. Chem.*, vol. 21, no. 12, pp. 2153–2163, 2010.

[393] H. J. Lee and W. M. Pardridge, "Pharmacokinetics and delivery of tat and tat-protein conjugates to tissues in vivo," *Bioconjug. Chem.*, vol. 12, no. 6, pp. 995–999, 2001.

[394] R. S. Shukla, W. Tai, R. Mahato, W. Jin, and K. Cheng, "Development of streptavidin-based nanocomplex for siRNA delivery," *Mol. Pharm.*, vol. 10, no. 12, pp. 4534–4545, 2013.

[395] A. Jain, A. Barve, Z. Zhao, W. Jin, and K. Cheng, "Comparison of Avidin, Neutravidin, and Streptavidin as Nanocarriers for Efficient siRNA Delivery," *Mol. Pharm.*, vol. 14, no. 5, pp. 1517–1527, 2017.

[396] E. Song *et al.*, "Antibody mediated in vivo delivery of small interfering RNAs via cell-surface receptors," *Nat. Biotechnol.*, vol. 23, no. 6, pp. 709–717, 2005.

[397] I. S. Ayene, "Ku protein targeting by Ku70 small interfering RNA enhances human cancer

cell response to topoisomerase II inhibitor and radiation," *Mol. Cancer Ther.*, vol. 4, no. 4, pp. 529–536, 2005.

[398] D. Peer, P. Zhu, C. V. Carman, J. Lieberman, and M. Shimaoka, "Selective gene silencing in activated leukocytes by targeting siRNAs to the integrin lymphocyte function-associated antigen-1," *Proc. Natl. Acad. Sci.*, vol. 104, no. 10, pp. 4095–4100, 2007.

[399] Y. Minakuchi *et al.*, "Atelocollagen-mediated synthetic small interfering RNA delivery for effective gene silencing in vitro and in vivo.," *Nucleic Acids Res.*, vol. 32, no. 13, p. e109, 2004.

[400] Y. Takei, K. Kadomatsu, Y. Yuzawa, S. Matsuo, and T. Muramatsu, "A small interfering RNA targeting vascular endothelial growth factor as cancer therapeutics," *Cancer Res.*, vol. 64, no. 10, pp. 3365–3370, 2004.

[401] F. Takeshita *et al.*, "Efficient delivery of small interfering RNA to bone-metastatic tumors by using atelocollagen in vivo," *Proc. Natl. Acad. Sci.*, vol. 102, no. 34, pp. 12177–12182, 2005.

[402] Z. Hao *et al.*, "Efficient delivery of micro RNA to bone-metastatic prostate tumors by using aptamer-conjugated atelocollagen in vitro and in vivo," *Drug Deliv.*, vol. 23, no. 3, pp. 874–881, 2016.

[403] M. C. Shin *et al.*, "Cell-penetrating peptides: Achievements and challenges in application for cancer treatment," *J. Biomed. Mater. Res. - Part A*, vol. 102, no. 2, pp. 575–587, 2014.

[404] W. Tai and X. Gao, "Functional peptides for siRNA delivery," *Adv. Drug Deliv. Rev.*, vol. 110–111, pp. 157–168, 2017.

[405] M. Dominska and D. M. Dykxhoorn, "Breaking down the barriers: siRNA delivery and endosome escape," *J. Cell Sci.*, vol. 123, no. 8, pp. 1183–1189, 2010.

[406] H. Margus, K. Padari, and M. Pooga, "Cell-penetrating peptides as versatile vehicles for oligonucleotide delivery," *Mol. Ther.*, vol. 20, no. 3, pp. 525–533, 2012.

[407] A. Erazo-Oliveras, N. Muthukrishnan, R. Baker, T. Y. Wang, and J. P. Pellois, "Improving the endosomal escape of cell-penetrating peptides and their cargos: Strategies and challenges," *Pharmaceuticals*, vol. 5, no. 11, pp. 1177–1209, 2012.

[408] S. M. Kronstadt, A. E. Pottash, D. Levy, S. Wang, W. Chao, and S. M. Jay, "Therapeutic Potential of Extracellular Vesicles for Sepsis Treatment," *Adv. Ther.*, vol. n/a, no. n/a, p. 2000259.

[409] A. E. Pottash, C. Kuffner, M. Noonan-Shueh, and S. M. Jay, "Protein-based vehicles for biomimetic RNAi delivery," *J. Biol. Eng.*, vol. 13, no. 19, 2019.